

22nd

GASEOUS ELECTRONICS

and HIGH-PRESSURE ARC SYMPOSIUM

Annual

CONFERENCE

Topical Conference of the American Physical Society

OCTOBER 27-31, 1969
GATLINBURG, TENNESSEE



OAK RIDGE NATIONAL LABORATORY
OPERATED BY UNION CARBIDE CORPORATION • FOR THE U.S. ATOMIC ENERGY COMMISSION

GASEOUS ELECTRONICS CONFERENCE COMMITTEE

G. J. Schulz, Chairman
Yale University

W. P. Allis, Honorary Chairman
Massachusetts Institute of Technology

E. C. Beaty
Joint Institute for Laboratory
Astrophysics

G. H. Dunn
Joint Institute for Laboratory
Astrophysics

Thomas L. Bailey
University of Florida

L. H. Fisher
Lockheed Palo Alto
Research Laboratory

Robert H. Bullis
United Aircraft Corporation
Research Laboratories

A. V. Phelps
Westinghouse Research Labs.

P. J. Chantry
Westinghouse Research Labs.

W. W. Robertson
University of Texas

C. F. Barnett, Secretary
Oak Ridge National Laboratory

LOCAL ARRANGEMENTS COMMITTEE

L. G. Christophorou

M. O. Krause

R. N. Compton

R. E. Minturn

W. D. Jones

I. A. Sellin

Mrs. Donna Cobble
Ladies Program

PROGRAM AND ABSTRACTS

TWENTY SECOND ANNUAL
GASEOUS ELECTRONICS CONFERENCE

&

HIGH PRESSURE ARC SYMPOSIUM

28 31 OCTOBER

1969

OAK RIDGE NATIONAL LABORATORY
OAK RIDGE, TENNESSEE

RIVERSIDE MOTEL
GATLINBURG, TENNESSEE

PROGRAM
HIGH PRESSURE ARC SYMPOSIUM

Monday Evening, 27 October

4:00 - 9:00 p.m.

Registration Lobby, Riverside Motel
Own-Host Reception in the Hideaway
Lounge, Riverside Motel.

Tuesday Morning, 28 October

8:00 a.m.

Registration Lobby, Riverside Motel

9:00 - 10:25 a.m.

Session A SPECTRAL CHARACTERISTICS
OF ARCS

Stephen Whaley Hall

Chairman: W. L. Wiese, NBS

A-1 MEASUREMENTS OF LINE SHIFTS AND OF THE FREE-FREE CONTINUUM OF ARGON FOR THE 20000 TO 30000°K TEMPERATURE REGION
R. U. Morris and J. C. Morris

A-2 THE CONTINUOUS EMISSION OF ARGON IN THE VISIBLE SPECTRAL RANGE
E. Schulz-Gulde

A-3 ABSORPTION CORRECTIONS FOR HIGH PRESSURE ARCS
H. N. Olsen

A-4 DEVELOPMENT OF A STABLE ARC SOURCE FOR QUANTITATIVE SPECTROSCOPIC STUDIES OF IRON
J. M. Bridges

A-5 INVESTIGATION OF HIGH PRESSURE ARC JET
J. Meyer and R. Beck

10:25 - 10:45 a.m. Coffee Break

10:45 a.m. - 12:25 p.m.

Session B TRANSPORT AND THERMODYNAMIC
PROPERTIES AND LTE PANEL

Panel Chairman: E. E. Soehngen,
Wright-Patterson AFB

B-1 TOTAL RADIATION SOURCE STRENGTH OF ARGON PLASMAS
P. W. Schreiber, A. M. Hunter and K. R. Benedetto

B-2 RADIATIVE AND TRANSPORT PROPERTIES OF SF₆ AND THEIR USE IN MODEL
ARC STUDIES
J. J. Lowke, R. W. Liebermann and L. S. Frost

B-3 INFLUENCE OF DIFFUSION ON THE BEHAVIOUR OF HE-ARCS UNDER NORMAL
PRESSURE
J. Uhlenbusch

- B-4 MEASUREMENTS OF ELECTRICAL AND THERMAL CONDUCTIVITY OF HYDROGEN, NITROGEN AND ARGON AT HIGH TEMPERATURES
J. C. Morris, R. P. Rudis and J. M. Yos
- B-5 THE MEASUREMENT OF PLASMA TRANSPORT PROPERTIES IN A FREE-BURNING ELECTRIC ARC
C. G. Stojanoff
- B-6 THE ELECTRICAL CONDUCTIVITY OF ARGON AT HIGH PRESSURES
Uwe H. Bauder and R. S. Devoto

12:30 p.m. Lunch

Tuesday Afternoon, 28 October

Session C ARC CHARACTERISTICS

Stephen Whaley Hall

Chairman: J. Uhlenbusch, I. Phys.
Inst. Techn. Hochschule
Aachen

2:00 - 5:10 p.m.

- C-1 EFFECTIVE PERIPHERY OF A HIGH PRESSURE ARC
W. T. Lord
- C-2 HIGH PRESSURE ARC TEMPERATURE AND RADIATIVE ENERGY DISTRIBUTIONS
C. H. Marston, G. Frind, B. L. Damsky and A. M. Schorn
- C-3 ANALYTIC MODEL FOR INFINITE CYLINDRICAL HIGH PRESSURE ARCS
D. M. Cap
- C-4 ENERGY DISSIPATION MECHANISMS IN INTENSE MERCURY-VAPOR ARCS
L. P. Harris
- C-5 THE INFLUENCE OF IONIZATION TO EXCITATION POTENTIAL RATIO ON ARC TEMPERATURE PROFILE OF METAL IODIDE ARCS
John F. Waymouth
- C-6 THE EFFECT OF ABSORPTION OF RADIATION ON ARC TEMPERATURE PROFILES OF METAL IODIDE ARCS
John F. Waymouth

3:25 - 3:45 p.m. Coffee Break

- C-7 THEORETICAL ANALYSIS OF THE BEHAVIOR OF Hg + T&I ARC DISCHARGES WITH VARIABLE MERCURY LOADINGS
C. F. Gallo
- C-8 A TWO ZONE MODEL FOR THERMAL INDUCTION PLASMAS
H. U. Eckert
- C-9 THE CONFINED ELECTRODELESS ARC
D. R. Keefer, J. A. Sprouse and F. C. Loper
- C-10 THE THERMAL ELECTRODELESS ARC IN AIR
Donald D. Hollister

Wednesday Morning, 29 October

9:00 - 11:00 a.m.

Session D ARCS IN FLOW AND MAGNETIC
FIELDS

Pearl Room

Chairman: H. Stine, NASA

- D-1 CHARACTERISTICS OF A HIGH PRESSURE ARC CONFINED IN A TRANSPIRATION-COOLED TUBE
E. Pfender and J. Heberlein
- D-2 BOUNDARY LAYER ANALYSIS OF AN SF₆ CIRCUIT BREAKER ARC
B. W. Swanson and R. M. Roidt
- D-3 ARCS IN TURBULENT FLOWS
G. Frind and B. L. Damsky
- D-4 THREE-DIMENSIONAL TEMPERATURE DISTRIBUTION WITHIN A STEADY-STATE CROSS-FLOW ARC
D. M. Benenson, A. A. Cenkner, Jr. and A. J. Baker
- D-5 SOME EXPERIMENTAL FINDINGS FOR AN ARC IN A SWIRL FLOW
H. Muntenbruch, S. F. Giannotta and H. O. Schrade
- D-6 EXPERIMENTAL RESULTS ON THE SHAPE AND MOTION OF A D.C. ARC IN AN EXTERNAL MAGNETIC FIELD
R. F. Neubauer
- D-7 INVESTIGATIONS ON A STATIONARY MAGNETICALLY STABILIZED HELIUM ARC
K. Bergstedt, P. Grassmann, O. Klueber and H. Wulff

11:00 - 11:30 a.m. Coffee Break

11:30 a.m.

Session H Plenary Session

Stephen Whaley Hall

Chairman: A. V. Phelps, Westinghouse
Research Laboratories

INVITED PAPER

H. H. Maecker, Technische Hochschule
München, Germany

MOTION AND DISPLACEMENT OF ARCS

12:15 - 2:00 p.m. Lunch

2:00 - 2:50 p.m.

Session E TIME VARYING ARCS

Pearl Room

CHAIRMAN: R. L. Phillips, Univ. of
Michigan

- E-1 A METHOD OF OBTAINING HIGH PLASMA TEMPERATURES USING PULSED CONSTRICTED ARCS
J. C. Morris and R. U. Morris

E-2 RESPONSE CHARACTERISTICS OF PULSED CESIUM VAPOR ARCS
 R. D. Buhler and W. F. Hug

E-3 INVESTIGATION OF THE DIELECTRIC RECOVERY OF HIGH CURRENT AIR GAPS
 J. F. Perkins and A. B. Parker

2:50 - 4:35 p.m.*

Session F ELECTRODE EFFECTS

Pearl Room

Chairman: T. H. Lee, G.E. Co.

F-1 IN SITU MEASUREMENT OF THERMIONIC CURRENT IN AN ARGON ARC WITH A
 TUNGSTEN CATHODE
 M. M. Chen, R. Thorne and E. F. Wyner

F-2 SPECTROSCOPIC STUDY OF A TUNGSTEN ARC CATHODE
 E. F. Wyner and M. M. Chen

F-3 ELECTRODE EROSION IN HIGH-CURRENT ELECTRIC ARCS
 K. T. Shih

F-4 A THEORY OF THE CATHODE SPOT
 D. Mitrovich

F-5 RECENT DEVELOPMENTS ON THE LONGINI MODEL OF THE CATHODIC SPOT
 M. F. Hoyaux

*No coffee break, but coffee will be available at 3:40 p.m.

PROGRAM
 TWENTY-SECOND ANNUAL
 GASEOUS ELECTRONICS CONFERENCE

Tuesday Morning, 28 October

8:00 a.m. - 8:00 p.m. Registration Lobby, Riverside Motel
 8:00 - 11:00 p.m. Own-Host Reception, Hideaway Lounge,
 Riverside Motel

Wednesday Morning, 29 October

8:00 a.m. Registration Lobby, Riverside Motel
 9:00 - 11:00 a.m. Session G ELECTRON COLLISIONS PANEL
 Stephen Whaley Hall Panel Chairman: W. R. Garrett, Oak
 Ridge National Lab.

- G-1 RELATIVE CROSS SECTION MEASUREMENTS FOR ELECTRON SCATTERING BY
 ATOMIC NITROGEN (0.2-3 eV)
 T. M. Miller, B. B. Aubrey, P. N. Eisner and B. Bederson
- G-2 ANGULAR DISTRIBUTION OF PROTONS PRODUCED BY DISSOCIATIVE IONI-
 ZATION OF H₂ NEAR THRESHOLD
 R. J. Van Brunt and L. J. Kieffer
- G-3 CROSS SECTION MEASUREMENT FOR DISSOCIATIVE RECOMBINATION OF
 ELECTRONS AND D₂⁺
 Martin K. Vogler and Gordon H. Dunn
- G-4 DIRECT EXCITATION OF MOLECULAR VIBRATIONS BY SLOW ELECTRON IMPACT
 E. V. Puttkamer
- G-5 CALCULATION OF CROSS-SECTIONS FOR INELASTIC ELECTRON-ATOM COLLI-
 SIONS
 H. H. Michels and F. E. Harris
- G-6 OUTER SHELL IONIZATION OF ARGON BY ELECTRON IMPACT; ANGULAR DIS-
 TRIBUTIONS IN A CENTRAL POTENTIAL MODEL
 Steven T. Manson
- G-7 ELECTRON SCATTERING BY POLAR MOLECULES
 W. R. Garrett and V. E. Anderson
- G-8 VARIATIONAL PRINCIPLE FOR SCATTERING
 K. J. Miller

11:00 - 11:30 a.m. Coffee Break

11:30 a.m. - 12:15 p.m.	Session H Plenary Session
Stephen Whaley Hall	Chairman: A. V. Phelps, Westinghouse Research Laboratories
INVITED PAPER	H. H. Maecker, Technische Hochschule München, Germany
MOTION AND DISPLACEMENT OF ARCS	

12:15 - 2:00 p.m. Lunch

Wednesday Afternoon, 29 October

- | | |
|---------------------|--|
| 2:00 - 3:40 p.m. | Session I RECOMBINATION PANEL |
| Stephen Whaley Hall | Panel Chairman: M. A. Biondi, Univ.
of Pittsburgh |
- I-1 PRESSURE AND ELECTRON DENSITY DEPENDENCE OF THE ELECTRON-ION RECOMBINATION COEFFICIENT IN HELIUM
J. Berlande, M. Cheret, R. Deloche, A. Gonfalone and C. Manus
- I-2 ELECTRON-ION RECOMBINATION IN HELIUM AT 77°K
J. B. Gerardo and M. A. Gusinow
- I-3 THE DISSOCIATIVE RECOMBINATION OF O_2^+ IONS INTO SPECIFICALLY IDENTIFIED FINAL ATOMIC STATES
E. C. Zipf
- I-4 MEASUREMENT OF THE RATE COEFFICIENT FOR THE RECOMBINATION OF He^+ WITH ELECTRONS IN A HIGH PRESSURE AFTERGLOW
W. E. Wells and C. B. Collins
- I-5 AFTERGLOWS IN AIR
Robert C. Gunton

Wednesday Afternoon, 29 October

- | | |
|------------------|---|
| 2:00 - 3:40 p.m. | Session J NEGATIVE IONS |
| Espalier Room | Chairman: R. N. Compton, Oak Ridge
National Laboratory |
- J-1 CHARGE TRANSFER FROM NEGATIVE HALOGEN IONS TO NO_2
S. J. Nalley, J. A. D. Stockdale and R. N. Compton
- J-2 SPURIOUS DISSOCIATIVE ATTACHMENT PEAKS FROM INELASTIC ENERGY LOSS REACTIONS
P. J. Chantry
- J-3 TEMPERATURE DEPENDENCE OF SF_6^- , SF_5^- , AND F^- PRODUCTION FROM SF_6
C. L. Chen and P. J. Chantry

- J-4 ATTACHMENT OF ELECTRONS TO SF₆, ION CHEMISTRY OF SF₆ AND CLUSTER ION FORMATION FROM ALKALI METAL IONS
F. C. Fehsenfeld
- J-5 MEASUREMENT OF ELECTRON ATTACHMENT RATES IN A THERMAL PLASMA
J. H. Mullen and R. L. Cowperthwaite
- J-6 ELECTRON ATTACHMENT IN THE FIELD ON THE GROUND AND EXCITED ELECTRONIC STATES OF THE AZULENE MOLECULE
E. L. Chaney, L. G. Christophorou, P. M. Collins and J. G. Carter
- J-7 ELECTRON ATTACHMENT CROSS SECTIONS AND NEGATIVE-ION LIFETIMES FOR p-BENZOQUINONE AND 1,4-NAPHTHOQUINONE
P. M. Collins, L. G. Christophorou, E. L. Chaney and J. G. Carter

3:40 p.m. Coffee and hiking

Wednesday Evening, 29 October

8:00 - 10:00 p.m.

Session K AFTERGLOWS AND ION REACTIONS

Pearl Room

Chairman: A. L. Schmeltekopf, ESSA

- K-1 WATER-CLUSTER IONS IN AIR, N₂, AND CO₂
P. N. Eisner, M. N. Hirsh and E. Poss
- K-2 NEUTRAL CHEMISTRY EFFECTS IN THE POSITIVE ION SPECTRUM OF ELECTRON-IRRADIATED AIR
M. N. Hirsh, P. N. Eisner and E. Poss
- K-3 REACTIONS IN IONIZED AIR-LIKE MIXTURES
F. E. Niles
- K-4 FLOWING AFTERGLOW STUDIES OF THE REACTIONS OF THE RARE-GAS MOLECULAR IONS He₂⁺, Ne₂⁺, and Ar₂⁺ WITH MOLECULES AND RARE-GAS ATOMS
D. K. Bohme, N. G. Adams, M. Mosesman, D. B. Dunkin and E. E. Ferguson
- K-5 FLOWING AFTERGLOW STUDIES OF FORMATION AND REACTIONS OF CLUSTER IONS OF O₂⁺ and O₂⁻
N. G. Adams, D. K. Bohme, D. B. Dunkin, F. C. Fehsenfeld and E. E. Ferguson
- K-6 REACTIONS OF NO⁺ IN ATMOSPHERIC GASES
L. J. Puckett and M. W. Teague
- K-7 A NUMERICAL STUDY OF THE TRANSIENT HYDROGEN AFTERGLOW
C. C. Limbaugh and W. K. McGregor
- K-8 PROBE MEASUREMENTS OF DIFFUSION COOLING
Edwin Blue

- K-9 THEORY OF ADIABATIC COOLING OF ELECTRONS IN A DIFFUSION-CONTROLLED AFTERGLOW PLASMA
J. H. Ingold

Wednesday Evening, 29 October

8:00 - 10:00 p.m.

Session L EXCITATION BY ELECTRON IMPACT PANEL

Stephen Whaley Hall

Panel Chairman: S. J. Smith, JILA

- L-1 ELECTRON IMPACT EXCITATION AND IONIZATION STUDIES OF He, Ne, AND Ar
J. T. Grissom, R. N. Compton and W. R. Garrett
- L-2 RESONANCE FEATURES IN THE EXCITATION FUNCTIONS OF NEON
K. G. Walker and R. M. St. John
- L-3 OPTICAL IONIZATION-EXCITATION FUNCTIONS OF ZINC, CADMIUM AND MERCURY BY ELECTRON IMPACT
Richard J. Anderson and Edward T. P. Lee
- L-4 ELECTRON EXCITATION CROSS SECTIONS OF THE FIRST NEGATIVE BANDS OF OXYGEN AND NITROGEN
Walter L. Borst and E. C. Zipf
- L-5 ELECTRON-IMPACT CROSS SECTIONS FOR SIMULTANEOUS IONIZATION AND EXCITATION OF He TO THE 4s,p,d,f STATES BY HIGH-RESOLUTION FABRY-PEROT INTERFEROMETRY
William D. Evans, James K. Ballou, Fred L. Roesler and Chun C. Lin
- L-6 SIMULTANEOUS EXCITATION AND IONIZATION OF ARGON: $3p^4 4s^2 P$ UV EMISSION
G. M. Lawrence
- L-7 THE DISSOCIATIVE EXCITATION OF ATOMIC RESONANCE LINES BY ELECTRON IMPACT
M. J. Mumma and E. C. Zipf

Thursday Morning, 30 October

8:30 - 11:20*

Session M CO₂ LASER PANEL

Stephen Whaley Hall

Panel Chairman: R. H. Bullis, United Aircraft Res. Labs.

- M-1 DIAGNOSTICS OF PLASMA PROPERTIES IN A CO₂ LASER
P. Bletzinger and A. Garscadden
- M-2 ELECTRON RADIATION TEMPERATURE MEASUREMENTS IN A SEALED-OFF CO₂-LASER SYSTEM
J. Polman and W. J. Witteman

*Coffee Break at 10:00 a.m.

- M-3 EFFECT OF ELECTRON COLLISIONS IN A PULSED CO₂ DISCHARGE ON OPTICAL GAIN AT 10.6 μm
J. H. Noon, P. R. Blaszyk, E. H. Holt and R. G. Buser
- M-4 COLLISION PROCESSES IN A SEALED-OFF CO₂-LASER
J. Freudenthal
- M-5 CO FORMATION IN N₂-CO₂ LASERS
W. J. Wiegand, M. C. Fowler and J. A. Benda
- M-6 ELECTRON ENERGY DISTRIBUTION FUNCTIONS IN CO₂ LASER MIXTURES
W. L. Nighan
- M-7 VIBRATIONAL EXCITATION IN CO₂ AND POSITIVE COLUMN MAINTENANCE FIELDS IN CO₂ LASER MIXTURES
A. V. Phelps
- M-8 THEORY OF ENERGY TRANSFER MECHANISMS IN CO₂ LASERS
H. J. Kolker
- M-9 INFLUENCE OF COLLISIONS ON OPTICAL SATURATION IN THE CO₂ LASERS
T. Kan and G. J. Wolga
- M-10 CENTRAL TUNING PEAK AND INHOMOGENEOUS SATURATION WITH THE CO₂ LASER
H. T. Powell and G. J. Wolga

Thursday Morning, 30 October

8:30 - 11:20 a.m.

Session N IONIZATION COEFFICIENTS AND BREAKDOWN

Pearl Room

Chairman: G. S. Hurst, Univ. of Ky.

- N-1 HALL EFFECT IN FIELD EMITTING PROTRUSIONS INITIATING VACUUM BREAKDOWN
Alan Watson
- N-2 INFLUENCE OF THERMAL PROPERTIES OF ANODE MATERIAL ON VACUUM BREAKDOWN
F. Y. Tse and P. C. Bolin
- N-3 IONIZATION COEFFICIENTS AND COLLISION FREQUENCIES IN CROSSED ELECTRIC AND MAGNETIC FIELDS
S. C. Haydon and A. Simpson
- N-4 NON-EQUILIBRIUM IONIZATION IN SWARMS WITH HIGH MEAN ELECTRON ENERGIES
M. Folkard and S. C. Haydon
- N-5 THE RATIO OF TRANSVERSE AND LONGITUDINAL DIFFUSION COEFFICIENTS
C. E. Klots and D. R. Nelson

N-6 PHOTOMETRIC DETERMINATION OF THE ELECTRON IONIZATION FREQUENCY
IN DRY AIR
M. H. Mentzoni

N-7 DIGITAL COMPUTER SOLUTION OF LOEB'S STREAMER CRITERION
M. S. Abou-Seada and Essam Nasser

10:00 - 10:20 a.m. Coffee Break

N-8 THE EFFECT OF NITRIC OXIDE ON MICROWAVE BREAKDOWN OF NITROGEN
Donald L. Jones, Allen D. Ruess and Paul E. Bisbing

N-9 BREAKDOWN VOLTAGE OF CESIUM IN THERMIONIC DIODE
K. Shimada

N-10 THEORETICAL CONSIDERATIONS OF THE PREBREAKDOWN CHARACTERISTICS
IN A CESIUM THERMIONIC DISCHARGE
David Tai-ko Shaw

N-11 EFFECT OF LARGE ELECTRIC FIELDS ON THE ELECTRON ENERGY DIS-
TRIBUTION AND IONIZATION RATE IN A CESIUM DISCHARGE
David Tai-ko Shaw and S. G. Mangolis

N-12 APPROACH TOWARD IONIZATIONAL EQUILIBRIUM IN SHOCKED MERCURY GAS
Yong Wook Kim

Thursday Morning, 30 October

11:30 a.m. - 12:00 noon

Session 0 Plenary Session

Stephen Whaley Hall

Chairman: G. Schulz, Yale Univ.

BUSINESS MEETING

12:00 - 2:00 p.m. Lunch

Thursday Afternoon, 30 October

2:00 - 3:45 p.m.

Session P PENNING EFFECT PANEL

Stephen Whaley Hall

Panel Chairman: E. E. Muschlitz, Jr.
Univ. of Florida

P-1 VELOCITY DEPENDENCE OF THE IONIZATION OF ARGON ON IMPACT OF
METASTABLE NEON ATOMS
S. Y. Tang and E. E. Muschlitz, Jr.

P-2 THE KINETIC ENERGIES OF IONS RESULTING FROM IMPACT OF 2^3S AND
 2^1S He^* ON H_2 , D_2 , O_2 AND NO
K. D. Foster and E. E. Muschlitz, Jr.

- P-3 DE-EXCITATION RATE CONSTANTS FOR HELIUM METASTABLE ATOMS WITH SEVERAL ATOMS AND MOLECULES
A. L. Schmeltekopf
- P-4 PENNING CROSS SECTIONS FOR He^M -Cd COLLISIONS
L. D. Schearer and F. A. Padovani
- P-5 POLARIZATION OF IONS AND ELECTRONS VIA PENNING COLLISIONS WITH OPTICALLY PUMPED METASTABLE HELIUM ATOMS
L. D. Schearer
- P-6 ROTATIONAL STRUCTURE OF N_2 2ND POSITIVE BANDS IN PENNING EXCITATION BY ARGON METASTABLE ATOMS
Wheeler K. McGregor, Jr.

Thursday Afternoon, 30 October

2:00 - 3:45 p.m.

Session Q HEAVY PARTICLE COLLISIONS I

Pearl Room

Chairman: D. W. Martin, Georgia
Institute of Technology

- Q-1 ELECTRON TRANSFER IN O-Cs COLLISIONS
B. W. Woodward, W. C. Lineberger and L. M. Branscomb
- Q-2 EXPERIMENTAL OBSERVATION OF ION IMPACT EXCITATION OF PURE VIBRATIONAL AND ELECTRONIC TRANSITIONS IN DIATOMIC MOLECULES
John H. Moore, Jr. and John P. Doering
- Q-3 ANALYSIS OF KINETIC ENERGY LOSS IN N^+ -A AND O^+ -Kr COLLISIONS AT KEV ENERGIES
H. C. Hayden and E. J. Knystautas
- Q-4 SMALL-ANGLE SCATTERING OF STRIPPING COLLISIONS OF HYDROGEN ATOMS ON VARIOUS GASES
H. Fleischmann, C. F. Barnett and J. A. Ray
- Q-5 TOTAL CROSS SECTION FOR SINGLE ELECTRON LOSS BY Ne AND Ar IN NITROGEN, OXYGEN AND AIR
G. J. Lockwood
- Q-6 IONIZATION OF ATOMIC AND MOLECULAR GASES BY 1-25 KEV HYDROGEN ATOMS
R. J. McNeal, D. C. Clark and R. A. Klingberg
- Q-7 ANALYTIC CROSS SECTIONS FOR INELASTIC COLLISIONS OF PROTONS AND HYDROGEN ATOMS WITH ATOMIC AND MOLECULAR GASES
A. E. S. Green and R. J. McNeal

Thursday Afternoon, 30 October

4:00 - 5:00 p.m.

Session R RARE GAS LASERS

Stephen Whaley Hall

Chairman: R. H. Bullis, United Aircraft Research Labs.

- R-1 ELECTRON COLLISIONAL PROCESSES IN ARGON ION LASER DISCHARGES
W. C. Jennings, J. H. Noon, E. H. Holt and R. G. Buser
- R-2 ELECTRON DENSITIES FROM REFRACTIVE INDEX MEASUREMENTS IN CW
ARGON ION LASER PLASMAS
P. S. Zory and C. B. Zarowin
- R-3 ANOMALOUS HYPERFINE LASER OSCILLATION IN THE HELIUM-IODINE LASER
C. S. Willett
- R-4 THE EFFECT OF HELIUM ON POPULATION INVERSION IN HE-NE LASER DIS-
CHARGES
R. T. Young, C. S. Willett and R. T. Maupin

SOCIAL HOUR

Hideaway Lounge

6:15 P.M.

BANQUET

Pearl Room
Riverside Motel

7:15 P.M.

Speaker: D. J. Rose, Assistant Director
Oak Ridge National Laboratory

"THE FUTURE OF NATIONAL LABORATORIES"

Friday Morning, 31 October

8:30 a.m. - 12:30 p.m.

Session S PHOTONS AND MOLECULAR
STRUCTURE

Stephen Whaley Hall

Chairman: F. R. Gilmore, Rand Corp.

- S-1 AFTERGLOW PROPERTIES OF NITROGEN EMISSION BANDS DUE TO TRANSITIONS FROM TRIPLET STATES
A. R. DeMonchy, G. N. Hays, C. J. Tracy and H. J. Oskam
- S-2 NON-RADIATIVE TRANSPORT OF RESONANCE EXCITATION ENERGY IN METAL VAPORS
A. V. Phelps and C. L. Chen
- S-3 STANDARD LIGHT SOURCES FOR THE VACUUM ULTRAVIOLET REGION
T. E. Stewart, J. E. Parks, G. S. Hurst, T. E. Bortner and F. W. Martin
- S-4 EMISSION FROM METASTABLE STATES IN A NITROGEN ION BEAM
William B. Maier, II and R. F. Holland
- S-5 EXPERIMENTAL VALUES OF SOME ArII TRANSITION PROBABILITIES
N. M. Nerheim and H. N. Olsen
- S-6 LIFETIMES OF THE $A^2\Sigma^+$ STATE OF NO
G. E. Copeland, R. T. Thompson and R. G. Fowler
- S-7 EMISSION SPECTRA OF ELECTRON BOMBARDED GASEOUS AND LIQUID HELIUM
G. K. Walters, W. S. Dennis, E. Durbin, Jr., W. A. Fitzsimmons and O. Heybey
- 10:15 a.m. Coffee Break
- S-8 MULTIPLE ELECTRON IONIZATION OF NEON BY ELECTRON AND PHOTON IMPACT
M. O. Krause, F. A. Stevie, L. J. Lewis, T. A. Carlson and W. E. Moddeman
- S-9 HIGH RESOLUTION MEASUREMENT OF S^- PHOTODETACHMENT NEAR THRESHOLD
W. C. Lineberger, B. W. Woodward and L. M. Branscomb
- S-10 PHOTOELECTRON SPECTRA OF DIBORANE
T. L. Rose, R. Frey and B. Brehm
- S-11 ENERGY ANALYSIS OF ELECTRON EJECTED IN SLOW ION-ATOM COLLISIONS
G. Gerber, R. Morgenstern and A. Niehaus
- S-12 CALCULATION OF THE DOUBLY EXCITED AUTOIONIZING STATES OF H_2
A. U. Hazi and H. S. Taylor
- S-13 INELASTIC ROTATIONAL COLLISIONS IN ALKALI DIMERS
M. McClintock and W. Demtroder

- S-14 THE ENHANCEMENT OF $H\alpha$ (6563 Å) RADIATION IN A NEON-HYDROGEN PULSED DISCHARGE
John A. McNally

Friday Morning, 31 October

8:30 a.m. - 12:30 p.m.

Session T GLOWS AND DISCHARGES

Pearl Room

Chairman: A. Garscadden, Wright-Patterson AFB

- T-1 THE COULOMB LOGARITHM FOR IONS SLOWING DOWN ON ELECTRONS IN A PLASMA
J. Rand McNally, Jr.
- T-2 A NEW METHOD FOR SOLVING THE KINETICS OF GAS DISCHARGES FOR ATOMS WITH MANY ENERGY LEVELS
W. G. Valance and A. Heller
- T-3 A VARIATIONAL SOLUTION FOR THE POSITIVE COLUMN CHARACTERISTIC CURVE
Frederick J. Mayer
- T-4 MEASUREMENTS OF THE RELAXATION TIME OF METASTABLE ATOMS IN A NEON DISCHARGE USING AN EXTERNAL SOURCE OF LIGHT
G. G. Cloutier, J. P. Novak and V. Fuchs
- T-5 TIME-RESOLVED ENERGY DISTRIBUTIONS IN A STRIATING DISCHARGE
R. F. Weber, A. Garscadden and P. Bletzinger
- T-6 CATAPHORETIC SEGREGATION PROCESSES IN A NON-PENNING GAS MIXTURE
A. K. Bhattacharya
- T-7 GAS FLOWS GENERATED BY NOBLE GAS DC DISCHARGES
C. C. Leiby, Jr. and C. W. Rogers
- T-8 AXIAL PRESSURE GRADIENTS IN DC DISCHARGES WITH BY-PASS CONNECTIONS
R. B. Tombers and L. M. Chanin
- T-9 EFFECT OF ARGON ATOMS ON SELF-ABSORPTION OF Hg 2537 Å RADIATION IN Hg + Ar DISCHARGES
T. J. Hammond and C. F. Gallo
- T-10 CHARACTERISTICS OF A LOW-DENSITY HELIUM PLASMA IN A MAGNETIC FIELD
S. Gavril, D. Schieber and M. S. Erlicki
- T-11 DISSOCIATION OF WATER VAPOR IN THE POSITIVE COLUMN OF A GLOW DISCHARGE
K. K. Corvin and R. M. St. John
- T-12 DIELECTRIC CONSTANT OF AN ELECTRON-FREE Ti^+I^- PLASMA
P. Davidovits and J. L. Hirshfield

T-13 NON-LINEAR THEORY OF THE POSITIVE COLUMN SPIRAL INSTABILITY
J. N. Shiau and Albert Simon

T-14 ENERGY DISTRIBUTION OF MO IONS RETURNING TO THE SPUTTERING CATHODE
IN AN ARGON GLOW DISCHARGE
J. E. Houston

Friday Afternoon, 31 October

2:00 - 5:00 p.m.*

Session U ION-MOLECULE COLLISIONS
USING DRIFT TUBES PANEL

Stephen Whaley Hall

Panel Chairman: E. W. McDaniel, Georgia
Institute of Technology

U-1 POSSIBLE SOURCES OF LARGE ERROR IN DETERMINATIONS OF REACTION RATES
WITH DRIFT TUBE-MASS SPECTROMETERS
E. W. McDaniel

U-2 MOBILITIES AND LONGITUDINAL DIFFUSION COEFFICIENTS OF MASS-IDENTI-
FIED OXYGEN AND POTASSIUM IONS IN OXYGEN
R. M. Snuggs, D. J. Volz, J. H. Schummers, D. W. Martin and
E. W. McDaniel

U-3 MONATOMIC AND DIATOMIC IONS IN OXYGEN
R. N. Varney

U-4 DRIFT VELOCITIES AND INTERACTIONS OF NEGATIVE IONS IN OXYGEN
L. G. McKnight and J. M. Sawina

U-5 MOBILITIES OF NEGATIVE IONS IN SF₆
P. L. Patterson

U-6 THEORY OF KINETIC ION TEMPERATURE
S. B. Woo and J. H. Whealton

U-7 DRIFT TUBE MEASUREMENTS OF THE FORMATION OF ALKALI ION-WATER
CLUSTERS
R. Johnsen, H. L. Brown and M. A. Biondi

U-8 CLUSTERING REACTIONS OF THE HYDRONIUM ION
C. E. Young, D. Edelson and W. E. Falconer

U-9 IONIC PROCESSES IN HELIUM-ARGON MIXTURES
G. E. Veatch and H. J. Oskam

* 3:30 - 3:50 p.m. Coffee Break

Friday Afternoon, 31 October

2:00 - 5:00 p.m.

Session V HEAVY PARTICLES II

Pearl Room

Chairman: T. L. Bailey, Univ. of Fla.

- V-1 A SMATTERING OF SCATTERING
H. Sugiuchi, J. F. Aebischer and M. G. Menendez
- V-2 EXACT PHASE SHIFTS FOR THE SUTHERLAND ION-MOLECULE POTENTIAL
John W. Sheldon
- V-3 THE EFFECTS OF VIBRATIONS ON LIFETIMES OF ION-MOLECULE COMPLEXES
IN ION-DIPOLE COLLISIONS
J. V. Dugan, Jr., R. B. Canright, Jr. and J. L. Magee
- V-4 A SIMPLE MODEL FOR THE HIGH ENERGY REACTION OF O^+ IONS WITH N_2
Thomas F. O'Malley
- V-5 ON THE DEPENDENCE OF ION-MOLECULE REACTIONS ON THE REACTANT
VIBRATIONAL ENERGY
F. A. Wolf
- V-6 MECHANISMS IN REACTIONS OF O^+ WITH N_2 AND CO_2
John F. Paulson
- V-7 LOW ENERGY $NO^+ + Cs$ CHARGE EXCHANGE-MEASUREMENTS
T. L. Churchill

3:30 - 3:50 p.m. Coffee Break

- V-8 THE EFFECTS OF VIBRATIONAL EXCITATION ON $N_2^+ + N_2$ and $N_2^+ + Ar$ CHARGE TRANSFER COLLISIONS
B. Van Zyl and N. G. Utterback
- V-9 VIBRATIONAL EXCITATION IN THE COLLISIONS OF LOW ENERGY ION BEAMS
WITH NEUTRAL MOLECULES
T. F. Moran
- V-10 CROSS SECTION FOR METASTABLE PRODUCTION IN VERY LOW ENERGY $He^+ - He$ COLLISIONS
P. J. MacVicar-Whelan and Walter L. Borst
- V-11 VACUUM ULTRAVIOLET PHOTON PRODUCTION IN LOW-ENERGY COLLISIONS
BETWEEN NEUTRAL ARGON ATOMS
Paul O. Haugsjaa and Robert C. Amme
- V-12 OPTICAL AND MASS SPECTROSCOPIC STUDIES OF THE REACTIONS OF He^+
AND $He(2^3S)$ WITH O_2
D. L. Albritton

Fla.

SESSION A

ES

Tuesday Morning, 28 October

9:00 a.m.

SPECTRAL CHARACTERISTICS
OF ARCS

MS

Chairman: *W. L. Wiese*, National Bureau of Standards
Washington, D. C.

ABSTRACTS

HIGH PRESSURE ARC SYMPOSIUM

28, 29 OCTOBER

1969

RIVERSIDE MOTEL

GATLINBURG, TENNESSEE

A1. Measurements of Line Shifts and of the Free-Free Continuum of Argon For the 20000 to 30000 °K Temperature Region.* R. U. Morris and J. C. Morris, Avco, Wilmington, Mass. Experimental measurements of two of the basic parameters, ionic line shifts and the free free effective nuclear charge, for the major radiating systems of Argon in the 20000 °K to 30000 °K temperature regions have been made. These data have been obtained using photoelectric and photographic techniques for observing a pulsed constricted electric arc. The results of these measurements are compared with theory.

*Work supported by Aerospace Research Laboratories, Office of Aerospace Research of the U. S. Air Force, (Contract No. F33615-68-C-1081.)

A2. The Continuous Emission of Argon in the Visible Spectral Range. E. SCHULZ-GULDE, Westinghouse Research Laboratories.--The continuous emission of a cascade arc operated in argon at atmospheric pressure was investigated using side-on intensity measurements in the spectral range 3700 Å - 7000 Å. Agreement to within the accuracy of the measurement was found between the present experimental continuum data and Schlüter's¹ theoretical values. Recently published experimental results² for $\lambda \leq 4000$ Å and $\lambda \approx 6500$ Å were confirmed.

¹Schlüter, D., Z. Phys. 210, 80 (1968).

²Schnapauff, R., Z. Astrophys. 68, 431 (1968).

A3. Absorption Corrections for High Pressure Arcs,*
 H. N. OLSEN, Plasma Sciences Laboratories,--An iterative procedure is described for correcting measured integrated spectral intensities to true emission coefficients for absorbing plasmas. The method is applied to the argon arc plasmas operating at pressures of 0.5, 1.1 and 2 atm. The strong 4s-2p transition lines which are usually avoided because of their self-absorption have been treated in detail. The absorption correction is applied to total line intensity with no need for reflection optics or for detailed wavelength profile measurements. Griem's broadening parameters, used for constructing the line profiles, have been reduced by about 20% in order to obtain consistent results. The final judgement of the results is based on comparison of measured transition probabilities with theoretical values computed by Garstang. The serious discrepancies existing between published experimental transition probabilities cannot be explained solely on the basis of self-absorption.

*Work supported by USAF under Contract F33615-67-C1071.

A4. Development of a Stable Arc Source for Quantitative Spectroscopic Studies of Iron.* J.M. Bridges, NBS.--A wall-stabilized arc source has been developed for measuring f-values and line widths of Fe I and Fe II lines, possessing several improvements over arcs previously used for similar measurements. We operate a wall-stabilized arc at 25 A in a mixture of argon and FeCl₃. By flowing the argon through ovens containing heated FeCl₃, a suitable amount of FeCl₃ vapor is mixed with the argon and carried into the arc chamber. The FeCl₃ is prevented from depositing out by keeping the entire chamber at a temperature greater than 300°C. In order to keep the density of Fe atoms constant at a given point in the arc, we monitor the intensity of an Fe line emitted from the arc and use a feedback system to control the rate of gas flow into the chamber. The arc can be operated for more than an hour with the Fe density remaining constant to within about 5%; during several minutes, it may vary less than 1%. This permits the measurement of a large number of lines using photoelectric detectors.

*Research supported by the Advanced Research Projects Agency of the Department of Defense under the Strategic Technology Office.

A5. Investigation of High Pressure Arc Jet.
J. MEYER and R. BECK, UBC, Vancouver -- The plasma of an arc jet burning in several atmospheres of hydrogen has been investigated. By variation of pressure the densities of electrons and hydrogen atoms can be varied over an order of magnitude. This indicates that the discharge is suited for the investigation of spectral line broadening. Results are presented showing the broadening of a silicon line produced by interaction with hydrogen atoms.

SESSION B

Tuesday Morning, 28 October

10:45 a.m.

TRANSPORT AND THERMODYNAMIC
PROPERTIES AND LTE PANEL

Panel Chairman: *E. E. Soehngen*, Wright-Patterson AFB,
Ohio

B1. Total Radiation Source Strength of Argon Plasmas. P.W. Schreiber, A.M. Hunter, Aerospace Research Laboratories, and K.R. Benedetto, Systems Research Laboratories.-- A review of measured total radiative source strengths for argon at one atmosphere indicates that significant discrepancies exist among the results of several investigators. These discrepancies may be caused by: absorption of radiation in the plasma and other media; an unknown contribution to the radiative energy transport in the vacuum ultraviolet region of the spectrum, temperature measurement errors, plasma impurities, and assumptions required to reduce measured data to radiative source strength. In the present investigation, the total effective radiation source strength is determined by a new approach. A direct-current discharge one meter long, one inch in diameter and having developed laminar flow is used as a plasma source. The large diameter provides a constant temperature region concentric with a cross-section of the discharge. The energy loss on the discharge axis is due to the net radiative loss which is determined from the energy balance by measuring the power input on the axis with electric and magnetic probes. These data are compared with radiometer measurements which are significantly smaller than the internal measurements. This discrepancy is being investigated.

B2. Radiative and Transport Properties of SF₆ and Their Use in Model Arc Studies. J.J. LOWKE, R.W. LIEBERMANN and L.S. FROST, Westinghouse Research Laboratories--Equilibrium composition of SF₆ from 1000 to 45,000°K at 1 to 16 atm pressure have been calculated, and used to derive the corresponding transport properties and spectral absorptivities. Using these, the temperature profile for a 100 amp cascade arc is calculated and shown to be in good agreement with recent experimental measurements of Motschmann.¹ An estimate is made of central arc temperatures and electric field strengths as a function of current and arc radius using an isothermal approximation and results are given at pressures of 1 and 8 atmospheres for radii up to 2 cm and currents up to 60,000 amperes. A comparison of these results is made with data obtained from detailed temperature profile calculations for a radius of 0.25 cm at 8 atmospheres.

* H. Motschmann, Z. Phys. 214, 42 (1968).

83. Influence of Diffusion on the Behaviour of He-Arcs under Normal Pressure. J. UHLENBUSCH, 1. Phys. Inst. Techn. Hochschule Aachen. - Measurements of arc characteristics and temperature in cascaded arcs burning in He under normal pressure suggest strong deviations from LTE of the arc plasma.^{1,2} Here the non-LTE behaviour is studied theoretically by solving the rate equations, where collisions and radiation effects as well as diffusion processes are included. The energy balance completes the set of equations. As a result radial intensity distributions of some He I lines are given under various conditions. The calculated data are compared with experiments.

- ¹ H. W. Emmons, Phys. Fluids 10, 1125 (1967)
² E. Fischer, J. Hackmann, J. Uhlenbusch, 9. Int. Conf. on Ion. Phen. in Gases, Bucharest (1969)

84. Measurements of Electrical and Thermal Conductivity of Hydrogen, Nitrogen and Argon at High Temperatures.* J. C. Morris, R. P. Rudis and J. M. Yos, Avco, Wilmington, Mass. The electrical and thermal conductivities of hydrogen, nitrogen and argon have been measured up to 14000 °K for pressures between 0.5 and 2.0 atmospheres using a wall stabilized electric arc as a plasma source. Generally satisfactory agreement is noted between theory and experiment for the electrical conductivity. Equally good agreement is found for the thermal conductivity for nitrogen and argon when the energy transfer by vacuum ultraviolet radiation is included in the energy transport calculations. For hydrogen a difference between theory and experiment of as much as a factor of two is observed at the lower temperatures; this difference is dependent on arc current and may be the result of non-equilibrium effects.
 *Work supported in part by Aerospace Research Laboratories, Office of Aerospace Research of the U. S. Air Force, (Contract No. F33615-68-C-1081.), and National Aeronautics and Space Administration Research Division, Office of Advanced Research and Technology, (Contract No. NASW-1188.)

85. The Measurement of Plasma Transport Properties in a Free-Burning Electric Arc. * C.G. STOJANOFF, Riverside Res. Inst., New York. -- A free-burning arc with fluid convection into the arc column via the cathodic boundary of the arc is used for the determination of the plasma transport properties from measured arc parameters. The measurements include the arc electric gradient, the current density, the arc temperature field, the radiant power density and the flow velocity. Values of the DC electrical conductivity, thermal conductivity and the dynamic viscosity of 1 atm equilibrium argon plasma are calculated from these measurements in the temperature range from 8000°K to 15000°K. The arc parameters are measured spectroscopically and by means of direct immersion probes. The plasma transport coefficients are obtained as solutions of Ohm's law and the energy and momentum equations for the fully developed, cylindrically symmetric, laminar arc column. The measured transport coefficients are in good agreement with the theoretical data available in the literature. Although in outward appearance the arc is perfectly quiescent and reproducible there exist regimes of operating conditions for which the arc instabilities and the perturbation effects of the probes inhibit the accuracy of the measurements.

* Work supported by AFOSR and ARL-Wright-Patt. AFB

86. The Electrical Conductivity of Argon at High Pressures. UWE H. BAUDER, Aerospace Research Laboratories, and R. S. DEVOTO*, Stanford Univ., -- Computation of the electrical conductivity in argon at pressures to 100 atm have been carried out in conjunction with experiments performed in a 5 mm diameter cascade arc. The voltage/current characteristic at 50 atm and currents to 200A was obtained by measuring the potential distribution along the cascade channel. Temperature distributions were deduced from side-on observation of continuum radiation at 4000-4600Å and of the AI 4300 line where a self-consistency check showed that the plasma is optically thin. For higher arc currents, the temperature distributions are nearly flat over a major part of the arc cross section with center-line temperatures reaching 12000°K at 200A. The electrical conductivity up to 12000°K has been computed from the data and is compared with calculations based on four different models of the charged-particle interactions: cut-off Coulomb potential, shielded-Coulomb potential with inclusion of order unity terms or numerical evaluation of the cross sections, and inclusion of order unity terms using a collision form with dynamic shielding.

*Research supported by Aerospace Research Laboratories

Faint, illegible text at the top of the page, possibly bleed-through from the reverse side.

SESSION C

Tuesday Afternoon, 28 October

2:00 p.m.

ARC CHARACTERISTICS

Chairman: J. Uhlenbusch, I. Phys. Inst. Techn. Hochschule Aachen

Faint text below the chairman's name, likely a list of participants or topics for the session.

Faint text at the bottom of the page, possibly a footer or additional information.

C1. Effective Periphery of a High Pressure Arc.
 W.T.LORD, Rocket Propulsion Est. Westcott, England. --
 The question of the definition of the effective periphery of a high pressure electric arc is reviewed. In particular, the specification of the periphery as an isothermal of fixed temperature for a given gas at a given pressure is compared with that in which the peripheral temperature is determined by some special condition such as the principle of minimum field strength. Some evidence is given which demonstrates the utility of the former definition provided the fixed value of the peripheral temperature is determined empirically. This evidence is then used to provide a complete relationship between electric conductivity and heat flux potential for nitrogen at one atmosphere pressure. Finally, some comments are made on the boundary conditions which should be applied at an arc periphery of fixed temperature.

C2. High Pressure Arc Temperature and Radiative Energy Distributions.* C.H. MARSTON, G. FRIND, B.L. DAMSKY and A.M. SCHORN, General Electric Co.--
 An analytical model has been developed for computation of a high pressure electric arc. The steady-state, LTE model includes the effects of self-absorption by considering radiant interchange among a series of constant property annuli. Temperature profile, based on non-optically thin Abel inversion of continuum intensity measurements is a necessary input. Practically all vacuum ultra-violet radiation is shown to be reabsorbed within the arc column. An uncooled, quasi-steady (1-5ms) arc has been operated in air at 100 atm. sufficiently quiescent to measure a temperature profile at 100 amp., but great care had to be taken to start symmetrically and avoid disturbances. Temperature profiles were also determined for 250 amp. arcs in ablating Delrin $(COH_2)_n$ constrictors at 100 and 150 atm. Voltage gradient was constant along the axis (as high as 500 v/cm.) and pressure gradient was negligible, indicating that this type arc is uniform axially.

*Work supported in part by USAF Systems Command

C3. Analytic Model for Infinite Cylindrical High Pressure Arcs. D. M. Cap, General Electric, Lamp Division. An analytic model is used to examine the effects of joule heating, effective thermal conduction and optically thick and thin radiation upon the characteristics of high pressure arcs. A three-zone boundary matching problem is obtained by piece-wise linearization of the energy balance equation for an infinite cylindrical plasma column. Known argon material functions, the temperature dependence of the electrical conductivity, power radiated per unit volume, and heat transfer function are inserted into the model and yield arc characteristics in agreement with known argon cascade arc characteristics.

C4. Energy Dissipation Mechanisms in Intense Mercury-Vapor Arcs.* L.P. HARRIS, General Electric R&D Center, Schenectady--Measurements have been made of the volt-ampere characteristics of mercury-vapor arcs in long narrow channels (0.5 to 2 mm thickness or diameter) at pressures of several atmospheres and average current densities near 10^4 A/cm². These arcs exhibit positive incremental resistances and voltage gradients of 100-500 V/cm that depend mainly on average current density and very little on channel dimensions. A parallel analytical study has been conducted to determine the dominant dissipation mechanisms in these arcs. This study has indicated that the most likely candidate is thermal radiation by free electrons. A simple calculation assuming equilibrium ionization and dissipation by thermal radiation gives satisfactory agreement with experiment.

*Work supported in part by NASA Cont. NAS12-675

C5. The Influence of Ionization to Excitation Potential Ratio on Arc Temperature Profile of Metal Iodide Arcs.

JOHN F. WAYMOUTH, Sylvania Electric Products.--Numerical integration of the heat flux equation in a high pressure arc, $\nabla(\chi \nabla T) = -P_{\chi}$, has been carried out for a mixed metal vapor arc. In the absence of absorption of radiation, P_{χ} is equal to the difference between electrical power input per unit volume and radiation power loss per unit volume. The former varies in proportion to the electrical conductivity, as $\exp(-eV_i/2kT)$, while the latter varies as $\exp(-eV/kT)$, where V_i is ionization potential and V is average excitation potential. If $V_i \leq 2V$, P_{χ} remains positive for all values of T less than the axial value, and the temperature profile is wall stabilized. Conversely if $V_i > 2V$, P_{χ} reverses sign at lower temperatures, and bell-shaped, constricted, non-wall-stabilized temperature profiles result. The latter condition is frequently found in metal iodide arcs.

C6. The Effect of Absorption of Radiation on Arc Temperature Profiles of Metal Iodide Arcs. JOHN F.

WAYMOUTH, Sylvania Electric Products.--The effect of absorption of radiation was incorporated into the integration of the heat flux equation for a high pressure arc, $\nabla(\chi \nabla T) = -P_{\chi}$ by adding a term, $+\Gamma h\nu\alpha$, to the net production of heat, P_{χ} , where Γ is the photon flux, $h\nu$ the average photon energy, and α the absorption coefficient. The photon flux must then be calculated from a separate divergence equation. A method of successive approximations is used to solve these equations; the temperature profile is calculated first for zero photon flux, and the resulting profile used to calculate the photon flux, which is then used to calculate a new temperature profile. Convergence is ordinarily obtained after 20-30 approximations. The effect of absorption has thus far been studied assuming values of V_i and V leading to a constricted non-wall stabilized arc in the absence of absorption. Maximum broadening of the temperature profile is observed when the absorption length is approximately 10% of the arc tube diameter.

C7. Theoretical Analysis of the Behavior of Hg + TlI Arc Discharges with Variable Mercury Loadings. C.F. GALLO*, Westinghouse Research, Pittsburgh 35, Pa. — A theoretical analysis of the behavior of Hg + TlI arc discharges with variable Hg loadings is performed. In these arcs, the Hg pressure is greater than the TlI pressure by a factor ~ 500 . Even though the Tl 5350Å line does not terminate on the lowest ground state, it is shown that self-absorption is an important factor in the attenuation of the intensity of this line. With the assumption of local thermodynamic equilibrium, it is quantitatively shown that, as the Hg loading is doubled, the following effects occur: (1) The effective arc temperature decreases from 5,100°K to 4,800°K, (2) The effective radius increases by $\sim 10\%$, (3) The escape factor for the imprisoned Tl 5350Å line increases $\sim 40\%$ due to collisions with the increased number of Hg atoms, (4) The power radiated in the Tl 5350 Å line increases $\sim 10\%$, and (5) The power radiated in the Hg visible lines decreases $\sim 15\%$. These calculations are in agreement with the experimental observations of Larson. The experimental observations are reasonably consistent with the assumption of local thermodynamic equilibrium.

*Present Address: Xerox Research, Rochester, N.Y. 14603

C8. A Two Zone Model for Thermal Induction Plasmas.* H. U. ECKERT, The Aerospace Corp. -- Approximate solutions of the Elenbaas-Heller equation have been obtained for thermal induction plasmas with small radiation losses. The plasma column is divided into two zones. Most of the ohmic heat is generated in the external zone and balanced by conduction. The major portion is lost to the wall, the minor to the internal zone where it accounts for most of the radiation losses. Under these conditions the distribution of the heat conduction potential assumes a parabolic shape for the internal zone whereas it can be described by Bessel functions of the first and second kind in the external zone. Matching of the zonewise solutions yields temperature distributions which are continuous to the first derivative and display the characteristic minimum known from experiments. Application to an argon discharge at atmospheric pressure yields temperatures in agreement with experimental data.

C9. The Confined Electrodeless Arc.* D. R. KEEFER, University of Florida, and J. A. SPROUSE and F. C. LOPER, ARO, Inc.--An energy balance has been performed for a confined cylindrical arc column heated inductively by high-frequency fields. The analysis includes the convective energy transport due to a radial inflow in addition to the radiative and conductive energy transport usually considered. The resulting non-linear two-point boundary value problem was solved numerically and extensive calculations were performed for an argon arc operating at atmospheric pressure. The characteristic parameter, plasma radius to skin depth ratio, was found not to have a unique value. The plasma diameter is determined primarily by the diameter of the confining tube. Radial inflow can significantly reduce the conductive transport to the wall with a small reduction in plasma diameter. It was found that in excess of 60 percent of the input power could be removed by convection.

*The research reported in this paper was sponsored by Arnold Engineering Development Center, Air Force Systems Command, Arnold Air Force Station, Tennessee, under Contract No. F40600-69-C-0001, with ARO, Inc. Further reproduction is authorized to satisfy the needs of the U. S. Government.

C10. The Thermal Electrodeless Arc in Air.* DONALD D. HOLLISTER, Philco Corp.--The Flenbaas-Heller equation is enhanced by a radiation term and combined with the electromagnetic equations to form a set which is descriptive of the high frequency induced discharge and amenable to numerical integration. An existence condition, which is theoretically derived from considerations of the minimum entropy state of the discharge, is found necessary to un-mix boundary conditions and enable finding the unique solution for stated conditions of discharge pressure, and magnitude and frequency of the induction field. This solution is found by an iterative process. The results of several hundred such iterations are summarized and the properties of the electrodeless arc in air at pressures between one and one hundred atmospheres are predicted in order to indicate what appear to be important trends for this discharge. The fundamental importance of radiative transport is discussed in connection with the existence condition and with the choice of the radiation model employed in this study, and an appraisal is given of the limits of the present theory.

*Work supported by the United States Air Force.

SESSION D

Wednesday Morning, 29 October

9:00 a.m.

ARCS IN FLOW AND MAGNETIC FIELDS

Chairman: *H. Stine*, NASA, Moffett Field,
California

D1. Characteristics of a High Pressure Arc Confined in a Transpiration-Cooled Tube.* E. PFENDER and J. HEBERLEIN, Univ. of Minnesota.--The peak enthalpy attainable in a constricted electric high intensity arc is limited by the heat flux density which the wall is able to withstand. By employing porous transpiration-cooled constrictor tubes a large fraction of the heat flux to the wall may be intercepted by the radially-oriented gas flow through the porous wall. Therefore, higher power inputs per unit length of the arc and correspondingly higher axis temperatures should be feasible. Measured characteristics of various parameter combinations (field strength-current; field strength-mass flow rate; wall heat flux-mass flow rate; inside wall temperature-mass flow rate) using porous ceramics and porous tungsten constrictor tubes with argon at atmospheric pressure as working fluid indicate that a comparison with corresponding theoretical predictions based on solutions of the conservation equations is of limited validity only. The same is true for temperature profiles determined spectrometrically or by means of enthalpy probes. The reason for the ensuing poor agreement between theory and experiment over a rather wide parameter range is mainly attributed to the existence of turbulent flow components.
*Research supported by ARL Contract F33-615-67-C-1353.

D2. Boundary Layer Analysis of an SF₆ Circuit Breaker Arc. B. W. SWANSON and R. M. ROIDT., Westinghouse Research Laboratories.--The energy equation for an arc in a gas flow has been integrated, using boundary layer concepts, to obtain a partial differential equation for the dynamic arc radius. Starting from an arc radius at peak current, the dynamic arc equation is solved for a linear current ramp to obtain the arc radius at current zero. For both convection-controlled and radiation-diffusion-controlled arcs, the arc radius at current zero can be expressed as the product of the peak current arc radius and heat transfer attenuation factors. Numerical examples indicate that convection, augmented by radiation and diffusion, can produce constricted arc columns at current zero. Arc constriction is important for current interruption in gas blast circuit breakers, because it permits radial diffusion to play a key role in the post-arc energy transient. Finally it is shown that the partial differential equation for the dynamic arc radius can be integrated to obtain a "Cassie" type equation for arc resistance which applies to the pre-zero arcing period.

D3. Arcs in Turbulent Flows.* G. FRIND and B. L. DAMSKY, General Electric Co.--Heat, mass and momentum transfer were experimentally investigated in very long, cylindrical axial flow arcs in laminar and turbulent flow and with special interest in the fully developed flow section of such plasmas. Strong evidence is presented for the existence of turbulence by the fact that all three transfer mechanisms are considerably accelerated in what we consider the "turbulent mode," also by direct optical studies of the three dimensional structure of such arcs by high speed photography and a light probe. The onset of turbulence is found with all our methods to occur around 1.5 grams/sec. gas flow rate. A considerable number of measurements of heat and momentum transfer are reported upon, covering the laminar and the turbulent mode, in the following ranges: Gases: Argon and Nitrogen; Tube Diameters: 0.5 to 1.0 cm; Tube Lengths up to 100 cm; Mass Flow Rates: 0.1 to 15 gram/sec; Ambient Pressures: 1-20 atm.; Currents: 25-200 amps. (some higher).

* Work support by USAF Aerospace Res. Lab.

D4. Three-Dimensional Temperature Distribution within a Steady-State Cross-Flow Arc.* D.M. BENENSON, A.A. CENKNER, JR., and A.J. BAKER, St. Univ. of N.Y. at Buffalo.--Using a unique optical system¹, temperature distributions have been obtained through the column of an Argon cross-flow plasma, to within about 3mm of electrodes spaced 11.2mm apart vertically (operating conditions: cross-flow velocity = 65.7cm/sec, arc current = 60.3 amperes, arc voltage = 15.0 volts, pressure = 1.1 atmospheres). Plasma cross-section was non-circular throughout the column length, with major axis in the flow direction. Highest maximum temperatures within a given horizontal cross-section were nearest the electrodes (cathode about 10,920K, anode about 10,665K), lowest near mid-height between electrodes (about 10,400K). Largest characteristic axial dimension was near mid-height (8.85mm), smallest near the electrodes (cathode about 5.45mm, anode about 6.58mm). In profile, isotherm distributions along the mirror plane of symmetry indicated presence of both the double vortex and jet flow modes.²

* Work supported by National Science Found. Grant GK-1174.

¹ D.M. Benenson, A.J. Baker, and A.A. Cenknner, Jr., IEEE Trans. on Power Appar. and Syst., PAS-88, 513 (1969).

² H.O. Schrade, Aero. Res. Labs., ARL 67-0119 (1967).

D5. Some Experimental Findings for an Arc in a Swirl Flow* H. MUNTENBRUCH, The Ohio State University Research Foundation, S.F. GIANNOTTA and H.O. SCHRADE, Aerospace Research Laboratories.--An experimental study of an electric arc subjected to a gaseous swirl with and without an applied axial magnetic field was conducted. An argon or nitrogen arc was drawn between colinear tungsten electrodes along the axis of a water-cooled, cylindrical copper chamber positioned within the core of the field coils. Gas inlet/outlet was achieved through 2 peripheral slits extending over the entire 20" tube length; both the arc position and length were variable during operation. Arc characteristics were determined for the following ranges of parameters: $0 \leq B \leq 2 \text{ KG}$; $105 \leq \text{steady } I \leq 900 \text{ A}$; $1/4" \leq \text{gap length} \leq 16"$ and $.08 < \dot{m} (\text{lbs/sec}) < .25$. Most tests were conducted without magnetic field; all runs were performed using the swirl flow. Measurements show a linear relationship between voltage and gap length for gaps greater than 2"; the voltage gradients found in the fully-developed column were consistently lower than 1 V/cm. With $B \neq 0$, electrode effects and other anomalies produce certain arc instabilities.

*This work was conducted at the Thermomechanics Research Laboratory, Aerospace Research Laboratories, WPAFB, Ohio.

D6. Experimental Results on the Shape and Motion of a D.C. Arc in an External Magnetic Field. R. F. NEUBAUER, DFVLR Braunschweig.--The shape and the motion of a D.C. arc burning between two coaxial cylindrical electrodes at atmospheric pressure in an external magnetic field are investigated. Pictures are taken with the aid of a rotating mirror camera. To get further information on the light emitted by the arc, the time-dependent intensity of spectral lines and continuum radiation is recorded by photo-multiplier and an oscillograph. If the inner-electrode is used as anode (polarity A), these results differ widely from those obtained when using the inner-electrode as cathode (polarity B). The shape and the motion of the arc are analyzed in both cases. Having polarity A, the arc rotates in the gap. Besides the arc column there is a strong luminosity at the outer-electrode (cathode) which looks like a "Foot" and follows the arc column. The time-dependent signals obtained by short-time spectroscopy give further details about the luminosity. Using polarity B an arc column can be detected only at low arc currents.

D7. Investigations on a Stationary Magnetically Stabilized Helium Arc. K. BERGSTEDT, P. GRASSMANN, O. KLUEBER, H. WULFF, Institut für Plasmaphysik - EURATOM, Garching, Germany. -- A stationary helium arc plasma in a constant magnetic field up to 80 kG was investigated. The axial temperatures are several 10^5 °K, and the electron density is $\sim 1.5 \times 10^{16}$ cm⁻³. Three important results emerge: (1) There are azimuthal diamagnetic currents perpendicular to the longitudinal magnetic field and the radial temperature gradient (Nernst effect). Interaction of these currents with the magnetic field causes a large radial pressure gradient, while the pinch effect is comparatively small. (2) The potential distribution in the plasma is such that the axial current is confined almost entirely to the magnetic flux tube enveloping the electrodes, although plasma of high electrical conductivity also exists outside. This high current concentration produces very effective heating near the axis. (3) Owing to the diffusion currents of the ion species parallel to the temperature and partial density gradients of the ions, the degree of ionization in such plasmas is determined by the continuity equations of the ion species and not by an expression for homogeneous plasmas, e.g. Saha equation.

SESSION E

Wednesday Afternoon, 29 October

2:00 p.m.

TIME VARYING ARCS

Chairman: *R. L. Phillips*, University of Michigan
Ann Arbor, Michigan

E1. A Method of Obtaining High Plasma Temperatures Using Pulsed Constricted Arcs* J. C. Morris and R. U. Morris, Avco, Wilmington, Mass. A simple method of pulsing constricted electric arcs to high power inputs is described. Using this method, peak power inputs of some six times greater than can be run continuously have been achieved. An analysis of this method has been made for argon to determine the maximum temperature to be expected as a function of arc channel diameter and generator construction material. In addition, the results of a number of methods used for electric and spectroscopic diagnostic studies of the arc column are discussed.

*Work supported by Aerospace Research Laboratories, Office of Aerospace Research of the U. S. Air Force, (Contract No. F33615-68-C-1081.)

E2. Response Characteristics of Pulsed Cesium Vapor Arcs.* R.D.BUHLER and W.F.HUG, EOS-XEROX.--Pulsed cesium vapor arcs in a cylindrical sapphire envelope have been investigated over a range of vapor pressures up to ~ 5 atm peak, pulse energies up to ~ 20 J/cm of arc, and peak pulse power levels up to ~ 200 kW/cm. Time and spectrally resolved radiation output measurements (in $\sim 1/2\mu$ bands from $\sim .35\mu$ to 5.0μ) as well as electrical characteristics were obtained. A simple theoretical model describing the non-steady thermal characteristics of the arc plasma has been formulated and used to correlate the experimental data. Over the range of operating conditions investigated the instantaneous conductance and total radiant output correlated adequately with the volume averaged instantaneous internal energy of the arc plasma which can be closely estimated from an energy balance. The energy integral approach presented should be applicable to the dynamic analysis of many other pulsed or ac arcs.

*Work supported by U.S. Naval Air Systems Command

E3. Investigation of the Dielectric Recovery of High Current Air Gaps.* J. F. PERKINS, Westinghouse Research Laboratories and A. B. PARKER, University of Liverpool.-- Measurements of dielectric recovery in air at 1 atmosphere following a critically damped 190 kA spark discharge of 100 μ s duration have been made. By using measurements of gas temperature, Paschen's law and a knowledge of the general gas law, recovery characteristics have been derived on the assumption that the sole mechanism operative in the post-spark channel is the reduction in gas density. It is shown in this paper that detailed discrepancies between measured and derived curves may be explained by variations in the values of the Townsend primary (α) and secondary (γ) ionization coefficients, and of the attachment coefficient (a). It is concluded that an increase in the secondary ionization coefficient is the most important mechanism in the early recovery period, and that at later recovery times when γ has decreased to its pre-discharge value, an overall increase in electron attachment due to the formation of impurity products is the predominant mechanism.

*Work supported in part by the U.K. Science Research Council.

Faded text at the top of the page, likely bleed-through from the reverse side.

SESSION F

Wednesday Afternoon, 29 October

2:50 p.m.

ELECTRODE EFFECTS

Faded text block, likely bleed-through from the reverse side, containing technical details.

**Chairman: T. H. Lee, General Electric Company, 100
Broad Street, Philadelphia, Pennsylvania**

Faded text block, likely bleed-through from the reverse side.

Faded text block, likely bleed-through from the reverse side.

F1. In Situ Measurement of Thermionic Current in an Argon Arc with a Tungsten Cathode.* M.M. CHEN, R. THORNE and E.F. WYNER. Mason Lab, Yale University.--The contribution of thermionic emission to the total cathode current is measured by observing the decay of arc current as the discharge is extinguished. This is accomplished by suddenly reducing the arc voltage with a constant voltage shunt, thus curtailing the production of ions, excited atoms, and photons in the vicinity of the cathode. The subsequent decay of the ion current, the secondary and photo-emission, and effects associated with the ion space charge field take place within 10^{-5} sec and can be easily separated from thermionic emission. The latter, unaided by Schottky effect, persists to 10^{-2} sec without significant decay, if care is taken to prevent electron space charge limit. The observed thermionic current is about 30% of the total current for a rod shaped cathode of 1.6mm. diam operating in the diffuse mode at 3-8A in argon at 0.5atm. These observations are used as a basis to infer other current components and establish an upper bound for the ion current, which is found to be less than estimates based on the energy considerations.

*Research support by NASA, Grant NGR 07-004-015

F2. Spectroscopic Study of a Tungsten Arc Cathode.* E.F. WYNER and M.M. CHEN. Mason Lab, Yale University.--Spectroscopic measurements have been made on the gas close to a tungsten arc cathode operating in a diffuse mode at $65\text{A}/\text{cm}^2$ and 3100°K in argon. With a gas pressure of 250 Torr, the density of atoms in the $5p_{10}$ (14.3V) and $4p_5$ (13.17V) states and the density of ions were obtained from total line intensities and from the broadening of the 6032\AA Al line respectively. These results show equilibrium with a maximum excitation temperature of 9200°K . By means of a diffusion calculation, the ion current at the cathode is predicted to be $7 \pm 3\text{A}/\text{cm}^2$. The low excited atom densities found indicate that they do not play a major role in the heating and emission from the cathode. Using the method of Chen et al¹ the thermionic emission current was found to be $15 \pm 5\text{A}/\text{cm}^2$. Schottky correction increases this current another 50%. Nonetheless there is still a large unexplained component of electron emission from the cathode.

*Research support by NASA, Grant NGR 07-004-015.

¹M.M. Chen, R. Thorne and E.F. Wyner; this meeting.

F3. Electrode Erosion in High-Current Electric Arcs.* K. T. SHIH, Convair division of General Dynamics, San Diego.--Experiments were conducted to simulate a magnetically driven arc using a high-current pulse. Situated in a uniform magnetic field, this current drives an arc in a single pass across a test sample. High-speed photographs indicate that electrode erosion due to the moving arc occurs mainly in the form of craters. These are generated by the constricted arc attachment, which is stationary for time intervals from 1 to 20 μ sec. In a test facility built to duplicate this stationary arc attachment, a variable-pulse-length arc discharge is generated on an anode test plate and maximum local value of the heat flux density is determined by measuring the time from striking an arc to the onset of surface melting. The anode heat flux density is found to be between 10^4 to 10^6 w/cm² for arc current of 50 to 2,000 amp. Heat flux density increases with increasing arc current and gas pressure and is higher in nitrogen than in argon. The initial anode surface temperature also has a strong effect on the anode attachment spot.

*Work supported by Office of Aerospace Research,
Contract No. F33615-67-C-1386.

F4. A Theory of the Cathode Spot.* D. MITROVICH, Harvard Univ. - Opposing electron flows through the cathode spot, both thermionic in nature, provide the basis for a model of the cathode region of a high pressure, D.C. arc. The difference between the ordinary thermionic electron flow from the cathode, and the thermionic back-flow from the plasma (the cathode potential drop acts as the work function) accounts for the arc current. These flows are the only significant means of energy transfer through the cathode spot. Within the plasma and cathode volumes energy transfer is assumed to be by thermal conduction. The nature of Richardson's equation closely restricts the cathode spot surface temperature, and essentially determines the thermal plasma-cathode system. Approximate solutions for an argon plasma and a tungsten cathode give cathode spot radii proportional to the arc current (0.43mm per 100 amps) and cathode drops of a few volts. Steady state stability is affected by three mechanisms: the cathode drop dipole layer, the coupled thermal-electrostatic system, and the arc circuit. Calculations show the first two are stable. The third mechanism appears to give the arc system stability properties qualitatively consistent with those observed experimentally.

* Work supported by the National Science Foundation.

F5. Recent Developments on the Longini Model of the Cathodic Spot. M.F. HOYAUX, Univ. of Pittsburgh.--The substance of some recent estimates relevant to the Longini model of the cathodic spot¹ is presented. The basic assumption is made that a cathodic spot is a location where a coupling exists between the departure of electrons by a modified form of field emission¹ and that of a lesser number of positive ions. The latter, doomed in their majority at being neutralized almost immediately, are released as a result of the weakening of cohesion bonds carried by the depletion of electrons. It is postulated that above a certain critical current density, of the order of 10^{12} A/m² or greater, the two help each other and a stable situation results. This stability, however, does not exclude that the phenomenon is actually made of bursts. The rate at which reticular planes are "peeled off" is approximately one per microsecond and corresponds to the frequency of luminous fluctuations observed by Ludwig.² The corresponding rate of erosion is in agreement with the lowest rate per coulomb observed experimentally.³

¹R.L. Longini, private communication, 1967. For a basic description of the model, see M.F. Hoyaux, Arc Physics, New York, Springer-Verlag, 1968, p. 190.

²H.C. Ludwig, private communication, 1968.

³R. Holm. J. Appl. Phys. 20, 7 (1949).

ABSTRACTS

TWENTY-SECOND ANNUAL
GASEOUS ELECTRONICS CONFERENCE

29-31 OCTOBER
1969

RIVERSIDE MOTEL
GATLINBURG, TENNESSEE

SESSION G

Wednesday Morning, 29 October

9:00 a.m.

ELECTRON COLLISIONS PANEL

Panel Chairman: *W. R. Garrett*, Oak Ridge National Laboratory
Oak Ridge, Tennessee

G1. Relative Cross Section Measurements for Electron Scattering by Atomic Nitrogen (0.2-3 eV).* T.M. MILLER, B.B. AUBREY, P.N. EISNER, and B. BEDERSON, New York University. -- Relative measurements have been made of the total cross section for electron scattering by atomic nitrogen, over the energy range of 0.2 to 3 eV, using the atom beam recoil technique. A prime motivation for the experiment was provided by the close-coupling calculation of Henry, Burke, and Sinfailam,¹ which gave a shape resonance in the e-N scattering cross section at low energy. The experiment to be reported implies that the peak of this resonance occurs at an energy below 0.5 eV and has a height roughly that predicted in Ref. 1. However, we have not as of this writing observed the decrease below the maximum on the low-energy side. Questions such as the beam dissociation, angular and energy resolution, presence of atomic metastable states, determination of the beam velocity distribution, systematic error checks, and absolute cross sections, will be discussed.

* Work supported by ARPA through ONR, Washington, ARO-Durham and NSF.

1. R.J.W. Henry, P.G. Burke, and A.-L. Sinfailam, *Phys. Rev.* 178, 218 (1969).

G2. Angular Distribution of Protons Produced by Dissociative Ionization of H₂ near Threshold.* R. J. VAN BRUNT and L. J. KIEFFER[†], University of Colorado and Joint Institute for Laboratory Astrophysics. -- From observations of the velocity distribution of protons at corresponding forward and backward angles with respect to the electron beam direction the momentum imparted to the dissociating H₂ molecule by the incident electron has been determined for electron energies up to 300 eV. At threshold the measured angular distribution of energetic protons when corrected to the center-of-mass system is symmetric about $\theta=90^\circ$ and the resulting anisotropic component deviates from a $\cos^2\theta$ dependence in a manner suggested by Zare.¹ The forward-backward asymmetry in the angular distribution observed by Dunn and Kieffer² at electron energies considerably above threshold is explained by including the effect of molecular recoil.

*Work supported in part by the Advanced Research Projects Agency.

[†]Staff member, Laboratory Astrophysics Division, National Bureau of Standards.

¹R. N. Zare, *J. Chem. Phys.* 47, 204 (1967).

²G. H. Dunn and L. J. Kieffer, *Phys. Rev.* 132, 2109 (1963).

G3. Cross Section Measurement for Dissociative Recombination of Electrons and D_2^+ .* MARTIN K. VOGLER and GORDON H. DUNN†, Joint Institute for Laboratory Astrophysics.--The cross section for dissociative capture of electrons by D_2^+ (dissociative recombination) has been measured using crossed beams of the reactant particles. The process was detected by observing Lyman alpha radiation from the resultant excited D atom. Electron energies between 1 eV and 7 eV were used, and the capture is thought to occur to repulsive states (resonances) of D_2 observed previously.¹ Calibration for absolute measurements of La flux is achieved by three different methods to be discussed. A cross section of $1.0 \pm 0.4 \times 10^{-17} \text{ cm}^2$ is obtained for the process at an electron energy of 6 eV.

*Work supported in part by the Controlled Thermonuclear Branch of the U. S. Atomic Energy Commission.

†Staff member, Laboratory Astrophysics Division, National Bureau of Standards.

¹E. R. Williams, J. V. Martinez, and G. H. Dunn, Bull. Am. Phys. Soc. 12, 233 (1967); Keith M. Burrows and Gordon H. Dunn, Bull. Am. Phys. Soc. 13, 215 (1968).

G4. Direct Excitation of Molecular Vibrations by Slow Electron Impact. E. v. PUTTKAMER, Institut für Physik.--Excitation functions of CO and H_2 into the first vibrational state $v=1$ show an excitation of the molecules outside the region of the 1.83 eV resonance in CO and the 3.5 eV shape resonance in H_2 respectively. Angular distribution measurements confirm, that in the region below 1 eV in CO and at about 11 eV in H_2 more than one partial wave contribute to the cross section. In CO the angular distribution is indicative for dipole excitation. In H_2 this excitation is comparable in magnitude to the resonant excitation via the resonant states around 11 eV. Similar measurements on CO_2 for low impact energies are discussed.

G5. Calculation of Cross-Sections for Inelastic Electron-Atom Collisions.* H. H. MICHELS, United Aircraft Res. Labs., and F. E. HARRIS, Univ. of Utah--The inelastic scattering of electrons from an atom is being studied using analytical expansions for representing the scattered electron. The stationary-state wavefunction is written as $\psi = \sum a_i \phi_i + \sum b_i \eta_i$ where the ϕ_i are the complete set of asymptotic eigenfunctions appropriate to the number of open channels and the η_i are short-range functions useful for approximating ψ within the range of the Hamiltonian. By application of a minimum-norm criterion, we have been able to develop a non-arbitrary method for identifying optimum-expansion approximations for both elastic and inelastic scattering processes. The method can be applied for any incident energy, including values at resonances resulting from stable or metastable negative ion states. This procedure has been tested both on a two-channel model problem and on studies of the excitation cross-sections for the scattering of electrons from a hydrogen atom.

*Work supported in part by the A.F. Office of Sci. Res.

G6. Outer Shell Ionization of Argon by Electron Impact; Angular Distributions in a Central Potential Model. STEVEN T. MANSON, Georgia State College -- Using a Hartree-Slater Central Potential appropriate to the ground state of Argon as tabulated by Herman and Skillman¹ Born approximation calculations have been carried out on the angular distribution of incident electrons which ionize the outer (3p) shell of Argon. We have considered ionized electron energies from 2 to 6 Rydbergs. We find that the angular distribution (and a related quantity, the generalized oscillator strength) has a single maximum for the lowest energy loss considered, but two maxima for higher energy losses. This is shown to be due to the vanishing of the transition matrix element in the 3p \rightarrow ed channel which also shows up as a minimum in the photo-ionization cross section of Argon.² The effect is large enough so that it should certainly be detected in an energy loss-angular distribution experiment.

1F. Herman and S. Skillman, Atomic Structure Calculations (Prentice-Hall, Inc., Englewood Cliffs, N.J., 1963)
 2S. Manson and J. Cooper, Phys. Rev. **165**, 126 (1968)

G7. Electron Scattering by Polar Molecules.* W. R. GARRETT and V. E. ANDERSON, Oak Ridge National Laboratory. -- Elastic and inelastic scattering of slow electrons by polar molecules are investigated through close coupling calculations. The general formalism of Arthurs and Dalgarno is utilized with a model interaction potential chosen to approximate that of a polar molecule. The potential function is expressed in a series of multipole components: dipole, quadrupole, and induced dipole. The relative importance on the scattering cross sections of each of the components of the total interaction has been studied for a range of dipole moments, D , from $D = 0$ to $D = 1$ atomic unit, and for incident electron energies from thermal to 1 eV. In the elastic channel results are particularly sensitive to the representation of the interaction potential.

* Research sponsored by the U.S. Atomic Energy Comm. under contract with Union Carbide Corporation.

G8. Variational Principle for Scattering.* K. J. Miller, Rensselaer Polytechnic Institute. -- A Variational Principle possessing a minimum, i.e. $I = \int (\mathcal{L}G)^* (\mathcal{L}G) dr \geq 0$, is being studied to calculate phase shifts. $\mathcal{L} = H - E$, where H may be either the effective one-electron or the total Hamiltonian operator for the scattering problem. The positive definite character of I eliminates the occurrence of false resonances which appear in the Kohn and Hulthén procedures. Bounds on the phase shift related to \sqrt{I} as well as to $\int |\mathcal{L}G| dr$ have been derived in order to estimate the accuracy of the calculation. Applications to elastic scattering off the static field of hydrogen will be discussed. The stationary state wave function used for s wave scattering off H is $G = \sum C_n r^n \exp(-\alpha r) + \sin(kr) + \tan \eta (1 - e^{-\alpha r}) \cos(kr)$.

* Work supported by the Petroleum Research Foundation.

11. Pressure and Electron Density Dependence of the Electron-Ion Recombination Coefficient in Helium

J. BERLANDE, M. CHERET, R. DELOCHE, A. GONFALONE and C. MANUS, Commissariat à l'Energie

Atomique - Saclay -- The recombination of He_2^+ ions and electrons has been studied in helium afterglow plasmas where electron and gas temperature are equal to 300°K, gas pressure ranges from 10 to 100 Torr and electron density from 10^9 to $5 \times 10^{11} \text{ cm}^{-3}$. The electron density decay, measured by microwave interferometry, is compared with computer solutions of a continuity equation for electrons which takes into account ambipolar diffusion and recombination effects. It is found that the recombination coefficient α is dependent on the gas density n_{He} and the electron density n_e and may be written as $\alpha_2 + k_e n_e + k_{\text{He}} n_{\text{He}}$ with $\alpha_2 \approx 5 \times 10^{-10} \text{ cm}^3 \text{ s}^{-1}$, $k_e = (2 \pm 0.7) \times 10^{-20} \text{ cm}^6 \text{ s}^{-1}$ and $k_{\text{He}} = (2 \pm 0.5) \times 10^{-27} \text{ cm}^6 \text{ s}^{-1}$. These values compare satisfactorily with results of theoretical computations¹ for a collisional-radiative recombination mechanism including both collisions with electrons and neutrals.

¹R. DELOCHE C.R. Acad. Sc. Paris 266B, 664 (1968)

12. Electron-Ion Recombination in Helium at 77°K.*

J. B. GERARDO and M. A. GUSINOW, Sandia Laboratories.--

The net decay of free electrons in an afterglow helium plasma with 77°K neutral and ion constituents is mainly controlled by the relative concentrations of He_2^+ , He_3^+ , the density of metastable atoms, and the temperature of the free electrons. All other electron loss processes can be made negligible by judicious selection of conditions. In a mass analyzed afterglow helium plasma with 77°K ions and neutrals, the recombination coefficient of He_2^+ was measured to be $(2.13 \pm 1.50) 10^{-6} (77/T_e)^{0.92 \pm 0.1} \text{ cm}^3 \text{ sec}^{-1}$ when the ratio of the densities $[\text{He}_3^+]/[\text{He}_2^+]$ was much less than unity. The net recombination coefficient increased with increased relative concentration of He_3^+ ions to a value $> 8 \times 10^{-6} \text{ cm}^3 \text{ sec}^{-1}$ when $[\text{He}_3^+]/[\text{He}_2^+] > 1$. At the present time we have not determined whether this value is indicative of recombination of He_3^+ or whether the larger value is accountable to preferential production (via He_3^+) of He_2^+ in a particular excited state which has an unusually large cross section for recombination.

* This work was supported by the U.S. Atomic Energy Commission.

13. The Dissociative Recombination of O_2^+ Ions into Specifically Identified Final Atomic States.* E. C. ZIPF, University of Pittsburgh.--Simultaneous measurements of the positive ion concentration, the average electron density, and the density of oxygen atoms in the metastable 1S and 1D states in the afterglow of a microwave discharge in oxygen-rare gas mixtures were used to study the dissociative recombination of O_2^+ ions into specifically identified final atomic states. The absolute microwave and optical measurements were corrected for time-dependent, spatial distribution effects by numerically solving the coupled, three dimensional, non-linear partial differential equations that govern the behavior of the charged particles and metastable atoms in the afterglow and using these results in the analysis. The total O_2^+ dissociative recombination coefficient had a value of 2.1×10^{-7} cm³/sec at 300°K while the branching ratio for the production of 3P , 1D , and 1S oxygen atoms was found to be 1.00: 0.90: 0.10, respectively. These results do not include cascading effects. The equivalent specific recombination coefficients are $\alpha(^3P) = 2.1 \times 10^{-7}$ cm³/sec, $\alpha(^1D) = 1.9 \times 10^{-7}$ cm³/sec, and $\alpha(^1S) = 2.1 \times 10^{-8}$ cm³/sec.

*Work supported, in part, by NASA

14. Measurement of the Rate Coefficient for the Recombination of He^+ with Electrons in a High Pressure Afterglow.* W.E.WELLS, and C.B.COLLINS, U. of Texas at Dallas.--An improved spectrometric system with a high sensitivity-resolution product has been used to measure the time-dependent, net rate of production of neutral helium atoms resulting from the recombination of He^+ with electrons in a pulsed helium afterglow at a neutral pressure of 44.6 Torr. The recombination rate coefficient of He^+ as a function of afterglow time has been obtained by dividing the data by the product of the electron and helium atomic ion densities, as determined absolutely from the intensity of radiation from levels in Saha equilibrium with the free electrons. Simultaneous measurement of the free electron density with a 35Gc microwave interferometer has given the rate coefficient as a continuous function of electron density without the need of a priori assumptions about the particular functional form. Results of such measurements at electron densities varying from 10^{12} to 10^{11} cm⁻³ have been found to be in reasonable agreement with theory.¹

*Work supported in part by NSF under Grant #GA-1551 and in part by NASA under Grant #NGL44-004-001.
1C.B. Collins, Phys. Rev. 177, 254 (1969).

15. Afterglows in Air. ROBERT C. GUNTON, Lockheed Palo Alto Research Laboratory.--Air at pressures near 1 torr was ionized by short (20 μ sec) microwave pulses. Electron density in the afterglow was monitored by cavity frequency shift and a wall probe. Ion density and composition were measured with probe and mass spectrometer. Electrons become unobservable following early removal dominated by electron-ion recombination and later removal by diffusion and attachment. The dominant early positive ion O_2^+ is converted by unknown processes to NO_2^+ and a small amount of NO^+ . The dominant negative ion is NO_2^- , observed mostly after electron disappearance. Afterglows were analyzed with a model having only one positive and one negative ion and including electron-ion recombination, ion-ion neutralization, attachment, and diffusion with space charge field terms. A computer program was developed using a 2-dimensional Crank-Nicholson alternating direction iterative scheme for integration. Results indicate that the electron-ion recombination coefficient is $2-3 \times 10^{-7} \text{ cm}^3 \text{ sec}^{-1}$, attachment frequencies are $400-500 \text{ sec}^{-1}$, and the ion-ion ambipolar diffusion coefficient D_p is about $65 \text{ cm}^2 \text{ torr sec}^{-1}$.

SESSION J

Wednesday Afternoon, 29 October

2:00 p.m.

NEGATIVE IONS

Chairman: *R. N. Compton*, Oak Ridge National Laboratory
Oak Ridge, Tennessee

J1. Charge Transfer from Negative Halogen Ions to NO₂. * S. J. NALLEY,† J. A. D. STOCKDALE, and R. N. COMPTON, Oak Ridge National Laboratory. -- Charge transfer to NO₂ was investigated in the manner described previously,¹ using the following ions from the indicated parents: I⁻/HI, I⁻/I₂, I⁻/C₆H₅I, Cl⁻/HCl, (Cl⁻ or Cl₂⁻)/CCl₄. NO₂⁻ was observed in each case. However, where CCl₄ was used, the simultaneous presence of Cl⁻ and Cl₂⁻ ions in the charge transfer region prevented precise interpretation. No evidence was obtained for the production of NO₂⁻ through three-body collisions, $e + \text{NO}_2 + \text{X} \rightarrow \text{NO}_2^- + \text{X}^*$, with X being C₂H₄, N₂, or He. Charge transfer cross sections were observed to increase rapidly with decreasing ion velocity.

* Research sponsored by the U.S. Atomic Energy Commission under contract with Union Carbide Corp.

† Radiological Health Physics Fellow.

¹J.A.D. Stockdale, R.N. Compton, and P.W. Reinhardt, Phys. Rev. Letters **21**, 664 (1968).

J2. Spurious Dissociative Attachment Peaks from Inelastic Energy Loss Reactions. * P.J. CHANTRY, Westinghouse Research Laboratories--Peaks in the electron energy dependence of negative ion production are usually the direct result of reactions of the type $e + \text{XY} \rightarrow \text{XY}^{*-} \rightarrow \text{X}^- + \text{Y}$ (1); each such peak being related to a particular XY^{-*} intermediate state whose energy in the Franck Condon region it approximately defines. The peak from reaction (1) may however be accompanied by a second peak at a higher electron energy at which the reaction $e + \text{XY} \rightarrow \text{XY}^{*-} + e'$ (2) leaves the electron e' with the appropriate energy for (1) to occur. The position of this second peak clearly does not correspond to a state XY^{-*}. Rather its separation from the first peak defines the energy lost via (2). An example of the above mechanism has been studied in O₂, where reaction (2) corresponds to excitation to the B ³Σ_u⁻ dissociation continuum and causes a peak in O⁻ production at 15 eV having a quadratic dependence on O₂ pressure. Previously reported¹ peaks in O⁻ production from N₂O, at 8.8 and 13 eV, are also found to be quadratically dependent on pressure, and are ascribed to the same general mechanism.

*This work was supported in part by ARPA through the ONR. ¹D. Rapp and D.D. Briglia, J. Chem. Phys. **43**, 1480 (1965); J.F. Paulson, Advances in Chem. Ser. **58**, 28 (1966).

J3. Temperature Dependence of SF₆⁻, SF₅⁻, and F⁻ Production from SF₆.* C.L. CHEN and P.J. CHANTRY, Westinghouse Research Laboratories--The attachment of low energy (0 - 1 eV) electrons to SF₆ has been studied as a function of gas temperature (300° - 1200°K) using a monoenergetic electron beam and mass analysis. At room temperature SF₅⁻ exhibits a previously unreported sharp peak coincident in energy with the predominant SF₆⁻ peak, i.e. at essentially zero energy. Increasing the gas temperature causes a rapid increase in this SF₅⁻ peak, while the SF₆⁻ signal decreases. Above 500°K the SF₅⁻ signal at zero electron energy exceeds the SF₆⁻ signal. The results of Hickam and Berg¹ are qualitatively consistent with the present work. Production of F⁻ at zero energy, observed at nominally room temperature by Curran,² was undetectable below 600°K in the present work, but increased rapidly with temperature. In contrast to the strong temperature dependence of the ions produced at zero energy the broader peak in SF₅⁻ production at 0.38 eV is found to be essentially independent of gas temperature.

*This work was supported in part by ARPA through the ONR. LW.M. Hickam and D. Berg, J. Chem. Phys. 29, 517 (1958).
2R.K. Curran, J. Chem. Phys. 34, 1069 (1961).

J4. Attachment of Electrons to SF₆, Ion Chemistry of SF₆ and Cluster Ion Formation from Alkali Metal Ions, F.C. FEHSENFELD, ESSA Research Laboratories. The attachment rate coefficient of electrons to SF₆ has been measured at 293°K and 530°K in the flowing afterglow. At both temperatures this attachment has a measured rate coefficient of 2.7×10^{-7} cm³/sec. At 293°K the dominant ion produced by the attachment is SF₆⁻ with the production of SF₅⁻ by dissociative attachment accounting for less than one part in 10⁴ of the total. However, at 530°K about ten percent of the reactions lead to dissociative attachment. It is found that SF₆⁻ charge-transfers to atomic oxygen and ozone while O₂⁻ charge-transfers to SF₆. The rates for these reactions will be reported. As a continuation of the metal ion chemistry first reported at the 1967 GEC the clustering reactions of H₂O to the alkali metal ions is being investigated. It is found that Na⁺ successively clusters with H₂O to form Na⁺·H₂O, Na⁺·(H₂O)₂, Na⁺·(H₂O)₃ and Na⁺·(H₂O)₄. Under our experimental conditions no clusters beyond the fourth were observed. The rate for the initial step Na⁺ + H₂O + M → Na⁺·(H₂O) + M has been measured to be 3×10^{-30} cm⁶/sec. This and other results will be reported.

J5. Measurement of Electron Attachment Rates in a Thermal Plasma.* J. H. MULLEN and R. L. COWPERTHWAITTE, McDonnell Douglas Corp., St. Louis.--A technique for measuring forward attachment rate constants in a high temperature argon plasma is presented. An rf induction plasma operating at 152 Torr and at 3000°-5000°K is used as the plasma source. The source gas is passed through a convergent-divergent nozzle into a low pressure (0.56 Torr) tank. Various target gases are injected in the throat of the nozzle. The target gas reacts for a short time, typically the order of μ secs, and then is rapidly frozen by the expansion nozzle. Electron concentrations of the expanded gas are measured with a K-band interferometer while the neutral gas temperature, electron density and electron temperature of the source is monitored with an optical spectrograph. The electron temperature of the source and expansion region is also monitored with an X-band radiometer. A quadrupole mass spectrometer is used to measure ion fluxes in the expansion region. A forward rate dominated theoretical attachment model is used to obtain the rate constants. Preliminary results will be given for a number of target gases, including SF₆, N₂O and O₂.

*Work conducted under the McDonnell Douglas Corporation Independent Research and Development Program.

J6. Electron Attachment in the Field of the Ground and Excited Electronic States of the Azulene Molecule.* E. L. CHANEY,† L. G. CHRISTOPHOROU, P. M. COLLINS,‡ and J. G. CARTER, Oak Ridge National Laboratory.--Azulene attaches thermal and near thermal-energy electrons forming a long-lived parent negative ion in the field of the electronic ground state with a peak cross section of $3.5 \times 10^{-15} \text{ cm}^2$ and a mean autoionization lifetime of $7 \pm 1.5 \mu\text{sec}$. Evidence is presented also for electron attachment in the field of a low-lying excited electronic state (possibly the lowest π -triplet state). Electron beam studies evidence the formation of long-lived, but metastable, negative ions in the energy range 5.0 - 9.0 eV. These are ascribed to electron capture by the parent molecule with simultaneous excitation of one or two orbiting electrons. The electron affinity of azulene in the ground state was found equal to 0.46 eV.

* Research sponsored by the U. S. Atomic Energy Commission under contract with Union Carbide Corporation.

†Oak Ridge Graduate Fellow, University of Tennessee, Knoxville, under appointment of Oak Ridge Associated Universities.

‡Radiological Health Physics Fellow, University of Tennessee.

J7. Electron Attachment Cross Sections and Negative-Ion Lifetimes for p-Benzoquinone and 1,4-Naphthoquinone.* P. M. COLLINS,† L. G. CHRISTOPHOU, E. L. CHANEY,‡ and J. G. CARTER, Oak Ridge National Laboratory. -- Formation and autoionization of polyatomic negative ions in ground and excited electronic states will be discussed with reference to p-benzoquinone (BQ) and 1,4-naphthoquinone (NQ). BQ attaches electrons via (i) a thermal process (cross section $\sigma_a = 3.5 \times 10^{-19} \text{ cm}^2$) associated with the benzene ring and (ii) a 2.1 eV process ($\sigma_a = 6.7 \times 10^{-17} \text{ cm}^2$) associated with capture in the field of the lowest triplet state T_1 resulting from an $n \rightarrow \pi^*$ transition at $\sim 2.35 \text{ eV}$. The parent negative-ion lifetime τ decreases from $48 \mu\text{sec}$ at 1.7 eV to $8 \mu\text{sec}$ at 3.2 eV. NQ forms long-lived parent negative ions at thermal and epithermal energies, the ion current evidencing structure associated with skeletal deformations. τ decreases from $\sim 350 \mu\text{sec}$ at thermal energies to $\sim 10 \mu\text{sec}$ at 1 eV.

*Research sponsored by the U.S. Atomic Energy Comm. under contract with Union Carbide Corporation.

†Radiological Health Physics Fellow, Univ. of Tennessee.

‡Oak Ridge Graduate Fellow, University of Tennessee.

SESSION K

Wednesday Evening, 29 October

8:00 p.m.

AFTERGLOWS AND ION REACTIONS

Chairman: *A. L. Schmeltekopf*, ESSA Research Laboratories
Boulder, Colorado

K1. WATER-CLUSTER IONS IN AIR, N₂, AND CO₂ * P. N. EISNER, M. N. HIRSH, and E. POSS, The Dewey Electronics Corp. -- Water-cluster ions are being studied in air, N₂, and CO₂ over the pressure range 1 to 8 Torr in a 700 -ℓ reaction chamber uniformly irradiated by 1.5 - MeV electrons. Positive and negative ions diffuse to a mass spectrometer at the chamber wall, and are studied as a function of irradiation history and water concentration. About 10 ppm of H₂O is sufficient to cause the hydronium ion sequence (H₃O⁺ · nH₂O, n = 0, 1, 2, 3) to dominate the positive ion spectrum in any of these gases, and water-related ions to dominate the negative ion spectrum in CO₂; in air the negative ions NO₂⁻ and NO₃⁻ remain dominant even with this H₂O concentration. Removal frequencies determined from the exponential decays observed for the water-cluster ions in the radiation afterglow suggest that chemical processes dominate the removal in almost all cases studied.

* Work supported by DASA.

K2. NEUTRAL CHEMISTRY EFFECTS IN THE POSITIVE ION SPECTRUM OF ELECTRON-IRRADIATED AIR* M. N. HIRSH, P. N. EISNER, and E. POSS, The Dewey Electronics Corp. -- We are studying the production of NO by fast electrons and the subsequent effects of NO on the positive ion spectrum in airlike N₂:O₂ mixtures at pressures above 1.0 Torr during continuous irradiation by these electrons. The NO density is deduced from measurements of the decay frequency of O₂⁺ in the afterglow as a function of prior irradiation of the gas, in a regime in which the O₂⁺ removal is controlled by charge exchange with NO. The measurements yield an NO density given by $1.1 \times 10^{11} p \sqrt{it} \text{ cm}^{-3}$ (p in Torr, i in $\mu\text{A}/\text{cm}^2$ of 1.0 Mev electrons, t in seconds); this NO density also accounts for the equilibrium ratios of NO⁺/O₂⁺ ion currents observed during irradiation. A set of six reactions will be presented which accounts for the observed behavior of the majority positive ion species, and predicts the neutral NO densities described above.

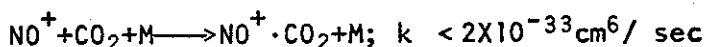
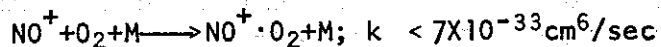
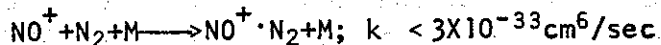
*Work supported by DASA.

K3. Reactions in Ionized Air-Like Mixtures. F. E. Niles, Ballistic Research Laboratories--The ionization of air-like mixtures initiates sequences of reactions which create secondary positive ions, negative ions, and new neutral constituents. Formation sequences for the positive ions and for the negative ions are represented by schematic diagrams. The formation of positive ions can be divided into three regions. Region I contains the ionization of neutral constituents and two-body reactions in dry air. Region II contains reactions involving ionic species which are formed by three-body reactions. Region III contains reactions requiring water vapor and shows the formation of the hydrated hydronium ions. The formation of negative ions proceeds predominately through O_2^- . The clustering of neutral molecules to O_2^- opens additional channels for the formation of NO_3^- . During continuous ionization, charge is transferred from the primary ions to the secondary ions by reactions. When the source of ionization is removed, the primary ions decay rapidly leaving the secondary ions. Comparison of calculated number densities with experimental measurements permits areas of agreement and disagreement to be identified. In general, qualitative agreement is achieved.

K4. Flowing Afterglow Studies of the Reactions of the Rare-Gas Molecular Ions He_2^+ , Ne_2^+ , and Ar_2^+ with Molecules and Rare-Gas Atoms, D.K. BOHME, N.G. ADAMS, M. MOSESMAN, D.B. DUNKLIN, and E.E. FERGUSON, ESSA Research Laboratories. The flowing afterglow technique has been used to measure rate coefficients and product channels for the reactions of He_2^+ , Ne_2^+ , and Ar_2^+ with the rare-gas atoms Ne, Ar, and Kr, and with the molecules NO, O_2 , CO, N_2 , and CO_2 at 200°K. These reactions are found to proceed principally by asymmetric charge-transfer. The experimental results for the reactions of the rare-gas molecular ions with rare-gas atoms indicate a correlation between reaction probability and reaction exoergicity analogous to that observed for asymmetric atomic ion-atomic neutral charge-transfer reactions. The reactions with molecules are found to proceed with unit reaction probability with the exception of the reactions $Ar_2^+ + O_2$ and $Ar_2^+ + NO$. The reaction probability for the reactions of the molecular rare-gas ions with molecules is not very sensitive to an energy resonance criterion. Finally, rate coefficients and reaction channels for the reaction of the mixed rare-gas molecular ions $HeNe^+$, $ArKr^+$, and $ArCO^+$ with Ne, Kr, and CO respectively, are reported.

K5. Flowing Afterglow Studies of Formation and Reactions of Cluster Ions of O_2^+ and O_2^- , N.G. ADAMS, D.K. BOHME, D.B. DUNKIN, F.C. FEHSENFELD, and E.E. FERGUSON, ESSA Research Laboratories. Rates of association of H_2 , N_2 , O_2 , CO_2 , N_2O , and SO_2 to O_2^+ have been measured with helium third body in a flowing afterglow at temperatures below $300^\circ K$. Rates for association of N_2 , O_2 , and CO_2 to O_2^- at $200^\circ K$ have been measured. Rate constants for a number of binary "switching" reactions have been measured, e.g. $O_2^+ \cdot O_2 + N_2O \rightarrow O_2^+ \cdot N_2O + O_2$, $k = 2.5(-10) \text{ cm}^3/\text{sec}$, and $O_2^- \cdot H_2O + CO_2 \rightarrow O_2^- \cdot CO_2 + H_2O$, $k = 5.8(-10) \text{ cm}^3/\text{sec}$. These reactions allow an ordering of cluster bond energies. The order of binding energies to O_2^+ (increasing) is N_2 , O_2 , N_2O , SO_2 , and H_2O . For O_2^- the increasing order is N_2 , O_2 , H_2O , CO_2 , and NO . In some cases, equilibria are observed allowing a determination of binding energy differences. Some free energy differences so obtained are: $\Delta F(O_2^- \cdot CO_2) - \Delta F(O_2^- \cdot O_2) \approx 0.26 \text{ eV}$, and $\Delta F(O_2^+ \cdot N_2O) - \Delta F(O_2^+ \cdot O_2) \approx 0.13 \text{ eV}$. The three body association rate constants increase with increasing association bond energy, in accord with theoretical expectation.

K6. Reactions of NO^+ in Atmospheric Gases. L. J. PUCKETT and M. W. TEAGUE, Ballistic Research Laboratories. Stationary afterglow techniques have been utilized to observe NO^+ ions reacting in atmospheric gases. Studies in $NO-N_2$, $NO-O_2$, $NO-CO_2$, and $NO-H_2O$ mixtures revealed that all the reactions products observed for NO^+ ions in laboratory air could be explained by NO^+-H_2O reactions. In afterglows of NO at $\sim 200 \text{ mTorr}$ and H_2O from 0.5 to 15 mTorr the dominate ions is $H_3O^+ \cdot 3H_2O$, although at 15 mTorr H_2O pressure the ion $H_2O^+ \cdot 3H_2O$ becomes dominant. The rate constants for NO^+ clustering in N_2 , O_2 , and CO_2 are



K7. A Numerical Study of the Transient Hydrogen Afterglow.* C. C. LIMBAUGH** AND W. K. MCGREGOR**, ARO, Inc., Arnold Air Force Station, Tenn.--The set of differential equations describing the transient behavior of an ionized gas are solved numerically for an idealized, constant pressure, optically thin, field free, atomic hydrogen plasma.¹ The study concerns plasmas in which the free electron velocity distribution is Maxwellian and electron-atom encounters totally dominate atom-atom encounters. The fundamental consistency of the mathematical model is examined as well as the existence and location of the "critical level." Comparison of the decay of a normal atomic hydrogen plasma to one in which the radiative metastability in the $2 S_{1/2}$ level has been removed are made. Results show that the inclusion of the metastability will significantly elevate the excited state population densities.

¹D. R. Bates, A. E. Kingston, and R. W. P. McWhirter, Phys. Rev., 267, 297 (1962).

*The research reported in this paper was sponsored by Arnold Engineering Development Center, AFSC, Arnold AF Station, Tenn. under Contract No. F40600-69-C-0001 with ARO, Inc. Further reproduction is authorized to satisfy the needs of the U. S. Government.

**Research Engineer, Research Branch, Rocket Test Facility.

K8. Probe Measurements of Diffusion Cooling.* EDWIN BLUE, Lockheed Palo Alto Res. Lab.--Pulsed electrostatic probe techniques¹ have been used to study the behavior of low pressure helium afterglow plasmas. Current-voltage characteristics were measured with symmetric double probes and with triple probes. Analysis of the characteristics shows clear and direct evidence to support the Biondi diffusion cooling mechanism.² Earlier measurements with double probes were regarded as evidence in support of diffusion cooling,³ however, the results were not conclusive since double probe measurements are limited to sampling only a small portion of the electron energy distribution. The pulsed triple probe measurements which are reported here show that the electrons have in fact achieved a Maxwellian distribution corresponding to a temperature well below room temperature.

*Supported by Lockheed Independent Research funds.

¹E. Blue and J. E. Stanko, Jour. Appl. Phys. 40 (1969)

²M. A. Biondi, Phys. Rev. 93, 1136 (1954)

³E. Blue, Bull. Amer. Phys. Soc. II 14, 257 (1969)

K9. Theory of Adiabatic Cooling of Electrons in a Diffusion-Controlled Afterglow Plasma.

J. H. INGOLD, General Electric Lighting Research Laboratory.--The electron-density-temperature history in a diffusion-controlled afterglow plasma is calculated theoretically in the ambipolar limit. It is shown that adiabatic cooling (previously termed "diffusion cooling") of the electrons below the gas temperature takes place when the electron-atom energy relaxation time is long compared to the electron diffusion time. The calculation is based on the assumption that the electron velocity distribution function is Maxwellian throughout the afterglow. This assumption is justified on the grounds that the electron-electron energy relaxation time is short compared to the electron diffusion time. The concept of adiabatic cooling is discussed briefly.

SESSION L

Wednesday Evening, 29 October

8:00 p.m.

EXCITATION BY ELECTRON IMPACT PANEL

Panel Chairman: *S. J. Smith*, Joint Institute for
Laboratory Astrophysics, Boulder,
Colorado

L1. Electron Impact Excitation and Ionization Studies of He, Ne, and Ar.* J. T. GRISSOM, R. N. COMPTON, and W. R. GARRETT, Oak Ridge National Laboratory. -- Electron impact excitation spectra and ionization cross sections of He, Ne, and Ar have been studied from 10 to 150 eV using a trapped electron apparatus with energy resolution of 0.2 to 0.3 eV. Energy scale calibration was performed by direct comparison to the 19.31 eV He transmission resonance and the He 2^3S level at 19.82 eV. New structure is observed corresponding to inner-shell, single electron excitations; outer-shell double, electron excitations; and negative ion formation. "Dips" in the positive ion cross section of He at 57.2 and 58.3 eV are attributed to negative ion resonances previously observed¹ in the elastic scattering cross section. The cross sections for slow electron production vs energy and the energy distributions of slow electrons in the ionization continuum have been measured.

*Research sponsored by the U.S. Atomic Energy Commission under contract with Union Carbide Corporation.

¹C. E. Kuyatt, A. Arol Simpson, and S. R. Mielczarek, *Phys. Rev.* 138, A385 (1965).

L2. Resonance Features in the Excitation Functions of Neon.* K. G. WALKER and R. M. ST. JOHN, Univ. of Okla. -- Resonance structure has been found a few hundredths of an eV above onset for the excitation functions of the $2p_3$, $2p_4$, $2p_6$, $2p_8$, $2p_9$ and $2p_{10}$ levels of neon. The resonant feature on the $2p_{10}$ excitation function has been associated with the compound state of the neon atom and an electron at 18.56 eV as found by Kuyatt, Simpson and Mielczarek⁽¹⁾ in electron transmission experiments. The other resonant features are possibly originating from higher states of the Ne^- ion not detected by Kuyatt, *et. al.*

*Work supported by AFOSR Grant 252-67.

¹C. E. Kuyatt, J. A. Simpson, S. R. Mielczarek, *Phys. Rev.* 138, A385 (1965).

L3. Optical Ionization-Excitation Functions of Zinc, Cadmium and Mercury by Electron Impact.* RICHARD J. ANDERSON, University of Arkansas, and EDWARD T. P. LEE, Optical Physics Laboratory Air Force Cambridge Research Laboratories (CROR).--The cross sections for the production of some sixteen lines of the Zn^+ , Cd^+ , and Hg^+ spectra by ionization-excitation collisions between electrons and neutral atoms have been measured over the energy range 0-260 eV. The spectral lines are characterized by excitation functions which reach their maximum values within the energy range 40-90 eV, and by emission cross section values of approximately 10^{-18} cm² to 10^{-21} cm² at 200 eV. For example, at 200 eV the $7^2S_{1/2} \rightarrow 6^2P_{3/2}$ transition of the Hg^+ ($\lambda 2848 \text{ \AA}$) has a cross section of 3×10^{-20} cm². Theoretical branching ratios have been calculated and are used to obtain estimates of the $7^2S_{1/2}$ (Hg^+), $6^2S_{1/2}$ (Cd^+) and $5^2S_{1/2}$ (Zn^+) direct excitation cross sections. In addition the corresponding theoretical values have been estimated by means of Born approximation.

*Work supported in part by the Research Corporation.

L4. Electron Excitation Cross Sections of the First Negative Bands of Oxygen and Nitrogen.* WALTER L. BORST AND E. C. ZIPF, University of Pittsburgh. -- Absolute cross sections for the excitation of the (0-0), (1-0), and (2-0) bands of $O_2^+(b^4\Sigma_g^- \rightarrow a^4\Pi_u)$ by electron impact were measured from threshold to 400 eV. The maximum values are 2.14, 5.30, and 2.10×10^{-18} cm² \pm 10% at 100 eV, respectively. The relative values agree with an independent measurement of band intensities obtained in a microwave discharge. All three excitation functions exhibited the same shape. The square of the electronic transition moment for $O_2(X^3\Sigma_g^-) \rightarrow O_2^+(b^4\Sigma_g^-)$ increases linearly from $v'=0$ to $v'=2$. The total cross section of the $b^4\Sigma_g^-$ state is 3.2×10^{-17} cm² at 100 eV. The excitation cross section of the (0-0) band of $N_2^+(B^2\Sigma_u^+ \rightarrow X^2\Sigma_g^+)$ was determined from threshold to 10 keV and had a maximum value of 1.74×10^{-17} cm² \pm 10% at 100 eV. The polarization of the emitted light was less than 5% over the entire energy range. The experimental technique involved a rotatable electron gun - collision chamber assembly providing a well collimated, electrostatically focused beam ($\sim 1 \mu A$). Low gas pressures ($< 10^{-4}$ Torr), narrow band pass filters, and single photon counting techniques were used.

*Work supported, in part, by NASA and ARPA.

15. Electron-Impact Cross Sections for Simultaneous Ionization and Excitation of He to the 4s,p,d,f States by High-Resolution Fabry-Perot Interferometry. *WILLIAM D. EVANS, JAMES K. BALLOU, FRED L. ROESLER, AND CHUN C. LIN, University of Wisconsin. --The thirteen lines of the 4s,p,d,f \rightarrow 3s,p,d transitions of He⁺ produced by passing an electron beam through helium gas have been recorded with a high-resolution, high-luminosity scanning Fabry-Perot interference spectrometer. At 200 eV incident electron energy, the measured relative intensities of the stronger components¹ 1,2,3,4,5+6, 9,12 are 7.4,0.1,5.4,0.1,12,10,9.0 from which we obtain the ionization-excitation cross section of the 4s state of He⁺ as $7.6 \times 10^{-21} \text{ cm}^2$ in good agreement with the theoretical value $8.1 \times 10^{-21} \text{ cm}^2$. The experimental cross sections of 4p,d,f are much larger than the theoretical estimates. At pressure above 0.06 Torr, the intensities of the 4s \rightarrow 3p lines decrease relative to the others indicating collisional transfer effects.

*Supported by the Air Force Office of Scientific Research and the National Science Foundation.

¹F. Roesler and J. Mack, Phys. Rev. 135, A58 (1964).

16. Simultaneous Excitation and Ionization of Argon: 3p⁴4s 2P UV Emission. G. M. LAWRENCE, Douglas Advanced Research Laboratories. -- One step excitation functions of the 723A° (2P_{3/2}) and 726A° (2P_{1/2}) lines of Ar II excited from ground state argon have been measured from threshold to 1Kv with an electron beam, monochromator, multichannel analyzer system. A time domain decay curve analysis was used to determine the fraction of 8-10 nsec cascading which feeds these (3p⁴4s 2P) states. Between 83 and 158 volts the cascading is (60±5)% of the total excitation for 2P_{1/2} and (55±5)% for 2P_{3/2}. Absolute excitation functions¹ for the major cascading levels have been used to normalize the 723A° and 726A° excitation functions. The total cross sections for 2P_{1/2} and 2P_{3/2} are quite similar, rising to a maximum at ~1.5 times threshold, with an E⁻¹ dependence at large E, and having peak values of $1.60 \times 10^{-18} \text{ cm}^2$ and $3.0 \times 10^{-18} \text{ cm}^2$, respectively.

¹I. D. Latimer and R. M. St. John, VI ICPEAC, MIT press, Cambridge, July 1969, p. 287.

L7. The Dissociative Excitation of Atomic Resonance Lines by Electron Impact. M. J. MUMMA and E. C. ZIPP, University of Pittsburgh.--The resonance lines of H, O, N, and [C and O] produced by the dissociative excitation of H₂, O₂, N₂ and CO₂ respectively by electron impact have been observed. Vacuum ultraviolet transitions in addition to the first resonance lines have been observed for both Cl and Ni. Evidence will be presented showing that the peak cross section for dissociative excitation can be very large ($> 5 \times 10^{-18}$ cm² for H₂, N₂, and O₂). Marked differences in the shape of the excitation functions have been observed and will be discussed.

*Work supported by ARPA and NASA

SESSION

Thursday Morning, 30 October

8:30 a.m.

CO₂ LASER PANEL

Panel Chairman: *R. H. Bullis*, United Aircraft
 Research Laboratories, E. Hartford,
 Connecticut

M1. Diagnostics of Plasma Properties in a CO₂ Laser. P. BLETZINGER and A. GARSCADDEN. Aerospace Rsch Labs, WPAFB.--Using a second derivative apparatus, the influence of different gas additives on the electron energy distributions in a CO₂ laser is reported. It is demonstrated that since the distribution is non-Maxwellian conventional microwave methods and semi-logarithmic Langmuir probe data are not sufficient to define the electron energy. The influence of gas pressure and collisional effects on the probe measurements have also been investigated and the results have to be considered for the CO₂ laser discharge. The effects of laser action on the plasma have been measured using probe and spectroscopic methods. The laser action causes a marked decrease of the number of electrons over a wide energy range. It is therefore possible to determine the range of electrons energies involved in pumping the laser. In addition to examining the basic laser oscillator, the diagnostics have been applied to an amplifier discharge in an oscillator-amplifier configuration.

M2. Electron Radiation Temperature Measurements in a Sealed-off CO₂-laser System. J. POLMAN and W.J. WITTEMAN, Philips Research Laboratories, Eindhoven, Netherlands.--Measurements of the noise temperature in the L-band were used to investigate the effect of several constituents of the gas mixture on the discharge properties of the CO₂-laser. Addition of He and H₂O to the discharge gives no significant change in the temperature. On the contrary addition of 4 Torr N₂ to 2 Torr CO₂ increases the noise temperature from 1.3 to 1.5 eV. Increase of the current in an optimum CO₂-N₂-He-H₂O mixture leaves the temperature nearly constant (1.5eV). This result deviates from those of Tyte and Sage¹, who found an anomalous rise of noise temperature with increasing current. Within the 5% experimental error the radiation temperature does not depend on laser action. A comparison of the present results with those of probe measurements will be given.
¹D.C.Tyte, R.W.Sage, IERE(London) to be publ.

M3. Effect of Electron Collisions in a Pulsed CO₂ Discharge on Optical Gain at 10.6 μm.* J. H. NOON, P. R. BLASZUK, E. H. HOLT, Rensselaer Polytechnic Institute, and R. G. BUSER, U. S. Army Electronic Command, Fort Monmouth.
 --A repetitively pulsed CO₂ discharge shows drastic variations in optical gain at 10.6 μm as a function of gas history, negative gain on a millisecond time scale being observed in the afterglow of pure CO₂. Using microwave measurements of free electron number density and electron radiation temperature, quantitative comparison has been made between observed gain relaxation times and solutions of the time-dependent rate equations involving population of excited states by electron collisions. It is shown that it is not only the laser level lifetimes but also the temporal behavior of the free electrons which determines the gain decay rate in the pure CO₂ afterglow. Repetitive pulsing with attendant evolution of CO, or admixture of N₂ or He destroys negative gain behavior.

*Supported by U. S. Army Electronics Command.

M4. Collision Processes in a Sealed-off CO₂-laser,* J. FREUDENTHAL, University of Minnesota - The active plasma of a CO₂-laser discharge was investigated mass spectrometrically. The neutral and ionic constituents of the plasma were sampled through a small hole in the wall of the discharge tube and they were analyzed by means of a quadrupole mass spectrometer. The following mixtures were investigated: He-N₂-CO₂, He-N₂-CO₂-H₂O and He-CO₂. The time dependence of the CO₂ was measured at the cathode and anode side of the discharge. The dissociation of the CO₂ was compensated by a strong oxidation process in the first two mixtures. For the He-N₂-CO₂ this might be CO + O('D) → CO₂ or CO₂ + O('D) → CO₃, CO₃ + CO → 2CO₂. In the He-N₂-CO₂-H₂O there is an additional oxidation process CO + OH → CO₂ + H. In the mixture He-CO₂ the oxidation is much less pronounced than in the other mixtures.

*This work was supported by the Office of Naval Research under Grant No. N00014-67-0002, project THEMIS.

M5. CO Formation in N₂-CO₂ Lasers.* W. J. WIEGAND, M. C. FOWLER, AND J. A. BENDA, United Aircraft Research Laboratories.--The CO-CO₂ chemistry in a N₂-CO₂-He laser has been studied under typical laser operating conditions. Dissociation in the discharge reduces the CO₂ concentration and opens a number of new electron inelastic loss channels in CO resulting ultimately in a decrease of laser power. By monitoring intensities of representative CO Angstrom bands and N₂ second positive bands the variation of CO concentration with position and velocity has been determined. Absolute concentrations of CO and CO₂ were obtained from mass spectrometer and gas chromatograph analysis of discharge gas samples. Under the conditions of this experiment a time constant of about 0.5 second for the establishment of the CO-CO₂ equilibrium was observed. In addition, the changes of E/N and laser output power were measured. The details of the CO formation and its effect on discharge properties and laser performance will be discussed.

*Portions of this work were supported by the Office of Naval Research under Contract N00014-69-C-0309.

M6. Electron Energy Distribution Functions in CO₂ Laser Mixtures.* W. L. NIGHAN, United Aircraft Research Laboratories.--The electron energy distribution function has been determined for CO₂ laser plasmas in gas mixtures of CO₂, N₂, and He by numerically solving the Boltzmann-Fokker-Planck equation. Calculations were made for a variety of experimentally interesting circumstances and in general, the distribution functions were found to be non-Maxwellian. Using the calculated distribution functions, electron-molecule energy exchange rates were evaluated. With this information the relationship of the various electron-molecule energy exchange processes to laser performance was studied. For plasma conditions typical of CO₂ lasers, approximately 20% of the power transferred to the CO₂ and N₂ was found to be available for conversion to optical power, in agreement with typical experimental values of laser efficiency. Estimates of maximum available optical power were also found to be consistent with experimental values.

*Portions of this work were supported by the Office of Naval Research under Contract N00014-69-C-0309.

M7. Vibrational Excitation in CO₂ and Positive Column Maintenance Fields CO₂ Laser Mixtures. A.V. PHELPS, Westinghouse Research Laboratories--Magnitudes of cross sections for excitation of the 010 and 001 vibrational levels of CO₂ using Born approximation energy dependences are determined from measured electron transport coefficients. Reasonable agreement ($\pm 20\%$) is obtained by increasing the 010 effective infrared transition probability to $8 \times 10^{-3} e^2 a_0^2$ and using the 001 experimental value of $1.6 \times 10^{-2} e^2 a_0^2$. Alternatively, the energy dependence of Boness and Schulz¹ for the 001 level requires that their magnitude be reduced by 0.5. CO₂, N₂ and He cross sections² are used to calculate ionization rates for a CO₂ laser mixture (0.5, 1.5, and 8 Torr). A balance of ionization and ambipolar diffusion for a uniform positive column (radius 3.8 cm) requires an E/N of $1.5 - 2 \times 10^{-16} \text{ V-cm}^2$ and a mean electron energy of 1 to 1.5 eV.

¹M.J.W. Boness and G.J. Schulz, Phys. Rev. Letters 21, 1031 (1968).

²R.D. Hake, Jr. and A.V. Phelps, Phys. Rev. 158, 70 (1967); A.G. Engelhardt, A.V. Phelps, and C.G. Risk, Phys. Rev. 135, A1566 (1964); L.S. Frost and A.V. Phelps, Phys. Rev. 136, A1538 (1964).

M8. Theory of Energy Transfer Mechanisms in CO₂ Lasers. H. J. KOLKER, United Aircraft Res. Labs.--There are a number of molecular collisions, involving the near resonance transfer of vibrational or rotational energy, which play an important role in predicting the performance of a CO₂ laser. A wave mechanical theory of molecular collisions has been used to study the mechanisms of these near resonant collisions. An exact solution for an equivalent problem involving a resonant transfer of excitation is used as the basis for a distorted wave type of approximation to solve the nonresonance problem. Since the cross section for this type of collision decreases very rapidly as the degree of nonresonance increases, this should be a good approximation. Assuming that long range intermolecular forces are responsible for the energy transfer, it is possible to predict the temperature dependence of the relaxation rate of the upper and lower laser levels of CO₂. Special attention will be devoted to the deactivation of the 001 and 011 states of CO₂, by N₂, H₂, D₂, SF₆, and SiF₄, and the 010 state by H₂ and D₂.

M9. Influence of Collisions on Optical Saturation in the CO₂ Laser*. T. Kan, G. J. Wolga, Cornell University. The low pressure saturation behaviour of the CO₂ molecular laser has been studied by a probe of the saturated inversion in an oscillator exhibiting the Lamb dip. Individual rotation-vibration transitions are found to saturate in a mixed inhomogeneous-homogeneous broadened manner in which the differential inversion (unsaturated inversion-saturated inversion) contains a dominant Doppler component in addition to the Lorentzian holes expected from a pure inhomogeneous line. The Doppler component is a direct demonstration of elastic velocity-changing collisions which act as a spectral cross-relaxation mechanism within the Doppler line. The inversion probe technique therefore achieves an experimental separation of the effects of different collision processes not possible with studies using the Lamb dip alone. Rate equation treatment of collisions shows that saturation in both atomic and molecular transitions must in general be characterized by no fewer than three pressure dependent parameters and reveals that Lamb dip formation in the CO₂ laser is the result of a balance between elastic velocity-changing and rotational thermalizing collision processes.

* Work supported by ONR contract N00014-67-A-0077-0006

M10. Central Tuning Peak and Inhomogeneous Saturation with the CO₂ Laser* H.T. POWELL and G.J. WOLGA, Cornell Univ.-A 1.73 m, 400°C, intracavity CO₂ absorber inside a CO₂ laser was used to produce a central tuning peak on lines in the 00⁰1-10⁰0 CO₂ laser band. A CO₂/N₂, 0.25 m, D.C.-excited gain tube was employed at pressures greater than 4 torr for homogeneous saturation. The absorption tube was filled to various pressures between 0.25 and 0.65 torr to provide an inhomogeneously saturable absorber. The frequency width of the central peak is simply the collision determined Lorentz width. The measured width as a function of pressure was fit to a straight line and yielded 6.6±0.3 MHz/torr at 400°C for the Lorentz halfwidth. The hole width determined in this manner is in excellent agreement with that found from low pressure CO₂ laser tuning profiles exhibiting a Lamb dip. We also performed a simple analysis of such Lamb dip curves in view of strong intraline cross relaxation¹. The effect of such cross coupling is to reduce the dip strength in a manner that is formally equivalent to so-called "soft collisions" in the low intensity case.

*Work supported by the Office of Naval Research
¹T.Kan and G.J.Wolga, preceding abstract.

SESSION N.

Thursday Morning, 30 October

8:30 a.m.

IONIZATION COEFFICIENTS AND BREAKDOWN

Chairman: *G. S. Hurst*, University of Kentucky
Lexington, Kentucky

N1. Hall Effect in Field Emitting Protrusions Initiating Vacuum Breakdown, ALAN WATSON,* Ion Physics Corporation - Experimental evidence indicates that very weak transverse magnetic fields will either increase or reduce field emission while at the same time influencing breakdown voltage correspondingly.⁽¹⁾ The reduction of field emission is accounted for in terms of the magnetic transport properties of the cathode surface and breakdown voltage variations are shown to be consistent with the unified theory of vacuum breakdown.⁽²⁾

(1) Alan Watson, W. R. Bell and M. J. Mulcahy, "Factorially Designed Vacuum Breakdown Experiments II", Proceedings Third International Symposium on Discharges and Insulation in Vacuum, Paris, September, 1968.

(2) Alan Watson, "A Unified Theory of Vacuum Breakdown", Proceedings Third International Symposium on Discharges and Insulation in Vacuum, Paris, September, 1968.

* Sponsored by USAECOM under Contract No. DA-28-043-AMC-00394(E).

N2. Influence of Thermal Properties of Anode Material on Vacuum Breakdown. * F. Y. TSE and P. C. BOLIN, Ion Physics Corp., Burlington, Mass. -- Factorial investigations of vacuum breakdown in clean high vacuum at voltages up to 300 kV indicate the critical role of anode material, especially for well-conditioned electrodes subjected to many high energy discharges (~7000 J available). Linear regression analysis has been used to relate thermal properties of five metals (Cu, Ti, Ni, SS and Al) to their breakdown voltages. The assumed function is of the form $V_{bd} = A T_m^a C_s^b D_m^c$, where T_m is the melting point temperature, C_s is the specific heat and D_m is the density. Dependence of breakdown voltage on the thermal properties of the anode is discussed in terms of field emission and clump theories of vacuum breakdown.

* Work sponsored by USAECOM under Contract Number DA-28-043-AMC-00394(E)

N3. Ionization Coefficients and Collision Frequencies in Crossed Electric and Magnetic Fields. S. C. HAYDON†, Joint Institute for Laboratory Astrophysics, and A. SIMPSON, University of New England, Armidale, N.S.W.--Primary and secondary ionization coefficients have been measured in deuterium covering the range $40 < E/p < 350 \text{ V cm}^{-1} \text{ torr}^{-1}$ and $0 < B/p < 2000 \text{ G torr}^{-1}$ using a coaxial cylindrical crossed field geometry to minimize diffusion loss of electrons. Values of the effective collision frequency ν_{eff}/p varying from $3 \times 10^9 \text{ sec}^{-1} \text{ torr}^{-1}$ at $E/p' = 40$ to $2.3 \times 10^9 \text{ sec}^{-1} \text{ torr}^{-1}$ at $E/p' = 80$ have been obtained from the pre-breakdown data, where p' is the equivalent pressure given by $p' = p \sqrt{1 + \omega^2/\nu_{\text{eff}}^2}$ and ω is the electron cyclotron frequency. The effect of non-equilibrium ionization problems on the range of values of E/p' for which accurate values of ν_{eff}/p can be determined in various gases is briefly discussed and a critical comparison made with other determinations of collision frequencies based on breakdown voltage measurements.

*Work supported in part by the Australian Research Grants Committee and the Australian Institute for Nuclear Science and Engineering.

†Visiting Fellow 1968-69, permanent address: University of New England, Armidale, N.S.W.

N4. Non-equilibrium Ionization in Swarms with High Mean Electron Energies.* M. FOLKARD, University of New England, Armidale, N.S.W., and S. C. HAYDON†, Joint Institute for Laboratory Astrophysics.--The growth of pre-breakdown ionization at high values of E/p has been studied using thin film techniques for producing an initial swarm of electrons with low mean energy. Ionization currents have then been measured in strictly uniform field conditions and these yield 'effective' values of the primary ionization coefficient in H_2 very much lower than those previously reported for $E/p \gtrsim 250 \text{ V cm}^{-1} \text{ torr}^{-1}$. Diffusion effects have also been examined with split electrode geometry and within the experimental error presently available, values of the primary coefficient obtained in H_2 in the range $50 < E/p < 350$ do not show any marked influence from such effects. The nature of the non-equilibrium established at high mean electron energies is briefly discussed in relation to crossed-field and other ionization phenomena.

*Work supported in part by the Australian Research Grants Committee and the Australian Institute for Nuclear Science and Engineering.

†Visiting Fellow 1968-69, permanent address: University of New England, Armidale, N.S.W.

N5. The Ratio of Transverse and Longitudinal Diffusion Coefficients.* C. E. KLOTS and D. R. NELSON, Oak Ridge National Laboratory. -- A number of experiments have indicated large differences in the coefficients describing diffusion parallel and perpendicular to the direction of drift in an electric field. These differences can be satisfactorily rationalized in terms of the Boltzman transport equation.^{1,2} Nevertheless, a simple method for obtaining the ratio of the two coefficients would be useful. By supposing that the microscopic mobility as a function of local drift velocity is just that obtaining on the macroscopic scale, one derives $D_L = D_T [d \ln w / d \ln E/P]$ where D_L, T are the longitudinal and transverse coefficients, w the drift velocity and E/P the field per unit pressure. The limitations of this relation and its application to existing data will be discussed.

*Research sponsored by the U.S. Atomic Energy Comm. under contract with Union Carbide Corporation.

¹J. H. Parker and J. J. Lowke, Phys. Rev. 181, 200 (1969); ibid. 302 (1969).

²H. R. Skullerud, J. Phys. (B), Ser. 2, 2, 696 (1969).

N6. Photometric Determination of the Electron Ionization Frequency in Dry Air.* M. H. MENTZONI,** Sylvania Electronic Systems. -- The photometric method has been proven successful in the measurement of the ionization frequency, ν_i , in the dry air in the field range $40 \leq E_{eff}/p \leq 132$ volts/cm Torr. The ionizing agent was a 9.361 GHz rectangular pulse which traversed a fused quartz breakdown cell enclosed in a cylindrical wave guide. As in previous studies, the electron collision frequency was selected according to the value $\nu_c = 5.3 p \times 10^9 \text{ sec}^{-1}$. The pressures chosen ranged from .5 to 36 Torr. The measurements were confined to the last half portion of the formative time lag (FTL) interval but always before manifestation of breakdown occurred as seen by abrupt changes in reflection and transmission signal pulses. The ν_i/p versus E_{eff}/p curve thus found ran reasonably parallel to the curve obtained by other workers who used the FTL-method.¹ Compared to their results, however, the present curve was shifted towards higher ν_i/p -values by as much as a factor of 1.8 in the lower one-half portion of the E_{eff}/p -range.

*Work supported by U.S. Air Force Cambridge Research Laboratories.

¹W. Scharfman and T. Morita, J. Appl. Phys. 35, 2016 (1964).

N7. Digital Computer Solution of Loeb's Streamer Criterion.* M. S. ABOU-SEADA and ESSAM NASSER, Iowa State University.--Since accurate knowledge of the electric field and its distribution with very large spatial resolution in some nonuniform field configurations has been recently obtained, the prediction of corona onset and streamer formation were attempted by the solution of Loeb's criterion for streamer development. This solution is carried out in steps. Assuming a certain voltage, the applied field is determined, then using known values of α , the first ionization coefficient, and v , the electron drift velocity, corresponding to the external electric field distribution and pressure, the electron multiplication and the avalanche transit time were computed using numerical integration techniques. Then the radius of the positive ion space charge is calculated by the diffusion equation. The space charge field is calculated and added vectorially to the external field. The new values of α are used again in Loeb's criterion equation which is then computed and compared with unity. If the difference is large, the voltage is incremented and the whole procedure is repeated. The voltage satisfying Loeb's criterion is the corona onset voltage. The effect of changing other variables, such as α , v , p , and the absorption coefficient, was studied.

*Work supported by the National Science Foundation.

N8. The Effect of Nitric Oxide on Microwave Breakdown of Nitrogen. DONALD L. JONES, ALLEN D. RUESS and PAUL E. BISBING, General Electric Co.--The effect of nitric oxide on high temperature air microwave breakdown is simulated by adding nitric oxide to dry nitrogen. The gas is broken down in a waveguide, with time to breakdown being the principal variable. A repetitive pulse is used with, typically, fifty pulses spaced two milliseconds apart. At constant power and gas pressure, time to breakdown is found to decrease as the fraction of nitric oxide increases. In general, breakdown in pure nitric oxide occurs an order of magnitude sooner than in dry nitrogen. For example, at a field strength of approximately 2 kV/cm and a pressure of 40 Torr, pure nitric oxide breaks down in approximately 0.4 microsecond. Under the same conditions it takes 4 microseconds to break down pure nitrogen. The data have been analyzed to infer the approximate variation of the ionization rate with nitric oxide concentration. The results indicate that nitric oxide may constitute at least a partial explanation of the effects of high temperature, such as are observed in shock tube experiments, on the microwave breakdown characteristics of air.

N9. Breakdown Voltage of Cesium in Thermionic Diode.*
 K.SHIMADA, Jet Propulsion Laboratory.—Volt-ampere curves of cesium diodes operated at relatively low emitter and cesium-reservoir temperatures exhibit both unignited and ignited modes. Transition between two modes occurs when cesium gas breaks down in the interelectrode gap. This breakdown is preceded by a rapid increase of the current and a visible glow near the anode. Such behavior is typical of the anode-glow mode in gas-discharge devices. Cesium breakdown voltages were measured in fixed-gap and variable gap diodes as functions of cathode, anode, and cesium-reservoir temperatures, for interelectrode distances D from 0.2 to 1.5 mm. Breakdown voltage varied from 5.0 to 1.4 V as a function of cesium pressure P , as in Paschen's curve. The breakdown voltage, however, was not a unique function of the product $P \times D$, and variations in voltage up to 1.5 V were observed at large values of D . We suggest that the dependence of such voltages on D indicates that the potential drop occurs in a dark plasma produced by electrons and ions emitted from the cathode, and that the cesium breakdown is initiated in a fairly small region adjacent to the collector.

*This paper presents the results of work sponsored by the National Aeronautics & Space Administration.

N10. Theoretical Considerations of the Prebreakdown Characteristics in a Cesium Thermionic Discharge.* DAVID TAI-KO SHAW, State University of New York at Buffalo.—The present theory is formulated on the basis of diffusion equations with uniform temperature, constant diffusion coefficient and mobilities. Special emphasis is placed on the plasma behavior near the collector because the processes occurring in this region play an important role in the prebreakdown characteristics. The solution is self consistent in that the division of the interelectrode plasma into several physically distinct regions is achieved in a natural way by the use of a limiting process on the governing equations. Spatial variations of the charged-particle density and electric fields are determined. The solution obtained is used to construct the volt-ampere characteristics of the prebreakdown discharge. It is found that most of the potential drop occurs in the anode sheath which can be divided into a free-fall, collisionless region, and a collision-dominated diffusion region. The dependence of this potential drop on diode currents and its effect on breakdown voltage are determined.

* The major part of this work was performed at the Jet Propulsion Laboratory, sponsored by NASA.

N11. Effect of Large Electric Fields on the Electron Energy Distribution and Ionization Rate in a Cesium Discharge.* DAVID TAI-KO SHAW, and S.G. MANGOLIS, State University of New York at Buffalo.--The present paper considers the nonequilibrium ionization in the near-emitter region of an ignited-mode thermionic converter. Numerical solutions are obtained for the Boltzmann equation with collisions terms which consist of elastic, inelastic, and electron-electron Coulomb interactions. The Fokker-Planck approximation of the Coulomb collision is used in the present study. It is found that at large electric fields (> 20 v/cm), the effect of the field acceleration causes a considerable departure from the Maxwellian function even in the elastic region. This effect is especially noticeable at low electron densities because of the small electron-impact collision frequencies. On the other hand, high electric fields usually yield high plasma temperatures, and consequently electron densities. When the Coulomb collisions become important; the distribution approaches that of Maxwellian. The effects of large electric fields and deviations from the Saha-Boltzmann population on the rate of ion generation is found by using the calculated distribution function.

*This research was supported in part by the National Science Foundation.

N12. Approach toward Ionizational Equilibrium in Shocked Mercury Gas*, Yong Wook Kim[†], University of Michigan. -- The ionizational relaxation times (τ) of shock-heated mercury have been spectroscopically measured at a variety of thermal states in a heated shock tube.¹ The activation energy is found to be 4.88 ± 0.28 eV for temperatures in a range $7,300^\circ$ to $11,000^\circ\text{K}$ and electron densities 2.8×10^{16} to 4.2×10^{17} cm^{-3} . It was also revealed that in this regime τ is independent of the particle density. A comparison with previous results on A, Kr, Xe and C_s enables us to conclude in general that the density dependence of τ is characteristic of the atom-atom process of ionization, whereas τ of the electron-atom process is characteristically void of such a dependence. It is then concluded that in the present case of shocked mercury, initial electrons are provided mainly by photo-excitation and -ionization processes ahead of the shock.

*Work supported by the A.F.O.S.R. Grant AF-AFOSR-934-67
[†]Present address: Lehigh University, Bethlehem, Penna.
 1. Y. W. Kim, O. Laporte, Phys. Fluids Suppl. 12, I-61
 (1969)

SESSION P

Thursday Afternoon, 30 October

2:00 p.m.

PENNING EFFECT PANEL

Panel Chairman: *E. E. Muschlitz, Jr.*, University of Florida
Gainesville, Florida

P1. Velocity Dependence of the Ionization of Argon on Impact of Metastable Neon Atoms.* S.Y.TANG and E.E. MUSCHLITZ, JR., Univ. of Florida.--Measurements of the velocity dependence of the total ionization cross section for collisions of $^3P_{2,0}Ne^*$ in Ar have been made using a velocity-selected beam of neon metastable atoms. A low voltage D.C. discharge is used as the source of excited atoms and velocity selection is accomplished by means of a rotating slotted-disc selector of standard design. Measurements were made in a collision chamber similar to that used previously,¹ and were of sufficient precision to allow simultaneous determination of both the cross section and the secondary electron ejection efficiency. In the velocity range investigated (330-840 meters sec⁻¹), the cross section was found to vary as $v^{-0.6}$ or (K.E.)^{-0.3}.

*Supported by the National Science Foundation.

¹W.P. Sholette and E.E. Muschlitz, Jr., J. Chem. Phys. 36, 3368(1962).

P2. The Kinetic Energies of Ions Resulting from Impact of 2^3S and 2^1S He* on H₂, D₂, O₂ and NO.* K.D. FOSTER and E.E. MUSCHLITZ, JR., Univ. of Florida.--Further experiments on Penning ionization using a thermal beam of metastable helium atoms have been performed with an apparatus previously described.¹ By measuring ion intensities as a function of retarding potential, information regarding the initial kinetic energies of the product ions can be obtained. Although the ion products for most of the systems studied appear to be formed with thermal kinetic energies, certain ions are formed with kinetic energies slightly in excess of thermal. Among these are H₂⁺(He*+H₂); D₂⁺(He*+D₂); O₂⁺, O⁺(He*+O₂); and NO⁺(He*+NO). H₂ and D₂⁺ were each found to have approximately 1.3 times thermal energy with H₂⁺ being slightly larger. For the reaction He*+O₂, O₂⁺ was found to have about 1.3 times thermal energy while the O⁺ fragment possessed ca. 2.5 times thermal energy. The behavior of NO⁺ was found to be similar to that of O₂⁺. Very small amounts of O⁺ from the reaction 2^1S He*+NO were also detected.

*Supported by the National Science Foundation.

¹J.A. Herce, J.R. Penton, R.J. Cross and E.E. Muschlitz, Jr., J. Chem. Phys. 49 958(1968).

P3. De-Excitation Rate Constants for Helium Meta-stable Atoms with Several Atoms and Molecules. A. L. SCHMELTEKOPF, ESSA Research Laboratories. The de-excitation rate constants for He(2^1S) and He(2^3S) metastables have been measured with the following gases: Ne, Ar, Kr, Xe, H₂, D₂, N₂, CO, NO, O₂, CO₂, NO₂, NH₃, SF₆, CH₄, C₂H₆, C₃H₈, and C₄H₁₀. These rate constants were measured in a flowing afterglow using the Neon 5689.8 Å and 7032.4 Å lines as detectors for the He(2^1S) and He(2^3S), respectively. In all of the above cases the He(2^1S) rate constants were the order of 2 to 3 times faster than those of the He(2^3S). The implications that these results have on the interpretation of data from Penning ionization electron spectroscopy will be discussed.

P4. Penning Cross Sections for He^M-Cd Collisions
L. D. Scheerer and F. A. Padovani, Texas Instruments, Incorporated.--The rate at which helium metastable atoms are quenched by cadmium atoms in a pulsed afterglow has been measured as a function of cadmium vapor pressure. At low vapor pressures the metastable density is monitored by absorption of 1.08 μ resonance radiation. At higher temperatures emission of cadmium ion radiation at 4416 Å and 3250 Å is observed. The decay of both levels follows the metastable loss indicating that Penning collisions between He^M and Cd atoms is the primary source of ion excitation. The quenching cross section is $3.2 \pm 0.1 \times 10^{-15} \text{ cm}^2$ at 200°C. The optical emission spectra of Cd⁺ resulting from the Penning collisions is obtained in a fast flowing afterglow and relative excitation rates for some of the levels is measured.

P5. Polarization of Ions and Electrons via Penning Collisions with Optically Pumped Metastable Helium Atoms. L. D. Scheerer, Texas Instruments, Incorporated.--Penning collisions between optically oriented metastable helium atoms and Group II atoms in a flowing afterglow yield polarized ions and electrons. The polarization of excited state ions is detected by monitoring the optical polarization of the light emitted by the ion as it decays radiatively. The polarized ions of Cd, Zn, Mg, Ca, Sr, and Ba have been observed in this manner. The ground state ion polarization is observed by monitoring circularly polarized ion resonance radiation transmitted through the reaction region. The magnetic resonance of Sr^+ and Ba^+ in the ground state has been detected in this manner. The ion density is on the order of $10^{10} - 10^{11} \text{ cm}^{-3}$ with a flow velocity of 10^4 cm sec^{-1} . The polarization of the Penning electron is detected by the spin polarization induced in sodium atoms following spin exchange collisions.

P6. Rotational Structure of N_2 2nd Positive Bands in Penning Excitation by Argon Metastable Atoms.* WHEELER K. MCGREGOR, JR., ARO, Inc., Arnold Air Force Station, Tenn.--The rotational structure of 2nd Positive bands of N_2 resulting from Penning excitation by collisions with metastable A atoms exhibit an alternation in intensities of successive rotational lines. In this study band spectra having rotational lines out to $K \sim 70$ were produced in the boundary of a low density, argon arc-jet plume by flowing a cold nitrogen sheath around the plume. The alternation of $I(K-1):I(K)$, where K is even, was found to be about 1.35:1 for all branches in a band. This alternation is explained by allowing for Q-branch excitation transitions from the $X^1\Sigma_g^+$ to the $C^3\Pi_u$ levels of N_2 as well as P- and R-branch transitions. Budó's† rotational strength factors for $1\Sigma \rightarrow 3\Pi$ transitions contain a constant, λ , usually taken as zero. The alternation ratio found experimentally requires that $\lambda \approx 0.9$.

*Research supported by Arnold Engineering Development Center, AFSC, under Contract No. F40600-69-C-0001.

†A. Budó, Z Physik 105, 579 (1937).

SESSION Q

Thursday Afternoon, 30 October

2:00 p.m.

HEAVY PARTICLE COLLISIONS I

Chairman: *D. W. Martin*, Georgia Institute of Technology
Atlanta, Georgia

Q1. Electron Transfer in O-Cs Collisions.* B. W. WOODWARD, W. C. LINEBERGER, and L. M. BRANSCOMB†, Joint Institute for Laboratory Astrophysics.--A crossed atomic beams measurement of the absolute cross section for the reaction $O + Cs \rightarrow O^- + Cs^+$ has been made for both the $3P$ and $1D$ states of the O atoms. The O atoms are obtained by photodetachment from a 1 keV negative ion beam using high power pulsed lasers. By a suitable choice of laser wavelength, O atoms are produced either entirely in the ground $3P$ state or with a known fraction in the metastable $1D$ state. The fraction of negative ions undergoing photodetachment is great enough that the absolute neutral flux can be determined by measuring the loss in the negative ion beam with a gated detector. The Cs beam is a collimated thermal beam produced in an effusive source. The reactant species, both charged particles, are electrostatically separated from the neutral atoms and accelerated to approximately 5 keV for detection by open electron multipliers of the venetian blind type. Individual events are counted in both channels, and delayed coincidence is employed to provide a high signal-to-noise ratio. Comparison is made with relevant theory.

*Work supported in part by the Advanced Research Projects Agency and in part by Bell Telephone Laboratories.

†Staff member, National Bureau of Standards.

Q2. Experimental Observation of Ion Impact Excitation of Pure Vibrational and Electronic Transitions in Diatomic Molecules,† JOHN H. MOORE, JR.* and JOHN P. DOERING, The Johns Hopkins University - An ion impact spectrometer has been constructed to measure the energy loss of ions inelastically scattered without charge exchange from molecular targets. H^+ and H_2^+ scattered from H_2 , D_2 and N_2 have been observed to have energy losses corresponding to pure vibrational transitions in the target molecules. The angular distribution of the scattered ions and the pressure dependence of the ion current were measured to determine the cross-sections for vibrational excitation. These cross-sections are unusually large. The (0-1) transition in H_2 was excited by 100-600 eV protons with a cross-section of $(1.7 \pm 0.5) \times 10^{-16} \text{cm}^2$. There was no detectable energy dependence. For 150 eV protons on N_2 , the cross-section for excitation of the (0-1) transition was estimated to be $3.6 \times 10^{-17} \text{cm}^2$. Less intense peaks corresponding to excitation of electronic levels were also observed in the energy loss spectra of several diatomic molecules. Some of the observed electronic transitions are optically forbidden.

†Work supported by the National Science Foundation

*Present address: Dept. of Chemistry, Univ. of Maryland

Q3. Analysis of Kinetic Energy Loss in N^+-A and O^+-Kr Collisions at keV Energies.* H. C. HAYDEN and E. J. KNYS-TAUTAS[†], University of Connecticut, Storrs, Ct., 06268.

Kinetic energy loss distributions have recently been reported for the large angle scattering reaction $N^+ + A \rightarrow N^{+m} + A^{+n} + (m+n-1)e$, and for the similar O^+-Kr reaction. The data are shown to be consistent with the assumption that, given an incident energy and a scattering angle, the energy received by the nitrogen follows a Gaussian distribution centered at \bar{E}_m' , and that this distribution is independent of the charge state n of the recoiling A^{+n} . A similar statement holds for the argon. The average kinetic energy loss $\bar{Q}_{mn} = \bar{E}_m' + \bar{E}_n''$. It is also shown that the Q -value varies linearly with the spectroscopic energy deficits specifying an (m,n) event: $\bar{Q}_{mn} = A + BU_m' + CU_m''$. Taking the energy term A to be equally distributed among the outer electrons in the colliding species allows calculation of the individual \bar{E}_m' and \bar{E}_n'' .

*The work was sponsored by the U.S. Air Force of Scientific Research.

[†]Now at Department de Physique, Universite Laval, Quebec
¹E. J. Knystautas, Q. C. Kessel, R. Del Boca, and H. C. Hayden (submitted to Physical Review).

Q4. Small-Angle Scattering of Stripping Collisions of Hydrogen Atoms on Various Gases.* H. FLEISCHMANN, Cornell University, C. F. BARNETT, J. A. RAY, Oak Ridge National Laboratory.--A beam of neutral hydrogen atoms with energies between 1.0-10 keV was produced by neutralization of a H^+ beam in hydrogen and oxygen. Using this beam and an open-ended collision chamber, the angular spread from collisions with He, Ar, Kr, H_2 , O_2 , H_2O , CO_2 and C_6H_6 was measured for angles up to 100 mrad with an angular resolution of 1 mrad at large and 2 mrad at low energies. All distributions were found to fall rapidly and smoothly with scattering angle. For N_2 and similarly for the other heavy gases, the $(1/10)$ -intensity angle increased from 2 mrad at 10 keV to 8 mrad at 1 keV. The distributions were decreased approximately a factor of 2 for collisions with H_2 and He.

*Research sponsored by the U. S. Atomic Energy Commission under contract with the Union Carbide Corporation.

Q5. Total Cross Section for Single Electron Loss by Ne and Ar in Nitrogen, Oxygen, and Air.* G. J. LOCKWOOD, Sandia Laboratories --Measurements of the total cross section for electron stripping σ_{01} of Ne and Ar in N_2 , O_2 , and air are reported here in the energy range of 25 keV to 90 keV. The method used was the direct detection of the fast ions formed in single electron stripping collisions. Ions produced in an rf ion source of the Oak Ridge type were neutralized by charge exchange prior to the collision chamber. The collision chamber geometry was such that all particles scattered into a cone of half-angle 1° were detected by a secondary electron detector. For all combinations the cross sections are observed to increase with increasing velocity. The dependence of the σ_{01} cross section on the neutralizing gas was measured by charge exchanging the ion in N_2 or air and its parent gas. In all cases studied the values of σ_{01} for neutrals formed in their parent gas were less than or equal to the value of σ_{01} for neutrals formed in N_2 or air. As expected, the cross section σ_{01} for Ne in air was found to equal 80 percent of σ_{01} for Ne in N_2 plus 20 percent of σ_{01} for Ne in O_2 .

*Work supported by the U. S. Atomic Energy Commission.

Q6. Ionization of Atomic and Molecular Gases by 1-25 keV Hydrogen Atoms.* R. J. McNeal, D. C. Clark, and R. A. Klingberg, Aerospace Corporation. - Cross sections have been measured for the production of positive ions and electrons in collisions between 1-25 keV hydrogen atoms and He, Ne, Ar, Kr, Xe, H_2 , and O_2 . Above 10 keV the data are in good agreement with previous, higher-energy measurements.¹ For He, Ne, Ar, and H_2 the results for electron production at 1 keV agree well with measurements in the range 50-1000 eV. Positive ions are produced by ionization and capture collisions and electrons by ionization and stripping. Ionization cross sections are obtained for the target gases by combining the present results with previous measurements of capture and stripping cross sections.³

*Work done under USAF Contract No. FO4701-68-C-0200

¹E. S. Solov'ev, R. N. Il'in, V. A. Oparin, N. V. Fedorenko, Soviet Phys. JETP 15, 459 (1962).

²H. H. Fleishman, R. A. Young, Phys. Rev. 178, 254 (1969).

³J. F. Williams, Phys. Rev. 153, 116 (1967).

Q7. Analytic Cross Sections for Inelastic Collisions of Protons and Hydrogen Atoms with Atomic and Molecular Gases.*

A. E. S. Green, University of Florida, and R. J. McNeal, Aerospace Corporation. - Convenient analytic formulas are given for inelastic cross sections for collisions of protons and hydrogen atoms with atomic and molecular gases in the 0.5 keV - 5 MeV energy range. The formulas, adaptations of those used in theoretical studies in the Born region, the intermediate energy region, and the low energy region, conveniently span the broad energy range important in atmospheric physics, astrophysics, radiation physics, and plasma physics. The parameters of the formulas are evaluated for noble and atmospheric gases with the aid of electron impact data and recent experimental results of proton and hydrogen atom impact. The systematics of the parameters are discussed.

*Work supported in part by AEC Contract No. AT-(40-1)-3798 and USAF Contract No. FO4701-68-C-0200.

SESSION R

Thursday Afternoon, 30 October

4:00 p.m.

RARE GAS LASERS

Chairman: *R. H. Bullis*, United Aircraft Research
Laboratories, E. Hartford, Connecticut

R1. Electron Collisional Processes in Argon Ion Laser Discharges.* W. C. JENNINGS, J. H. NOON, E. H. HOIT, Rensselaer Polytechnic Institute, and R. G. BUSER, U. S. Army Electronics Command, Fort Monmouth.--Predicting excitation of ion laser energy levels due to collisions between electrons and both neutral and ionized atoms, requires knowing the relative importance of different collisional processes which determine the mobility and mean free path of the electrons. A modified Tonks-Langmuir theory has been successfully applied to the high current density low pressure discharge required for the argon ion laser in order to calculate laser level pumping rates and expected output power. The relative importance of electron-neutral and electron-ion collisions are considered using available data on pertinent cross-sections and the theory is compared directly with experimental measurements. For a current density times tube radius product $jR \leq 30$ amps/cm, the optimum gas density for maximum laser output is shown to be determined by electron-neutral collisions, whereas for higher values of jR , electron-ion collisions dominate. The analysis also reveals that radiation trapping effects become significant at high currents.

*Supported by U. S. Army Electronics Command.

R2. Electron Densities from Refractive Index Measurements in CW Argon Ion Laser Plasmas, P. S. ZORY and C. B. ZAROWIN, IBM T. J. Watson Research Laboratory - A three mirror laser interferometer⁽¹⁾ has been utilized to measure the refractive index of a typical cw argon ion laser plasma as a function of pressure and current density. The electron density is obtained from the index measurements at the three probe wavelengths, 0.6328μ , 1.15μ and 3.39μ . This data and its relation to previous measurements⁽²⁾ and calculations⁽³⁾ will be discussed.

- (1) W. J. Witteman, Appl. Phys. Ltrs. 10, 347 (1967)
- (2) V. F. Kitaeva, Yu. I. Osipov, P. L. Rubin and N. N. Sobolev, IEEE J. Quant. Elec., QE5, 72 (1969)
- (3) C. B. Zarowin, Appl. Phys. Ltrs., 15, 36 (1969)

R3. Anomalous Hyperfine Laser Oscillation in the Helium-Iodine Laser.* C. S. WILLETT, Harry Diamond Laboratories. - Oscillation on a number of singly ionized iodine lines in the afterglow of a pulsed discharge in a Helium-Iodine mixture has been studied in which selective excitation is by charge transfer.¹ Oscillation in ionized iodine on the $6p'{}^3D_1 - 6s'{}^3D_1$ transition at 658.5 nm has been obtained simultaneously on three hyperfine components with two components of the $(6p'{}^3D_2 - 6s'{}^3D_1)$ 576.0 nm line. At high iodine vapour pressure oscillation occurs alone on the F 7/2-5/2 transition of the 658.5 nm line. This component has a lower theoretical intensity than the F 7/2-7/2 transition. With decreasing pressure oscillation commences on the F 7/2-7/2 transition, finally oscillating alone on this transition. As the two components have a common upper level the change in oscillation is not due to variation in population of upper-level sub-levels and can be attributed to non-equilibrium in sub-levels of the lower $6s'{}^3D_1$ level. Additional transitions into the F 7/2 or 5/2 levels cannot account for the oscillation behavior.

*Work conducted at the University of York, England with support by the Culham Laboratory.
¹G.R.Fowles and R.C.Jensen, Appl. Optics, 3, 1191(1964).

R4. The Effect of Helium on Population Inversion in He-Ne Laser Discharges. R. T. YOUNG, C. S. WILLETT, and R. T. MAUPIN, Harry Diamond Laboratories. - In a previous paper¹ we reported on a comparison of excitation rates of Ne 3s (Paschen notation) levels due to the two processes: $He^*(2^1S_0) + Ne \rightarrow He + Ne(3s_{2,3,4,5})$ and $Ne + e \rightarrow Ne(3s_{2,3,4,5}) + e$. This paper reports on an extension of our previous work to the processes $He^*(2^3S_1) + Ne \rightarrow He + Ne(2s_{2,3,4,5})$ and $Ne + e \rightarrow Ne(2s_{2,3,4,5}) + e$. The ratios of the excitation rates due to He metastables to the excitation rates due to electrons were obtained from spectral intensity measurements on discharges in He-Ne mixtures and in pure Ne with the pD values for the two cases adjusted to maintain the same electron temperature. For discharges representative of lasing conditions at 632.8 nm (He:Ne=5:1, pD=4 Torr-mm, j=130 mA cm⁻²) the ratios of the excitation rates for the Ne 3s levels are: 3s₂-7₂, 3s₃-4₄, 3s₄-7₇, 3s₅-7₇. For conditions representative of lasing conditions at 1.15 μm (He:Ne=10:1, pD=7.7 Torr-mm, j=130 mA cm⁻²) the same ratios for the Ne 2s levels are: 2s₂-11₁₁, 2s₃-20₂₀, 2s₄-5₅, 2s₅-10₁₀.

1. R. T. Young, Jr., C. S. Willett, R. T. Maupin, Bull. Am. Phys. Soc. Series II, 13, 206 (1968).

Robert T. Young
 Jr.
 545-6700

Faded text at the top of the page, likely bleed-through from the reverse side.

SESSION S

Friday Morning, 31 October

8:30 a.m.

PHOTONS AND MOLECULAR STRUCTURE

Faded text block, likely bleed-through from the reverse side.

**Chairman: F. R. Gilmore, Rand Corporation
Santa Monica, California**

Faded text block, likely bleed-through from the reverse side.

Faded text block, likely bleed-through from the reverse side.

S1. Afterglow Properties of Nitrogen Emission Bands Due to Transitions from Triplet States.*

A.R. DEMONCHY, G.N. HAYS, C.J. TRACY and H.J. OSKAM, University of Minnesota.--The properties of the emission intensities of the Vegard-Kaplan ($A^3 \Sigma_u^+ \rightarrow X^1 \Sigma_g^+$), second positive ($C^3 \pi_u \rightarrow B^3 \pi_g$), and Goldstein-Kaplan ($C^1 3 \pi_u \rightarrow B^3 \pi_g$) bands have been studied during the decay period of plasmas produced in nitrogen and helium-nitrogen mixtures. The time dependence of the densities of the various charged particles was determined using a quadrupole mass spectrometer. The second positive band emissions are due to mutual collisions between molecules in the A state. This was also found previously.¹ The intensity of the Goldstein-Kaplan band was found to be also determined by the A state. Detailed studies of the first positive system strongly indicated that more than one process determines its emission properties. Processes occurring at the wall of the plasma container seem to influence the emission spectrum during the late afterglow period.

*Work supported by the National Science Foundation and the Air Force Cambridge Research Laboratories.

¹Zipf, E. C. Bull. Am. Phys. Soc. 13, 219 (1968). D. H. Stedman and D. W. Setser, J. Chem. Phys. 50, 2256 (1968).

S2. Non-radiative Transport of Resonance Excitation Energy in Metal Vapors.* A.V. PHELPS and C.L. CHEN, Westinghouse Research Laboratories--Theoretical calculations of the kinetic diffusion coefficient and of the effective diffusion coefficient for excitation transfer or "hopping" for atoms excited to a resonance level have been used to estimate the effect of these processes on the magnitude and spectral distribution of backscattered resonance radiation. The kinetic diffusion coefficient varies as the reciprocal of the vapor density N while the effective diffusion coefficient for excitation transfer varies as $N^{1/3}$. In cesium vapor these coefficients are equal for densities near 10^{17} atom/cm³. Experimental evidence for the importance of non-radiative transport has been obtained from the spectral distribution of the backscattered radiation with white light incident on cesium vapor at densities of 1×10^{16} and 5×10^{16} atom/cm³. The importance of non-radiative transport is greatly enhanced when a narrow line source is used as in the experiments with the 2537 Å line of mercury vapor by Hansen and Webb.¹

*This work was supported in part by the Office of Naval Research.

¹J.M. Hansen and H.W. Webb, Phys. Rev. 72, 332 (1947).

S3. Standard Light Sources for the Vacuum Ultraviolet Region. T. E. STEWART, J. E. PARKS, G. S. HURST, T. E. BORTNER, F. W. MARTIN, University of Kentucky.--A method has been developed to determine the absolute intensity of photons excited by the passage of a beam of charged particles (e.g. protons) through a gas. For instance, it is known¹ that a proton beam passing through argon gas will excite a strong continuum in the region 1100-1400 Å and that this continuum originates from Franck-Condon emission in the two-body collision of $\text{Ar}(^1P_1)$ with $\text{Ar}(^1S_0)$. To achieve absolute calibration of the total number of photons emitted per cm of proton track, a channel electron multiplier (CEM) was used in a simple geometry to view the photons excited by 4 MeV protons from a van de Graaff accelerator. In such an arrangement the number of counts at gas pressure P is given by $C(P) = Ak(P) \int d\lambda s(\lambda)W(\lambda)n(\lambda)$ where $k(P)$ is the number of photons emitted per proton, A is a geometric constant, $s(\lambda)d\lambda$ is the normalized spectrum of photons, $W(\lambda)$ is the transmission of any windows required in the photon beam, and $n(\lambda)$ is the efficiency of the photon detector. From the measured $k(P)$ and $s(\lambda)$ one can determine $S(P,\lambda)d\lambda$ which is the number of photons emitted into 4π solid angle in the wavelength region between λ and $\lambda+d\lambda$ (per cm of track length).
¹G. S. Hurst et al., Phys. Rev. 178, 4 (1969).

S4. Emission from Metastable States in a Nitrogen Ion Beam.* WILLIAM B. MAIER II and R.F. HOLLAND, Los Alamos Scientific Lab.--Nitrogen ions are produced by electron impact on N_2 , confined by a magnetic field, accelerated, and directed down a tube. Observations of radiation from the beam are made with a photometer sensitive in the range 1050 to 3200 Å and with a spectrometer. Long-lived states in the ion beam are observed to radiate in the wavelength range 1700 to 3200 Å. Two lifetimes, 4.4 ± 2.0 and 44 ± 11 μsec, have been measured. The electron energy dependence of the excited radiation is similar to the energy dependence previously observed for the production of N_3^+ when N_2 is bombarded by electrons. Preliminary spectra show several features originating from the ion beam; these spectral data are briefly discussed.

*Work conducted under the auspices of the U.S. Atomic Energy Comm. and partially supported by the Advanced Research Projects Agency.

55. Experimental Values of Some ArII Transition Probabilities.* N.M. NERHEIM, JPL, and H.N. OLSEN, Plasma Sci. Lab.--Experimental transition probabilities of a number of ArII spectral lines have been determined from observations of a 1.1 atm free-burning arc. Techniques used in previous work¹ were modified to allow observations of lines in the uv spectral region and thereby extend the previous results to include the stronger lines with both 4p and 4d upper energy levels. The range of the upper energy levels of the lines studied is 5.6 eV. The transition probabilities obtained for the lines with the higher energy levels are lower than published theoretical² values by nearly a factor of 2 and higher than the available experimental³ values by about a factor of 4. In addition, the ArII transition probabilities found in the literature are compared by considering their use in plasma temperature measurements and estimating the temperature uncertainties that may be attributed solely to the difference in the transition probabilities.

*Work supported by NASA, Contract NAS7-100

¹H.N. Olsen, JQSRT, 3, 305 (1963)

²R.I. Rudko, C.L. Tang, J. Appl. Phys., 38, 4731 (1967)

³M.U. Beth, et. al., Z. Naturforschg., 21a, 1203 (1966)

56. Lifetimes of the $A^2\Sigma^+$ State of NO.* G.E. COPELAND, R.T. THOMPSON, and R.G. FOWLER, University of Okla.--The lifetimes of the $v'=0,1,2$ levels of the $A^2\Sigma^+$ state of NO have been measured by monitoring 19 transitions of the NO γ bands. A new cold cathode discharge tube was used in conjunction with the delayed coincidence technique for measurement of lifetimes. A non-linear least squares program was used for data analysis in order to estimate cascade contributions. No pressure dependence of the lifetimes is observed for pressures less than 200 microns Hg. Tentative values for lifetimes are $\tau(v'=0) = 99.8 \pm 5.5$ nsec, $\tau(v'=1) = 104. \pm 6.6$ nsec, and $\tau(v'=2) = 93.6 \pm 7.9$ nsec. These results are about one half previous values.⁽¹⁾ Using Morse potential Franck-Condon factors,⁽²⁾ the electronic transition moments are calculated to be 0.244, 0.231 and 0.236 (A.U.).

*Work supported by Kirtland AFB, New Mexico, F29601-67-0035.

¹M. Jeunehomme, J. Chem. Phys. 45, 4433 (1966).

²H.A. Ory, A.P. Gittleman, J.P. Maddox, Astrophys. J. 139, 346 (1964).

S7. Emission Spectra of Electron Bombarded Gaseous and Liquid Helium.* G.K.WALTERS, W.S.DENNIS[†], E.DURBIN, JR., W.A.FITZSIMMONS[‡], and O.HEYBEY, Rice Univ.--In the course of studies of the possible existence of localized excitations in simple liquids, we have recorded unexpected features in the optical and infrared emission spectra of dense helium gas and liquid helium bombarded by 160 kev electrons. We identify spectra of excited atomic and molecular helium in both gas and liquid, with only slight wavelength shifts in each case relative to the free species. The features are appreciably broadened in the liquid, but rotational and vibrational structure is surprisingly apparent. The metastable 2^3S_1 atomic and a $3^3\Sigma_u^+$ molecular states are efficiently populated, and may exist for long periods in the liquid without de-excitation. These results are particularly interesting because many of the molecular states observed have electron orbits that are much larger than the 3.7 Å average spacing of helium atoms in the liquid, thus suggesting the existence of stable microscopic local voids (or "bubbles") in which the molecules reside.

*Work supported in part by the U.S. Atomic Energy Comm.

[†]Present address: Biology Dept, Yale University

[‡]Present address: Physics Dept, U. of Wisconsin

S8. Multiple Electron Ionization of Neon by Electron and Photon Impact.* M. O. KRAUSE, F. A. STEVIE,† L. J. LEWIS,‡ T. A. CARLSON and W. E. MODDEMAN, Oak Ridge National Laboratory.--According to the shakeoff (sudden approximation) concept, multiple electron excitation and ionization relative to single ionization is to be independent of the primary excitation mode, provided electron correlation is negligible and excitation energy sufficiently high. By way of the K-Auger spectrum of neon we show that this holds true for photon energies greater than about $1.3 E_{KL}$ and for electron energies $\approx 3E_{KL}$ where E_{KL} is the ionization energy of a KL electron pair. In either case multiple excitation and ionization occurs in nearly 20% of the events.

*Research sponsored by the U. S. Atomic Energy Commission under contract with the Union Carbide Corporation.

[†]AEC Health Physics Fellow Vanderbilt University

[‡]Summer Student Morehouse College, Atlanta, Georgia.

S9. High Resolution Measurement of S⁻ Photodetachment Near Threshold.* W. C. LINEBERGER, B. W. WOODWARD, and L. M. BRANSCOMB†, Joint Institute for Laboratory Astrophysics.--The cross section for photodetachment of S⁻ has been measured with a resolution of approximately 1 Å in the region within 0.15 eV of threshold. The measurements were made with a crossed beam apparatus employing a tunable organic dye laser as the light source. Typical photon outputs are 10¹⁶ photons in 0.3 μsec with approximately 1 Å bandwidth. The S⁻ ions are extracted from a discharge in COS and are accelerated to 1 keV prior to entering the photodetachment region. The photodetachment rate is determined by time-gated detection of the fast S atoms with a windowless electron multiplier. The use of the tunable dye laser provides at least two orders of magnitude better resolution than the best previously attainable in crossed beam photodetachment studies. Structure in the photodetachment cross sections resulting from the spin-orbit splittings of both the S⁻ and S ground states is clearly resolved. Measurements of the electron affinity of S and the ²P_{3/2,1/2} splitting of the S⁻ ground state are reported.

*Work supported in part by the Advanced Research Projects Agency.

†Staff member, National Bureau of Standards.

S10. Photoelectron Spectra of Diborane. T. L. ROSE,* R. FREY, and B. BREHM, Physics Institute, University of Freiburg, Germany.--The energy levels of the electronic states of the diborane ion have been measured using photoelectron spectroscopy techniques. A molecular beam of diborane is crossed at right angles by a monochromatic light beam of 21.21 eV. The kinetic energy of the electrons ejected perpendicular to the plane of the crossed beams is measured by the retarding potential method using a planar grid. Energy resolution of the spectrometer for photoelectrons from argon is better than 10 meV. Five electronic states are found for diborane of which only the next to the lowest energy state exhibits any resolvable vibrational structure. The adiabatic ionization potential for the first state is 11.37 ± 0.01 eV. The observed vibrational structure of the second state leads to D (BH₃⁺-BH₃) ≤ 1.5 eV. The assignment of the molecular orbitals vacated for each ionic state will be discussed and compared with the theoretical calculations of Buenker, et al.¹

*Present address: Department of Chemistry, Texas A&M University

¹R. J. Buenker, S. D. Peyerimhoff, L. C. Allen and J. L. Whitten, J. Chem. Phys., 45 2835 (1966).

S11. Energy Analysis of Electrons Ejected in Slow Ion-Atom Collisions. G. GERBER, R. MORGENSTERN, A. NIEHAUS, Universität Freiburg. - We report on first results obtained with an apparatus designed for the investigation of Slow Ion-Atom Collisions, processes of the kind $A^+ + B \rightarrow A^+ + B^+ + e^-$. The measured energy spectra of electrons ejected in collisions of Ar^+ ions with Ar (and He^+ with Ar) at ion energies from 200 eV to 3 keV consist of a low energy part, extending from 0 to ca. 9 eV and a high energy part, extending from 9 to ca. 16 eV. The low energy part shows weak oscillatory structure. The high energy part shows pronounced peaks strongly dependent on ion energy. The structure in the energy range above 9 eV can be explained by autoionization of superexcited neutral Ar atoms at large separations of Ar^+ and Ar, in the states $\dots 3s3p^0ns, np$ and $\dots 3s^2 3p^4 4sns, np$. To the portion of the spectrum below 9 eV, process $A^+ + B \rightarrow A^+ + B^+ + e^-$ as well as process $A^+ + B \rightarrow A^+ + B^+ + e^-$, if it occurs at small separations, can contribute. However, a contribution of autoionizations at large separations can be excluded. Therefore the spectrum should be continuous in this region, and it is interesting that in spite of this some reproducible structure is resolved.

S12. Calculation of the Doubly Excited Autoionizing States of H_2 . A. U. HAZI, UCLA, and H. S. TAYLOR, University of Southern California. -- We have applied the stabilization method¹ of calculating resonance energies to the doubly excited autoionizing states of H_2 . For fixed internuclear separations the exact electronic Hamiltonian of H_2 was diagonalized in sets of exponentially decaying elliptic basis functions. The energies of the autoionizing states were calculated as a function of the internuclear separation. We have carefully examined the region in which the potential curves of the autoionizing states cross the potential curve of the $2\Sigma_g^+$ of H_2^+ . In order to obtain reliable results we studied the convergence properties of the several basis sets used in the calculations. The potential curves obtained in the present work will be compared to those obtained by O'Malley² using the projected atomic orbitals procedure. The role of autoionizing states in the dissociative excitation of H_2 and H_2^+ will be discussed.

¹H. S. Taylor, Adv. in Chem. Phys., to be published.

²T. O'Malley, VI. International Conference on the Physics of Electronic and Atomic Collisions, MIT, 1969.

S13. Inelastic Rotational Collisions in Alkali Dimers.
 M. McClintock, National Bureau of Standards and Dept. of
 Physics, U. of Colorado and W. Demtroder*, Joint Institute
 for Laboratory Astrophysics, Boulder, Colo.

Laser excitation of selected molecular states, provides a new spectroscopic technique for the study of certain collision processes in precise detail. The homonuclear molecule Na_2 has been excited to the $v'=6, J'=43$ level of the $B^1 \Pi_u$ state by the 4880\AA line of the argon laser, and well resolved spectral lines in emission have been observed which originate from adjacent levels populated by single collisions while in the excited electronic state. Both odd and even ΔJ collisions have been observed to as high as $\Delta J=+5$. Lines arising from odd ΔJ collisions are preferentially polarized perpendicular to the electric vector of the exciting radiation, as a consequence of the fact that the transition moment for P & R transitions is perpendicular to that for Q transitions. Depolarization of spectral lines, and therefore molecular reorientation, increases monotonically with ΔJ . As a consequence of parity conservation, lambda components do not mix in any of the observed collisions.

* physikalisches Institut der Universität, Freiburg,
 Germany

S14. The Enhancement of H α (6563 \AA) Radiation In A Neon-Hydrogen Pulsed Discharge, JOHN A. McINALLY, Xerox Research Laboratories, Rochester, N.Y. - The visible spectral output of pulsed discharges in pure hydrogen and mixtures of neon-hydrogen has been studied. In a 20% hydrogen mixture at 50 Torr the H α radiation was enhanced 2.5 times and H β and H γ to a lesser degree over a discharge of similar characteristics in pure hydrogen. A continuum to the violet side of H γ was also enhanced 2.5 times in the mixture, while the remaining continuum remained constant. A study of the line shapes of the Stark-broadened Balmer lines indicated that the hydrogen in both cases was about 50% ionized. An LTE temperature of about $15,000^\circ\text{K}$ was deduced for both discharges using corrected Saha-Eggert equations. However, line intensity ratios, line to continuum ratios and continuum to continuum ratios led to anomalous results indicating that LTE may not be applicable. The enhanced line spectrum might be explained on the basis of selective excitation of H_2^+ . Neon $1s_5$ metastables of 16.6 e.v. are in close resonance with vibrational states of H_2^+ ($1s \sigma g$) and could excite H_2 to them in collisions of the second kind. Subsequent ion-electron recombination and system crossing to repulsive states could account for the increased density of excited atoms.

SESSION T

Friday Morning, 31 October

8:30 a.m.

GLOWS AND DISCHARGES

Chairman: *A. Garscadden*, Wright-Patterson AFB
Ohio

T1. The Coulomb Logarithm for Ions Slowing Down on Electrons in a Plasma.* J. RAND McNALLY, JR., Oak Ridge National Laboratory.--The slowing down of ions due to collisions with a sea of electrons is frequently expressed in terms of an energy loss rate

$$\frac{dW}{dt} = \frac{4\pi z^2 (\Delta n_-) e^4}{mv_+} \ln \frac{b_{\max}}{b_{\min}}$$

where $\Delta n_- = \int_0^{v_- = v_+} f_- dE_-$ and b_{\max} and b_{\min} are the maximum

and minimum impact parameters. The Coulomb logarithm is usually defined in terms of $b_{\max} =$ Debye distance $= \sqrt{kT_- / 4\pi n_- e^2}$ and $b_{\min} \sim Ze^2 / 3kT_-$. It will be shown that these parameters are better describable as $b_{\max} = \sqrt{m_+ v_+^2 / 12\pi n_- e^2}$ and $b_{\min} = Ze^2 / m_+ v_+^2$. The new expressions are especially important in moderate temperature plasmas (10^4 - 10^7 °K) and can give rise to gross discrepancies between T_+ and T_- .[†] In fusion type plasmas ($T > 10^8$ °K) the error is not nearly as large (except for high Z and very high densities) but may account for a significant error since in general $v_+ \ll \sqrt{3kT_- / m_-}$.

*Research sponsored by the U.S. Atomic Energy Commission under contract with the Union Carbide Corporation.

1. J. Rand McNally, Jr., Plasma Physics 10, 903 (1968).

T2. A New Method for Solving the Kinetics of Gas Discharges for Atoms with Many Energy Levels. W. G. VALANCE*, and A. HELLER, General Telephone & Electronics Laboratories Inc., Bayside, N. Y. - A theoretical method for estimating the overall emission from a non-equilibrium gas discharge was developed. The kinetic equations for the discharge are solved for many-level atoms by many shot expansion techniques. The use of the concept of stochastic processes accounts accurately for collisional excitation, deexcitation, and emission processes. The technique allows the estimation of the emittance of low and medium pressure discharges in specific spectral lines or specific spectral regions at defined electron temperatures.

* Present address: Boston College, Newton, Mass.

T3. A Variational Solution for the Positive Column Characteristic Curve. FREDERICK J. MAYER, Case Western Reserve University.--A "least-squares" variational solution to the coupled, non-linear electron and ion conservation equations is used to predict the characteristic curve for the parallel-plane positive column of a low-density quiescent gas discharge. The well-known asymptotic limits of low and high density corresponding to "free" and "ambipolar" diffusion are shown to agree exactly if one introduces a cross-term mixing parameter, λ . The dependence of the characteristic curve upon the discharge parameters $n_0 = L^2/\lambda_D^2$ (L , width of discharge, λ_D Debye length), τ (ratio of electron to ion temperature), δ (ratio of ion to electron free-diffusion coefficients), and λ is presented in terms of the solutions to a cubic equation. The significance of the approximate results is discussed with regard to numerical integrations for exact solutions.

T4. Measurements of the Relaxation time of Metastable Atoms in a Neon Discharge Using an External Source of Light. G. G. CLOUTIER, J. P. NOVAK AND V. FUCHS, Research Institute of Hydro-Quebec, Montreal.--An external source of radiation was used to produce variations of the metastable atom population in a positive column of a glow discharge in neon. The source of light was another neon discharge tube driven in such a way as to produce a sinusoidal variation of frequency ω of the light intensity. Instantaneous variations of the electron temperature were observed by means of a two probe technique.¹ It was thus possible to measure directly the phase shift ϕ between the variations of the electron temperature of the light intensity. A relation between $\tan \phi$ and ω was derived using Gentle's description of the positive column.² The function $\tan \phi = g(\omega)$ derived from the theoretical analysis is linear and agrees with the experimental results in the frequency range studied. The total relaxation time of the metastable atoms is found to be of the same order of magnitude as the relaxation time derived from the parameters of p-type striations. These results support the suggestion that the p-type striations are controlled by stepwise ionization of metastable atoms.

¹M. G. Drouet, J. Sci. Instr. 44, 1023 (1967).

²K. N. Gentle, Phys. Fluids 9, 2203 (1966).

T5. Time-Resolved Energy Distributions in a Striating Discharge. R.F. WEBER, A. GARSCADDEN and P. BLETZINGER. Aerospace Research Laboratories, WPAFB.--Using a sample-and-hold diagnostic method, time-resolved Langmuir probe measurements have been made in a neon discharge plasma which supported large amplitude moving striations at frequencies of a few kHz. The system has been developed to obtain digital data with an accuracy $>0.3\%$ and compatible with computer reduction. Numerical analysis of the data provides the second-derivative and also calculates the electron energy distribution, having identified space potential from the second derivative. The measurements show that the distribution is non-Maxwellian; in particular, preceding the peak of the light intensity fluctuation, there exists a high energy group of electrons (~ 10 eV). The relaxation of this group through the phase of the striation is demonstrated and examples of the dependence on other discharge parameters are given.

T6. Cataphoretic Segregation Processes in a Non-Penning Gas Mixture. A. K. BHATTACHARYA, General Electric Lighting Research Laboratory.---The ion conversion processes occurring in plasmas produced in krypton admixed with small amounts of xenon was found to be analogous to those in He-Ne gas mixture^{1,2,3}. The ionic mass spectrometric study of plasmas produced in Kr admixed with 0.01% of Xe shows the presence of Kr^+ , Kr_2^+ , Xe^+ , Xe_2^+ and $(XeKr)^+$. A cataphoretic dc discharge (20 to 40 Torr, 40-60 ma) in a 1 meter long Pyrex tube with 8 mm id was able to remove the xenon impurity atoms. Afterglow studies showed that at gas pressures higher than a few torr Kr^+ is rapidly converted into Kr_2^+ , which then produces Xe^+ by charge exchange. Xe^+ is then quickly converted into $(XeKr)^+$ by triple collision with krypton atoms. Finally, $(XeKr)^+$ in collision with Xe and Kr atoms produces Xe_2^+ . The above reaction rates have been determined and were found to be quite large.

1. L. B. Loeb, J. Appl. Phys. 29, 1369 (1958).
2. H. J. Oskam, J. Appl. Phys. 34, 711 (1963).
3. G. F. Sauter, R. A. Gerber and H. J. Oskam, Physica 32, 1921 (1966).

T7. Gas Flows Generated by Noble Gas DC Discharges.
 C. C. LEIBY, JR. and C. W. ROGERS, A.F.C.R.L., Bedford,
 Mass.---Pressure differences (Δp) caused by electropho-
 retically induced gas flows in dc discharges were
 measured in He ($p_0 = 0.04$ to 22.3 Torr), Ne (0.02 to
 26.7), Ar (0.007 to 27.2), Kr (0.006 to 29.74) and Xe
 (0.006 to 53.23) at discharge currents $i = 60, 140$ and
 220 ma. Short term accuracy of our Baratron gage was \sim
 $\pm 0.03 \mu$. Reproducibility was excellent and unaffected by
 discharge current reversal. The 6 mm i.d. experimental
 tube (perimeter: 150 cm) was in the form of a racetrack
 with the discharge occupying one "straightaway" (length:
 53 cm). Δp was measured between the midpoints of the
 "turns". Comparison of Δp values with the high-pressure
 approximation to the Leiby-Oskam theory utilized electron
 temperatures and densities (microwave measurements),
 positive column electric fields (floating probe measure-
 ments), discharge gas temperatures (assumed equal to
 measured wall temperatures), and ion mobilities (pub-
 lished values). Agreement to within factors of 2 or
 better were obtained for He and Ne. For Ar, Kr, and Xe,
 $1 \leq \Delta p(\text{obsrvd})/\Delta p(\text{theory}) \leq 100$, depending upon degree of
 discharge constriction. At $i = 220$ ma, maximum observed
 (room temperature) gas flow velocities were: He, 31.7
 cm/sec; Ne, 30.5; Ar, 49.0; Kr, 35.5, and Xe, 36.6.

T8. Axial Pressure Gradients in DC Discharges with By-
 Pass Connections.* R. B. TOMBERS and L. M. CHANIN,
 University of Minnesota.--Return or by-pass tubes are
 frequently used in certain types of gas lasers to mini-
 mize axial pressure gradients and also cataphoretic
 effects.¹ Measurements have been made of the longitu-
 dinal pressure gradients in dc discharges of helium and
 xenon to determine the reduction achieved, using a
 return connection. Data were obtained for a 50 cm
 sampling length of the positive column of a 0.13 cm ra-
 dius discharge tube. The by-pass connection consisted of
 20 and 169 cm lengths of radii 0.19 and 0.16 cm res-
 pectively. Measurements were made for discharge currents
 varying from 20-100 mA and for gas pressures varying
 over at least one order of magnitude. Comparison of the
 results with the relation recently derived by Oskam,²
 shows good agreement, when gas temperature effects are
 considered.

*Work supported in part by Air Force Cambridge Research
 Laboratories.

¹E. I. Gordon and E. F. Labuda, Bell. Sys. Tech. J.
 43, 1827 (1964).

²H. J. Oskam (to be published Physics Fluids).

T9. Effect of Argon Atoms on Self-Absorption of Hg 2537A Radiation in Hg + Ar Discharges. T. J. HAMMOND & C. F. GALLO, Xerox Research Laboratories, Rochester, N.Y. — As previously reported,¹ the Hg 2537A radiation in Hg + Ar discharges was measured as an independent function of mercury pressure (8×10^{-4} to 3×10^{-2} Torr), argon pressure (5 to 400 Torr) and dc current (80 to 600 ma). Holstein² has shown theoretically that self-absorption depends upon the details of the line shape. We are particularly interested in the effect of argon pressure on the Hg 2537A self-absorption through its influence on the Hg 2537A line shape and width. Our present analysis indicates that there are four ways that additional argon reduces the Hg 2537A self-absorption: (1) The Hg 2537A line gets broader simply because the additional argon atoms increase the Hg-Ar collision frequency, (2) Adding argon causes the gas temperature to rise and this drives the Hg-Ar collision frequency still higher, (3) The rise in gas temperature also causes an increase in the Hg 2537A Doppler width, (4) The additional argon also changes the Hg 2537A line shape from Doppler dominated to a collision dominated profile.

1. T.J.Hammond & C.F.Gallo, Bull. Am. Phys. Soc. 12, 1038 (1967)
2. T. Holstein, Phys. Rev. 72, 1212 (1947); 83 1150 (1951)

T10. Characteristics of a Low-Density Helium Plasma in a Magnetic Field. S. GAVRIL, D. SCHIEBER, and M.S. ERLICKI. Faculty of Electrical Engineering, Technion, Haifa, Israel. — The influence of an external magnetic field (30-2000 Gauss) on a helium glow discharge was investigated. Highly regular dependence of the sparking voltage on the tube pressure in the range of 170-800 μ Hg was obtained with the ratio of gas pressure to magnetic pressure taken as the parameter of each characteristic. Investigation of spectral emissivity for the 3889 Å line as function of the magnetic field yielded the following basic results: (a) the "half-width" of the line remains constant; (b) line intensity increases with the magnetic field; (c) the normalized spectral line power, as function of the tube pressure, exhibits a regular pattern of minima for the magnetic pressure / tube pressure. As regards striations, there appears to be some regularity in their behaviour in weaker fields, whereas in stronger magnetic fields the discharge tends to be homogeneous and the striations are mainly located at the cathode.

T11. Dissociation of Water Vapor in the Positive Column of a Glow Discharge.* K.K. CORVIN and R.M. ST. JOHN, University of Oklahoma.

The electron-impact dissociation of water vapor was investigated in the positive column of a DC glow discharge for pressures between 0.3 and 4 Torr and discharge currents between 0.3 and 0.7 mA. The axial electric field of the positive column was obtained by varying the interelectrode distance in a hollow-cathode discharge. The molecular dissociation rates per unit column length were determined by separating and measuring the pressure of the non-condensable products formed. The accumulation of dissociation products was minimized so that E/p was measured as a function of reduced tube radius pR in essentially pure H_2O . The number of dissociating collisions by an electron drifting through unit length along the field direction were determined; the values of these rate coefficients ranged between 0.025 at an E/p of 34 and 0.65 at $43 \text{ v}\cdot\text{cm}^{-1}\text{Torr}^{-1}$.

*Supported in part by AFOSR-252-67.

T12. Dielectric Constant of an Electron-Free Tl^+I^- Plasma.* P. DAVIDOVITS and J. L. HIRSHFIELD, Yale Univ. — It has been known for some time that efficient photo-dissociation of thallium iodide into the ions Tl^+ and I^- is obtained by illuminating TII vapor with 2100 Å radiation. To date, however, no studies of the dielectric properties of this electron-free plasma have been reported. This paper reports the production of such a plasma, and the measurement of its dielectric properties. This was done by dissociating the TII vapor between the plates of a plane parallel capacitor and measuring the capacitance as a function of frequency. From these measurements the ion density and collision frequency were calculated. With continuous illumination obtained from a zinc spectral lamp, the ion density was $1.02 \times 10^{12} \text{ cm}^{-3}$, and the collision frequency was $1.35 \times 10^7 \text{ sec}^{-1}$. In this region both the kinetic ion-molecule collisions and ion-ion Coulomb collisions are of importance. With a pulsed light source it should be possible to produce a plasma density about a thousand times higher, thus obtaining a system in which the ion collisions are entirely Coulombic.

* This work was partially supported by NSF.

T13. Non-linear Theory of the Positive Column Spiral Instability.* J.N. Shiau and Albert Simon, University of Rochester.--Previous calculations¹ of the positive column spiral instability in the small amplitude regime were based on the quasi-linear approximation. Assuming pure He^+ in the column, the resultant slope of E versus B was in good agreement with experiment² except at the lowest pressure. We have now extended the treatment to include all mode-coupling terms as well as mixtures of He^+ and He_2^+ . The resultant theoretical slopes for pure He^+ and pure He_2^+ bracket the experimental result at all pressures. The percentage mixture required for exact fit varies monotonically with pressure in the expected manner (more He_2^+ at higher pressures). The occurrence of hysteresis at low pressure depends on the mixture ratio, as well. These results suggest the need for measurement of mixture ratios in order to make careful comparison with theoretical calculations. Additional information available from the theory (frequency shift, harmonic amplitudes) should also be measured for comparison.

* Work supported in part by the U.S. Atomic Energy Comm.
¹A. Simon and J.N. Shiau, *Physics of Fluids*, Nov. (1969)
²F.C. Hoh and B. Lehnert, *Proc. Fourth International Conf. on Ionized Phenomena in Gases*, Uppsala (1959)

T14. Energy Distribution of Mo Ions Returning to the Sputtering Cathode in an Argon Glow Discharge.* J. E. HOUSTON, Sandia Laboratories.--Davis and Vanderslice¹ showed that the energy distribution for gas ions incident on the cathode in an abnormal glow discharge could be adequately described by a simple resonant charge exchange model involving as parameters only the dark space length, the resonant charge exchange cross section and the gas pressure. In recent measurements extending this work to higher voltages and low pressures, we have found their model to be applicable to the energy distribution of sputtered atoms which are subsequently ionized and returned to the cathode. Data of this kind are presented for Mo^+ ions in an Argon discharge for a broad range of discharge parameters. The results are fitted to the Davis-Vanderslice theory and calculations made of the average density of Mo atoms in the cathode region.

* This work was supported by the U. S. Atomic Energy Commission.

¹W. D. Davis and T. A. Vanderslice, *Phys. Rev.* 131, 219 (1963).

SESSION U

Friday Afternoon, 31 October

2:00 p.m.

ION-MOLECULE COLLISIONS USING DRIFT TUBES PANEL

Panel Chairman: *E. W. McDaniel*, Georgia Institute of Technology
Atlanta, Georgia

U1. Possible Sources of Large Error in Determinations of Reaction Rates with Drift Tube-Mass Spectrometers.

E. W. McDANIEL, Ga. Inst. of Tech.--Drift tube-mass spectrometers have begun to be used extensively to measure the rate coefficients of ion-molecule reactions. In favorable cases, the accuracy which can be obtained is about ten percent. However, if attention is not paid to a number of factors, large errors can result. The purpose of this paper is to call attention to this fact, and to enumerate the factors which can lead to these large errors. Particular attention is paid to (1) the frequent failure to analyze properly the arrival time spectra of the ions in determining the mobility; (2) the necessity of properly accounting for the different rates of diffusion of the various ionic species, particularly at high E/p ; (3) indiscriminate use of the Wannier expression for average ionic energy; (4) failure to account for mass discrimination in the sampling of the ions at the end of the drift tube; (5) the desirability of having a variable drift distance; (6) the necessity of having ultra high vacuum pumping capability.

U2. Mobilities and Longitudinal Diffusion Coefficients of Mass-Identified Oxygen and Potassium Ions in Oxygen.*

R. M. SNUGGS, D. J. VOLZ, J. H. SCHUMMERS, D. W. MARTIN, and E. W. McDANIEL, Ga. Inst. of Tech.--The mobilities and longitudinal diffusion coefficients of O_2^+ , O^- , O_2^- , and K^+ ions in oxygen have been measured at $300^\circ C$ over an E/N from 6 to $300 \times 10^{-17} V/cm^2$ at pressures from 0.02 to 0.65 Torr using a pulsed time of flight method. The drift tube mass spectrometer on which these measurements were made is basically the same as that described by Albritton et al.¹ The mobilities are determined from the mean arrival time of the ions.¹ The longitudinal diffusion coefficients are determined from the shape of the arrival time histograms.² The zero-field reduced mobilities of O_2 , O^- , O_2^- , and K^+ were determined to be 2.24, 3.15, 2.16, and 2.68 $cm^2/Vsec$, respectively. Each mobility is free of the effects of ion-molecule reactions. The longitudinal diffusion coefficients agree with the values predicted from the mobilities by the Einstein relation at low E/N and increased as E/N was increased.

*Work supported by the Office of Naval Research in Project SQUID, Purdue University.

¹D. L. Albritton et al., Phys. Rev. **171**, 94 (1968).

²J. T. Moseley et al., Phys. Rev. **178**, 234 (1969).

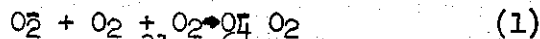
U3. Monatomic and Diatomic Ions in Oxygen.* R. N. VARNEY, Lockheed Palo Alto.--The reaction rates and cross sections for charge exchange reactions of O^- , O^+ , O_2^- , and O_2^+ with O_2 have been measured over a range of values of E/p_0 . The cross section for the O^- exchange rises from 0 at E/p_0 of 20 to 5.1 \AA^2 at E/p_0 of $300 \text{ V}(\text{cm Torr})^{-1}$. For O^+ , the cross section drops from about 2.8 \AA^2 at E/p_0 of 17 to about 1.7 \AA^2 at 35. The resonant charge transfer cross sections for O_2^+ and O_2^- in O_2 are 40 and 25 \AA^2 resp. The mobilities of the molecular ions are in excellent agreement with older observations, but the values for O^- are appreciably higher than those of Beaty¹ and of Eiber.² Comments will be made on a method of producing large currents of O^- ion.

* Work supported by Lockheed Independent Research funds.

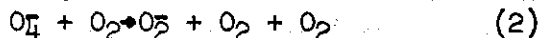
¹E. C. Beaty, L. M. Branscomb and P. L. Patterson, Bull. Am. Phys. Soc. 11,9, 535 (1964).

²H. Eiber, Z. Angew. Phys. 15, 461 (1963).

U4. Drift Velocities and Interactions of Negative Ions in Oxygen, L. G. MCKNIGHT and J. M. SAWINA, Bell Telephone Laboratories Incorporated, Whippany, New Jersey.--Drift velocity measurements in oxygen have been extended to include data on the O_4^- ion. The drift velocity of this ion is virtually identical to that of the O_2^- ion with a low field mobility (μ_N) of $5.6 \times 10^{19} \text{ (volt cm}^{-1} \text{ sec)}^{-1}$ at 315°K . The O_4^- ion is formed from the O_2^- ion in oxygen with a pressure dependence consistent with the reaction:



with a rate constant of $3 \times 10^{-31} \text{ cm}^6/\text{sec}$ at 315°K . Data were taken in a drift tube with time resolution and simultaneous mass analysis of the ion current at E/N between 2 and $40 \times 10^{-17} \text{ volt} \cdot \text{cm}^2$. The reaction rate was measured under conditions where the reaction rate forming O_4^- was much faster than the break-up of the O_4^- ion complex. At the lowest E/N where the ion drift time was long, the reverse reaction:



became important. Equilibrium concentrations of O_2^- and O_4^- were consistent with an equilibrium constant of $1.7 \times 10^{-17} \text{ cm}^3$ at 315°K , in good agreement with previous measurements by Conway and Nesbitt¹; giving a rate of $2 \times 10^{-14} \text{ cm}^3/\text{sec}$ for reaction (2).

¹Conway, D.C. and L.E. Nesbitt, J. Chem. Phys. 48, 509 (1968)

U5. Mobilities of Negative Ions in SF₆. * P. L. PATTERSON, Avco Everett Research Laboratory. -- A multiple shutter ion drift tube was used to measure the mobilities of negative ions formed by a pulsed spark discharge in SF₆. The ions studied were mass identified by means of a differentially pumped quadrupole mass spectrometer. Zero field mobilities of the four ion species, SF₅⁻, SF₆⁻, SF₆⁻(SF₆), and SF₆⁻(SF₆)₂ were found to be 0.595, 0.542, 0.470, and 0.420 cm² V⁻¹ sec⁻¹, respectively. All four experimental mobilities are significantly lower than the values predicted by the Langevin mobility theory in its polarization limit. Previously, the low mobility of SF₆⁻ was assumed to be due to resonant charge transfer with the gas. However, this explanation does not work for the other three ions. Rather, it appears that the observed low mobilities of all four ions is a consequence of the existence of complex internal structure in the ions. Similar deviations from the Langevin theory have been observed for polyatomic ions in several other gases.

*Work supported by the Advanced Research Projects Agency and the Air Force Space and Missile Systems Organization under Contract F04701-69-C-0122.

U6. Theory of Kinetic Ion Temperature. *S.B.WOO, and J.H.WHEALTON, University of Delaware. -- A theory of kinetic ion temperature is formulated. The significance of the theory is demonstrated by its ability to predict, through the use of the Einstein diffusion relationship, both the transverse and longitudinal diffusion coefficient of ions (and therefore their mean random kinetic energy) over a wide range of E/p₀ conditions (1 to 100 volts/cm-torr). Data from Beaty and Woo, and Mosley were used for comparison. Assuming dynamic energy equilibrium of the charged particles, the transverse ion temperature in degrees Kelvin is $T_T = [T_g + \sqrt{T_g^2 + (8A/F)(KE/p_0)^2}] / 2$, where T_g, K, A, F, and E/p₀ refer to neutral gas temperature in degrees Kelvin, reduced mobility in cm²/(volt-sec), reduced ion mass number, fraction of excess kinetic energy transferred to the neutral particle per collision, and the electric field strength over the pressure reduced to 0°C in volts/(cm-torr) respectively. The longitudinal ion temperature is $T_L = T_T + (Mv_d^2) / 2k = T_T + 8.9 \times 10^{-6} M(KE/p_0)^2 T_g$, where D_T, D_L, v_d, M and k refer to transverse and longitudinal diffusion coefficient, drift velocity, ion mass number, and Boltzman constant respectively. Considering the crudeness of the theory, the range of its applicability is surprising. Explanation shall be offered.

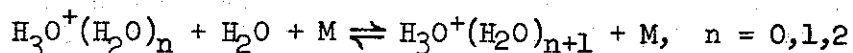
*Research supported in part by Ballistic Research Laboratories, Aberdeen, Maryland.

U7. Drift Tube Measurements of the Formation of Alkali Ion-Water Clusters*. R. JOHNSEN, H. L. BROWN, and M. A. BIONDI, Univ. of Pgh.-The attachment of water molecules to sodium and potassium ions is being studied in a mobility tube-mass spectrometer. Alkali ions produced by a Kunsman type ion source traverse a drift tube filled with water vapor and helium buffer gas where they may attach to the water molecules at near-thermal energy. Clusters of the form $\text{Na}^+(\text{H}_2\text{O})_n$ ($n=1$ to 5) and $\text{K}^+(\text{H}_2\text{O})_n$ ($n=1$ to 4) have been identified in the quadrupole mass spectrometer. Similar values of n were estimated by Munson and Tyndall¹ from the mobilities of clustered ions in rare gases. Assuming that the first clusters, $\text{Na}^+\cdot\text{H}_2\text{O}$ and $\text{K}^+\cdot\text{H}_2\text{O}$ are formed in 3 body collisions only, a 3-body clustering coefficient of $\sim 10^{-29} \text{ cm}^6/\text{sec}$ has been obtained for sodium ions. Surprisingly, the corresponding coefficient for potassium ions appears to be significantly smaller. Difficulties in the determination of water vapor concentrations have so far prevented a more accurate measurement of the rate constants.

*This research was supported, in part, by ARPA through the Army Research Office (Durham), DA-31-124-D-440.

¹R. J. Munson and A. M. Tyndall, Proc. Roy Soc. A172, 28 (1939).

U8. Clustering Reactions of the Hydronium Ion. C. E. YOUNG, D. EDELSON, and W. E. FALCONER, Bell Telephone Labs.-A drift tube with mass spectroscopic analysis was used to investigate the formation and decomposition of hydrates of H_3O^+ . These ion molecule reactions may be represented by



From time-resolved ion fluxes, rate constants and ion mobilities were determined near 350K, the operating temperature of the drift cell, as functions of H_2O concentration and total pressure at low E/p . With Ar as the third body, the rate constant for the hydration of H_3O^+ , $k_{01} = 1 \times 10^{-27} \text{ cm}^6 \text{ s}^{-1}$ and the rate constant for the reverse reaction, $k_{10} = 2 \times 10^{-13} \text{ cm}^3 \text{ s}^{-1}$. Less well defined initial conditions for the higher clustering reactions make estimates of their rate constants less accurate. Similar measurements were made using He as the inert buffer gas to circumvent problems due to long-lived Ar metastables and to investigate the effects of a different third body.

U9. Ionic Processes in Helium-Argon Mixtures.*
 G.E. VEATCH and H.J. OSKAM, University of Minnesota.--
 Ionic processes occurring in helium-argon have been studied by using the afterglow technique. A quadrupole mass spectrometer was used to measure the positive ion wall current. Simultaneous studies of the light emission established the occurrence of the collisional recombination process $\text{Ar}^+ + 2e \rightarrow \text{Ar} + e + h\nu$, while they confirmed the importance of the dissociative recombination process $\text{Ar}_2^+ + e \rightarrow \text{Ar} + \text{Ar} + h\nu$. The only conversion process observed for argon concentrations between 0.01% and 5% was $\text{Ar}^+ + \text{Ar} + \text{He} \rightarrow \text{Ar}_2^+ + \text{He}$. The conversion frequency was found to be $\nu_{\text{conv}} = 100p_0(\text{He})p_0(\text{Ar})$. The value of the mobility of Ar^+ in the helium-argon mixtures obeyed Blanc's Law.

*Work supported by the National Science Foundation and the Air Force Cambridge Research Laboratories.

Faded, illegible text at the top of the page, possibly a header or introductory paragraph.

SESSION V

Faded text following the session header, likely listing topics or speakers.

Friday Afternoon, 31 October

Faded text below the date header, possibly detailing the schedule or location.

2:00 p.m.

HEAVY PARTICLES II

**Chairman: T. L. Bailey, University of Florida
Gainesville, Florida**

VI. A Smattering of Scattering. H. SUGIUCHI, J. F. AEBISCHER and M. G. MENENDEZ,* Martin Marietta Corp. and Rollins College.--The measurement of the angular dependence of cross sections requires precise knowledge of the scattering geometry defined by the usual apparatus parameters. For a uniform source intensity the scattered intensity is given by a five-fold integral over the scattering volume and the detector window. In general, this quantity can not be integrated without the use of approximations. In the interest of accurately determining scattering geometries as a function of angle for double beam configurations we have developed a computer program based on Monte Carlo techniques which computes the scattering volume and calculates the weighting functions composing the differential intensity at a given angle. Use of a constant cross section in the intensity integral yields the "apparatus geometry." The computation allows one to make a detailed analysis of angular resolution and permits its quantification. The results of calculations using this method will be presented and compared with other analyses for in-plane and out-of-plane scattering configurations.

*Present address: Physics Department, The University of Georgia

V2. Exact Phase Shifts for the Sutherland Ion-Molecule Potential. JOHN W. SHELDON, Florida State Univ.--Spector¹ has shown that Mathieu functions are exact solutions to the radial Schrödinger equation for r^{-4} potentials, but he demonstrated its complete exact solution only for the repulsive case. In the present paper Spector's work is extended to the case of a long-range attractive r^{-4} (polarization) potential with a short-range infinite repulsive barrier. A relatively simple exact expression for the phase shifts is obtained which is applicable to potential parameters typical of ion-molecule collisions. Both the high and low energy asymptotic forms of the phase shift expression are also presented.

¹R. M. Spector, J. Math. Phys. 5, 1185 (1964).

V3. The Effects of Vibrations on Lifetimes of Ion-Molecule Complexes in Ion-Dipole Collisions. J.V. DUGAN JR., R.B. CANRIGHT JR., NASA-Lewis Research Center and J.L. MAGEE, Univ. of Notre Dame.--A classical harmonic oscillator has been added to the ion-dipole interaction model¹ to study the effects of vibration on collision lifetimes. The dipole moment of the polar molecule is assumed to be a gaussian function of equilibrium bond distance. Two hundred collisions have been studied via computer-plotter techniques^{1,2} for varying impact parameters at relative velocities of 5×10^4 and 2×10^5 cm sec⁻¹. The oscillator energies range from thermal (internal rotations) to .5eV (stiff oscillators). The collision systems are described in refs 1 and 2. Collision lifetimes depend critically on both oscillator force constant and mass. Stiff oscillators¹ generally lower the probability of multiple reflections whereas thermal oscillators increase the probability. The role of the oscillator also depends on initial ion velocity. Motion pictures will be shown which allow instantaneous correlation of translational, vibrational and rotational motion.

¹J.V. Dugan, Jr., J.H. Rice and J.L. Magee, Chem. Phys. Lett., 3 323 (1969).

²J.V. Dugan, Jr., R.B. Canright, Jr., R.W. Palmer and J.L. Magee, VI ICPEAC MIT Press, July, 1969, p.333-340

V4. A Simple Model for the High Energy Reaction of O⁺ Ions with N₂. THOMAS F. O'MALLEY, General Research Corporation.--A rough semi-empirical model is presented for the reaction $O^+ + N_2 \rightarrow NO^+ + N$ as it has been found to occur for either vibrationally excited Nitrogen¹ or high energy ($\gtrsim 1$ eV) O⁺ ions.² The model is based on an assumed crossing of potential energy surfaces. It finds the rapid energy dependence of the reaction rate on both vibrational state and on kinetic energy in the Franck-Condon overlap integral. This integral is constructed by parameterizing initial and final potential energy surfaces in their dependence on the N-N coordinate only, in such a way as to reproduce the experimental dependence on both vibrational and translational energy.

*Work supported by the Advanced Research Projects Agency.

¹A. L. Schmeltekopf, E. E. Ferguson and F. C. Fehsenfeld, J. Chem. Phys. 48, 2966 (1968).

²R. F. Stebbings, B. R. Turner and J. A. Rutherford, J. Geophys. Res. 71, 771 (1966).

*Langevin
to Swan ion
partial
waves*

V5. On the Dependence of Ion-Molecule Reactions on the Reactant Vibrational Energy.* F. A. Wolf, San Diego State College.--The statistical theory of reactions of the type $A_2^+ + A_2 \rightarrow A_4^+ \rightarrow A_3^+ + A$ is discussed. Because of resonant charge transfer the interaction energy in the back reaction channel is dependent on the vertical ionization energy. The cross section for a strong-coupling collision depends on the vibrational energy of the reactants such that the (lower, higher) the ionization energy the (stronger, weaker) becomes the coupling and hence the (larger, smaller) becomes the strong coupling cross section. Using hydrogen the cross section ratios (excited/unexcited) are displayed as functions of the reactant kinetic energy in the range from thermal to 10 eV. These ratios reach maxima in excess of unity in the neighborhood of 1 eV and decrease to minima below unity at energies corresponding to the dissociation threshold. These results are explained, for the former in terms of a "strong coupling barrier" effect, and for the latter as phase space competition between continuous and discrete energy state distributions.

*Sponsored by Air Force Grant AFOSR 1277.

V6. Mechanisms in Reactions of O^+ with N_2 and CO_2 . John F. Paulson, Air Force Cambridge Research Labs. --A time-of-flight technique has recently been developed for measuring the velocities of ionic reactants and products in low energy ion-neutral reactions in a longitudinal double mass spectrometer system. Measurements of Q , the energy transferred from internal to translational modes, can be made from these observed velocities. In the case of $O^+ + N_2 \rightarrow NO^+ + N$, the slope of Q vs E_1 (E_1 is the kinetic energy of the ionic reactant) changes abruptly at about 12 eV from that corresponding to formation of a reaction complex at low energies to that for an atom pickup process at high energies. The possibility of an N_2O^+ complex in this system has been discussed by several workers. Two channels for the reaction of O^+ with CO_2 have been studied, leading to $O_2^+ + CO$ and to $CO_2^+ + O$. For a given energy in the range of reactant ion kinetic energies from 0.8 to 6.5 eV, the Q -values for these channels are identical, as expected for reactions proceeding through a complex, and the slope of Q vs E_1 is that predicted for this mechanism.

C. g. M. cm-AM
to 3.6 eV

V7. Low Energy NO⁺ + Cs Charge Exchange-Measurements*
T. L. CHURCHILL, United Aircraft Research Laboratories.--
The low energy charge-exchange cross section of the NO⁺ + Cs reaction reported on a preliminary basis at the Twenty First GEC was remeasured in an experiment specially designed to achieve high resolution of energies below 1 eV. The apparatus was of the 90° crossed-beam type and included a curved, electroformed collision chamber and a homogeneous, transverse magnetic field for continuous energy selection of the ion beam. A quadrupole mass spectrometer provided analysis of the reaction products. The charge-exchange cross section remeasured in this precise experiment was found to occur primarily by small-angle scattering indicating near-resonant transfer without the formation of a temporary complex. Further evidence of this fact was the complete absence of interchange components such as CsN⁺ and CsO⁺ in the reaction products. Only Cs⁺ was observed. The magnitude of the charge-exchange cross section was found to vary monotonically from 10⁻¹⁵cm² at 8 eV to 5 x 10⁻¹⁴cm² at 0.6 eV.
*Work supported in part under AFCRL.

V8. The Effects of Vibrational Excitation on N₂⁺ + N₂ and N₂⁺ + Ar Charge Transfer Collisions. B. VAN ZYL and N. G. UTTERBACK, AC Electronics - Defense Research Labs.
- The effects of small amounts of vibrational energy carried into near resonant charge transferring collisions between molecules are assessed. An empirically derived expression based substantially on the work of Rapp and Francis¹ relating relative transfer cross section, collision velocity, and energy defect is evaluated for each unique set of vibrational level combinations occupied by initial and final collision members. After including Frank-Condon factors to predict weights of final levels and assigning initial ion vibrational population fractions, all important reaction channels are summed. The resulting relative cross section is then normalized to carefully selected experimental data which include a changing initial ion population distribution as a parameter. The technique, so far tested on N₂⁺ + N₂ and N₂⁺ + Ar collisions faithfully reproduces the dependence of these cross sections on experimental ion source electron energy, and hence on initial ion vibrational populations. Cross sections for charge transfer out of each of the low vibrational levels of the N₂⁺ ion are presented.

¹ D. Rapp and W. E. Francis, J. Chem Phys. 37, 2631(1962).

V9. Vibrational Excitation in the Collisions of Low Energy Ion Beams With Neutral Molecules.* T. F. MORAN and P. C. COSBY, Georgia Institute of Technology. --

Inelastic scattering in ion-molecule collisions has been measured in the 5-20eV kinetic energy range. The occurrence of such processes has been detected using a beam apparatus designed to direct reactant ions into a collision chamber containing neutral molecules and scan the mass, energy and angular distributions of charged reaction products. Ion-molecule rearrangement, charge transfer and elastic events are thus separated from the inelastic energy loss processes. Inelastic collisions with energy losses corresponding to discrete vibrational transitions have been measured for the interactions of O^+ and O_2^+ with atoms and diatomic molecules. For a given reactant ion kinetic energy, the probability of exciting higher vibrational levels increases with scattering angle. The probabilities for translational-vibrational energy exchange as a function of ion kinetic energy are in approximate agreement with those calculated on the basis of a forced harmonic oscillator model.

*Work supported in part by the National Aeronautics and Space Administration under Grant No. NsG-657.

V10. Cross Section For Metastable Production in Very Low Energy He^+ - He Collisions.* P. J. MACVICAR-WHELAN and WALTER L. BORST†, University of California, Berkeley. --

He^m atoms produced by charge exchange of ground state He^+ with He were detected by secondary electron emission from a tungsten target. The cross section for metastable production rose from a threshold near 22 eV to a sharp peak having a value of $2.2 \times 10^{-18} \text{ cm}^2 \pm 50\%$ at 27 eV and decreased to a minimum at 32 eV (c.m. energy). Subsequent rise was attributed to the increased production of He^m and to a smaller extent to kinetic emission of secondary electrons at the higher energies. The apparatus consisted of an ion gun ($10^{-9}A$) - collision chamber (10^{-4} Torr He) - metastable detector assembly. Ultra-high vacuum techniques were used. The surface detector was flashed at high temperatures and measurements were obtained within monolayer build-up times. The secondary electron yield γ_m was 0.13 ± 0.02 . Positive ion emission from the target was also noted. Only neutral particles were able to reach the detector surface.

*Work supported by the U.S. Office of Naval Research

†Present address: Department of Physics, University of Pittsburgh.

VII. Vacuum Ultraviolet Photon Production in Low-Energy Collisions between Neutral Argon Atoms.* PAUL O. HAUGSJAA⁷ and ROBERT C. AMME, University of Denver.-- Photons produced during collisions between two ground-state neutral argon atoms have been observed, using atomic beam techniques. The argon beam energy ranged between 30 and 1000 eV in the laboratory system. The beam was formed by charge-transfer neutralization of a ground-state argon ion beam. A Bendix magnetic electron multiplier, which is sensitive to photons of wavelengths between 2Å and 1500Å, was positioned so as to protect the collecting surface from scattered neutrals. The relative cross section was measured to within a few volts above threshold for the production of photons from the first excited states of argon. The cross section was found to rise rapidly with energy,¹ in a manner similar to the total ionization cross section.

*Work supported by a grant from the National Aeronautics and Space Administration.

⁷Now at the General Telephone and Electronics Laboratory, Bayside, N.Y.

¹H. C. Hayden and R. C. Amme, Phys. Rev. 141, 30 (1966)

VI2. Optical and Mass Spectroscopic Studies of the Reactions of He⁺ and He(23S) with O₂, D. L. ALBRITTON, ESSA Research Laboratories. With He⁺ ions as the only energetic component of a flowing helium afterglow, the O₂⁺b⁴Σ_g⁻-a⁴Π_u bands that originate from the v>2 levels of the b⁴Σ_g⁻ state are weakly excited. O⁺ is the vastly predominant product ion. The reaction is interpreted as a resonant charge transfer to the c⁴Σ_u⁻ state followed by an allowed predissociation, accounting for the O⁺ signal, and radiation to the upper levels of the b⁴Σ_g⁻ state, in agreement with calculated Franck-Condon factors. The He(23S) metastables excite the O₂⁺b⁴Σ_g⁻-a⁴Π_u and A²Π_u-X²Π_g bands, where the latter were found to require a vibrational renumbering of the ground state. A comparison of these metastable-induced spectra with those excited by 5 kV electrons shows that the Penning ionization into the b⁴Σ_g⁻ state is a vertical transition. The b⁴Σ_g⁻ rotational distribution is essentially that of the ground O₂ state. On the other hand, the vibrational distribution in the A²Π_u state differs markedly from that caused by the high-velocity electrons and the metastable-induced rotational excitation is extensive.

INDEX TO AUTHORS

Abou-Seada, M. S.	63	Borst, W. L.	50, 105
Adams, N.G.	44, 45	Bortner, T. E.	80
Aebischer, J. F.	101	Branscomb, L. M.	71, 83
Albritton, D. L.	106	Brehm, B.	83
Amme, R. C.	106	Bridges, J. M.	3
Anderson, R. J.	50	Brown, H. L.	98
Anderson, V. E.	32	Buhler, R. D.	21
Aubrey, B. B.	29	Buser, R. G.	55, 76
Baker, A. J.	17	Canright, R. B., Jr.	102
Ballou, J. K.	51	Cap, D. M.	11
Barnett, C. F.	72	Carlson, T. A.	82
Bauder, U. H.	8	Carter, J. G.	40, 41
Beck, R.	4	Cenkner, A. A., Jr.	17
Bederson, B.	29	Chaney, E. L.	40, 41
Benda, J. A.	56	Chanin, L. M.	90
Benenson, D. M.	17	Chantry, P. J.	38, 39
Bergstedt, K.	19	Chen, C. L.	39, 79
Berlande, J.	34	Chen, M. M.	24
Bhattacharya, A. K.	89	Cheret, M.	34
Biondi, M. A.	98	Christophorou, L. G.	40, 41
Bisbing, P. E.	63	Churchill, T. L.	104
Blaszuk, P. R.	55	Clark, D. C.	73
Bletzinger, P.	54, 89	Cloutier, G. G.	88
Blue, E.	46	Collins, C. B.	35
Bohme, D. K.	44, 45	Collins, P. M.	40, 41
Bolin, P. C.	60	Compton, R. N.	38, 49

Copeland, G. E.	81	Foster, K. D.	67
Corvin, K. K.	92	Fowler, M. C.	56
Cosby, P. C.	105	Fowler, R. G.	81
Cowperthwaite, R. L.	40	Freudenthal, J.	55
Damsky, B. L.	10, 17	Frey, R.	83
Davidovits, P.	92	Frind, G.	10, 17
Deloche, R.	34	Frost, L. S.	6
DeMonchy, A. R.	79	Fuchs, V.	88
Demtroder, W.	85	X Gallo, C. F.	13, 91
Dennis, W. S.	82	Garrett, W. R.	32, 49
Devoto, R. S.	8	Garscadden, A.	54, 89
Doering, J. P.	71	Gavril, S.	91
Dugan, J. V., Jr.	102	Gerardo, J. B.	34
Dunkin, D. B.	44, 45	Gerber, G.	84
Dunn, G. H.	30	Giannotta, S. F.	18
Durbin, E., Jr.	82	Gonfalone, A.	34
Eckert, H. U.	13	Grassman, P.	19
Edelson, D.	98	Green, A. E. S.	74
Eisner, P. N.	29, 43	Grissom, J. T.	49
Erlicki, M. S.	91	Gunton, R. C.	36
Evans, W. D.	51	Gusinow, M. A.	34
Falconer, W. E.	98	Harris, F. E.	31
Fehsenfeld, F. C.	39, 45	Harris, L. P.	11
Ferguson, E. E.	44, 45	X Hammond, T. J.	91
Fitzsimmons, W. A.	82	Haugsjaa, P. O.	106
Fleischmann, H.	72	Hayden, H. C.	72
Folkard, M.	61	Haydon, S. C.	61

Hays, G. N.	79	Kolker, H. J.	57
Hazi, A. U.	84	Krause, M. O.	82
Heberlein, J.	16	Lawrence, G. M.	51
Heller, A.	87	Lee, E. T. P.	50
Heybey, O.	82	Leiby, C. C., Jr.	90
Hirsh, M. N.	43	Lewis, L. J.	82
Hirshfield, J. L.	92	Liebermann, R. W.	6
Holland, R. F.	80	Limbaugh, C. C.	46
Hollister, D. D.	14	Lin, C. C.	51
Holt, E. H.	55, 76	Lineberger, W. C.	71, 83
Houston, J. E.	93	Lockwood, G. J.	73
Hoyaux, M. F.	26	Loper, F. C.	14
Hug, W. F.	21	Lord, W. T.	10
Hunter, A. M.	6	Lowke, J. J.	6
Hurst, G. S.	80	McClintock, M.	85
Ingold, J. H.	47	McDaniel, E. W.	95
Jennings, W. C.	76	McGregor, W. K.	46, 69
Johnsen, R.	98	McInally, J. A.	85
Jones, D. L.	63	McKnight, L. G.	96
Kan, T.	58	McNally, J. R., Jr.	87
Keefer, D. R.	14	McNeal, R. J.	73, 74
Kieffer, L. J.	29	MacVicar-Whelan, P. J.	105
Kim, Y. W.	65	Maecker, H. H. (Invited Paper)	
Klingberg, R. A.	73	Magee, J. L.	102
Klots, C. E.	62	Maier, W. B., II	80
Klueber, O.	19	Mangolis, S. G.	65
Knystautas, E. J.	72	Manson, S. T.	31

Manus, C.	34	Nerheim, N. M.	81
Marston, C. H.	10	Neubauer, R. F.	18
Martin, D. W.	95	Niehaus, A.	84
Martin, F. W.	80	Nighan, W. L.	56
Maupin, R. T.	77	Niles, F. E.	44
Mayer, F. J.	88	Noon, J. H.	55, 76
Menendez, M. G.	101	Novak, J. P.	88
Mentzoni, M. H.	62	O'Malley, T. F.	102
Meyer, J.	4	Olsen, H. N.	3, 81
Michels, H. H.	31	Oskam, H. J.	79, 99
Miller, K. J.	32	Padovani, F. A.	68
Miller, T. M.	29	Parker, A. B.	22
Mitrovich, D.	25	Parks, J. E.	80
Moddeman, W. E.	82	Patterson, P. L.	97
Moore, J. H., Jr.	71	Paulson, J. F.	103
Moran, T. F.	105	Perkins, J. F.	22
Morgenstern, R.	84	Pfender, E.	16
Morris, J. C.	2, 7, 21	Phelps, A. V.	57, 79
Morris, R. U.	2, 21	Polman, J.	54
Mosesman, M.	44	Poss, E.	43
Mullen, J. H.	40	Powell, H. T.	58
Mumma, M. J.	52	Puckett, L. J.	45
Muntenbruch, H.	18	Puttkamer, E. v.	30
Muschlitz, E. E., Jr.	67	Ray, J. A.	72
Nalley, S. J.	38	Roesler, F. L.	51
Nasser, E.	63	Rogers, C. W.	90
Nelson, D. R.	62	Roidt, R. M.	16

Rose, T. L.	83	Swanson, B. W.	16
Rudis, R. P.	7	Tang, S. Y.	67
Ruess, A. D.	63	Taylor, H. S.	84
Sawina, J. M.	96	Teague, M. W.	45
Schearer, L. D.	68, 69	Thompson, R. T.	81
Schieber, D.	91	Thorne, R.	24
Schmeltekopf, A. L.	68	Tombers, R. B.	90
Schorn, A. M.	10	Tracy, C. J.	79
Schrade, H. O.	18	Tse, F. Y.	60
Schreiber, P. W.	6	Uhlenbusch, J.	7
Schulz-Gulde, E.	2	Utterback, N. G.	104
Schummers, J. H.	95	Valance, W. G.	87
Shaw, D. T.	64, 65	Van Brunt, R. J.	29
Sheldon, J. W.	101	Van Zyl, B.	104
Shiau, J. N.	93	Varney, R. N.	96
Shih, K. T.	25	Veatch, G. E.	99
Shimada, K.	64	Vogler, M. K.	30
Simon, A.	93	Volz, D. J.	95
Simpson, A.	61	Walker, K. G.	49
Snuggs, R. M.	95	Walters, G. K.	82
Sprouse, J. A.	14	Watson, A.	60
St. John, R. M.	49, 92	Waymouth, J. F.	12
Stevie, F. A.	82	Weber, R. F.	89
Stewart, T. E.	80	Wells, W. E.	35
Stockdale, J. A. D.	38	Wheaton, J. H.	97
Stojanoff, C. G.	8	Wiegand, W. J.	56
Sugiuchi, H.	101	Willett, C. S.	77

Witteman, W. J.	54
Wolf, F. A.	103
Wolga, G. J.	58
Woo, S. B.	97
Woodward, B. W.	71, 83
Wulff, H.	19
Wyner, E. F.	24
Yos, J. M.	7
Young, C. E.	98
Young, R. T.	77
Zarowin, C. B.	76
Zipf, E. C.	35, 50, 52
Zory, P. S.	76